INAUGURAL-DISSERTATION

zur Erlangung der Doktorwürde

der Naturwissenschaftlich-Mathematischen Gesamtfakultät

der Ruprecht-Karls-Universität Heidelberg

vorgelegt von

Diplom-Biologin Helga Grötsch,

geboren in Lüneburg

Tag der mündlichen Prüfung: _____

Title:

Analysis of the recruitment of the class I myosin Myo5p to endocytic sites in *Saccharomyces cerevisiae*

Referees: Prof. Dr. Felix Wieland

Prof. Dr. Christine Clayton

Acknowledgments

First of all, I would like to thank Maribel Geli for giving me the opportunity to do my PhD in her lab and for all her support, not only concerning the work, but also personally.

I am very grateful to Prof. Dr. Felix Wieland and Prof. Dr. Christine Clayton for reviewing this thesis.

Also, I would like to thank Prof. Dr. Wieland and Barbara Schröter for pushing me a little bit to finish this thesis.

I am more than grateful to all the people of my group: Isabel Fernandez, Fatima Idrissi and Henrique Girao. “You are all fantastic!” It helped me a lot also in very hard days to enjoy your company!!! Gracias!!!! Thank you also for critically reading this thesis, this helped a lot. Un abrazo fuerte por todo!

Thank you also to Jonatan Perez, who made the work really easier when he was in our lab and who was a very pleasant person to have around. Also very nice company was Monica Pons, who helped a lot with the microscope.

I would also like to thank all the nice people who worked next to me at the BZH and at the IBMB, because all together they were creating a nice atmosphere at the working place.

VIELEN DANK and MUCHAS GRACIAS to all my friends!!! Although most of you were far away, it helped me a lot already to talk to you on the phone and when we saw each other it always gave me “good energy” for a longer time! Here in Barcelona, “the Cristinas” were really a big support always, muchas gracias para esto!!!

Vielen Dank auch an meine Eltern, meine Schwester Birgit und Florian, die mich immer unterstützt haben. Jetzt beginnt eine neue Zeit! Birgit danke ich auch besonders für die vielen tollen Pakete, die sie mir immer geschickt hat!

Paul, como esposo y como amigo me has ayudado muchisimo. Espero que un dia puedo aprender mas de ti como no estresarme siempre tanto.

Index

1. Zusammenfassung

In *Saccharomyces cerevisiae* sind dynamische Multiproteinkomplexe, die sich zu sogenannten kortikalen Flecken an der Plasmamembran aufbauen, als Orte der Endozytose identifiziert worden. Während der Bildung des endozytischen Vesikels assoziieren und dissoziieren Proteine an diesen Membrandomänen in hoch geordneter zeitlicher Abfolge. Myo5p, ein Myosin der Klasse I, ist eine essentielle Komponente des Endozytose-Apparates von *S. cerevisiae*. Es ist beschrieben worden, dass dieses Protein sich in einer kurzen, der Vesikelfusion vorausgehenden Zeitspanne am kortikalen Fleck aufhält.

In dieser Arbeit haben wir den Mechanismus der exakten Rekrutierung von Myo5p zu den kortikalen Flecken analysiert. Um zu untersuchen welche Proteindomänen von Myo5p an der Lokalisation des Myosins beteiligt sind, haben wir verschiedene Myo5p-Konstrukte mit GFP fusioniert und deren Lokalisation in lebenden Hefezellen untersucht. Durch diese Experimente fanden wir Hinweise auf eine intramolekulare Interaktion zwischen der zentralen TH1 Domäne und dem C-terminalen Teil von Myo5p, der eine SH3 Domäne mit einschließt. In weiteren Versuchen konnten wir die intramolekulare Interaktion bestätigen und zeigen, dass diese die SH3-vermittelte Interaktion mit Verprolin verhindert und die Rekrutierung von Myo5p an die kortikalen Flecken blockiert.

Mit verschiedenen experimentellen Methoden gelangen wir zu überzeugenden Hinweisen, dass die intramolekulare Interaktion in Myo5p durch die Dissoziation von Calmodulin von der Myo5p-Hals-Domäne (die oberhalb der TH1 Domäne liegt) gelöst wird. Unsere Experimente belegen auch, dass die Dissoziation von Calmodulin die Affinität der TH1 Domäne zu sauren Phospholipiden erhöht.

Basierend auf unseren Ergebnissen erstellen wir ein Modell für die durch Calmodulin regulierte Rekrutierung von Myo5p an den endozytischen Fleck. Demzufolge dissoziiert Calmodulin an der Plasmamembran von der Myo5p-Hals-Domäne und die Interaktion zwischen der TH1 Domäne und dem C-terminalen Teil von Myo5p wird folglich gelöst. Dies ermöglicht wiederum die Bindung der SH3 Domäne an Veprolin und die Interaktion der TH1 Domäne mit sauren Phospholipiden.

2. Summary

In *Saccharomyces cerevisiae*, dynamic complexes of multiple proteins that assemble in cortical patches at the plasma membrane have been identified as sites of endocytosis. During endocytic vesicle formation, proteins associate and dissociate at these membrane subdomains in a highly defined temporal order. The type I myosin Myo5p is an essential component of the endocytic machinery of *S. cerevisiae*. The protein has been shown to be localized to the cortical patches in a short time interval, preceding vesicle scission from the plasma membrane.

In the present work, we analyze the process of Myo5p recruitment to the endocytic patch. To investigate which domains are required for targeting of the myosin, we used GFP-tagged Myo5p mutants and life cell imaging. Starting with these experiments, we demonstrate the existence of an inhibitory interaction between the Myo5p tail homology 1 (TH1) domain and the most C-terminal portion of the myosin, which includes the SH3 domain. Such interaction precludes the SH3-mediated Myo5p association with Verprolin and Myo5p recruitment to the cortical patch. Using different kinds of experiments, we find strong evidence that the interaction between the Myo5p TH1 domain and the C-terminus is released at the plasma membrane by dissociation of calmodulin from the Myo5p neck domain, which lies immediately upstream of the TH1 domain. Further, we find that calmodulin release increases the affinity of the Myo5p neck and TH1 domains for acidic phospholipids.

Based on our results, we propose a model for calmodulin-regulated patch recruitment of Myo5p, whereby calmodulin dissociation from the Myo5p neck at the plasma membrane releases an intramolecular interaction between the Myo5p TH1 domain and the C-terminus, allowing the association of the Myo5p SH3 domain with Verprolin and the interaction of the Myo5p neck and TH1 domains with acidic phospholipids.

3. Abbreviations

aa	amino acid
ADP	adenosine 5’-diphosphate
ATP	adenosine 5’-triphosphate
bp	base pairs
DMSO	dimethyl sulfoxide
DNA	deoxyribonucleic acid
g	gravity
GFP	green fluorescent protein
GST	glutathion-S-transferase
GTP	guanosine 5’-triphosphate
GDP	guanosine 5’-diphosphate
GEF	guanine nucleotide exchange factor
IgG	immunoglobulin G
kDa	kilodalton
kd	dissociation constant
min	minute
OD_{600}	optical density at 600nm
ORF	open reading frame
PCR	polymerase chain reaction
PMSF	phenylmethanesulfonyl fluoride
P_i	inorganic phosphate
ProtA	protein A of *Staphylococcus aureus*
RT	room temperature
SDC	synthetic dextrose complete medium
SGC	synthetic galactose complete medium
Tris	tris-(hydroxymethyl)-aminomethane
s	second
ts	temperature-sensitive
U	unit
wt	wild-type
YPD	yeast peptone dextrose medium
YFP	yellow fluorescent protein
Ura	uracil
Leu	leucin
Trp	tryptophan

4. Introduction

4.1. Class I myosins

Many intracellular trafficking events are powered by motor proteins. While molecular motors of the kinesin and dynein protein family mediate microtubule-based motility, myosins are the only known motors that use actin filaments as tracks (Mallik and Gross, 2004).

Myosins comprise a big superfamily of proteins, all are characterized by a big N-terminal motor or “head” domain that bears an actin-dependent ATPase and transforms the chemical energy derived from ATP hydrolysis into mechanical movement (Sellers, 2000).

In most myosins, the N-terminal head domain is followed by a flexible neck region and a C-terminal tail (Mooseker and Cheney, 1995). The neck is an amphipathic helix, which acts as a lever arm, transforming small conformational changes in the motor domain into bigger movements that are transmitted to the C-terminal tail (Goldman, 1998). The neck domain also serves as the binding site for regulatory light chains, which are calmodulin molecules or other members of the EF-hand protein family (Bahler and Rhoads, 2002; Mooseker and Cheney, 1995). The C-terminal tails of different myosins show a striking diversity of structural elements. Via binding to specific proteins and cargoes, the tail is thought to determine the function and localization of the myosin (Krendel and Mooseker, 2005).

Based on sequence comparison of their conserved N-terminal catalytic domain, myosins are grouped into an ever-increasing number of classes (18 up to now) (Berg et al., 2001). Generally, members of a particular class of myosins also share a common organization of the C-terminal tail and are thus thought to fulfill similar cellular functions (Krendel and Mooseker, 2005; Mooseker and Cheney, 1995).

Only one class of myosin was known until 1973, the so called “conventional” or class II myosins, which promote actin filament movement in muscle cells. Pollard and Korn discovered then the first “unconventional” myosins in *Acanthamoeba castellani* and termed them myosins I, since, in contrast to the two-headed conventional myosins, they were single headed and incapable of forming bipolar filaments via their tails (Pollard and Korn, 1973).

The class I myosins are now the largest and best-characterized group of unconventional myosins and they have been found in a wide range of species from yeast to humans, indicating that they fulfill evolutionary conserved and essential functions (Hasson and Mooseker, 1996; Sellers, 2000).

Class I myosins are characterized by a short positively charged domain in the tail, the so-called tail homology 1 (TH1) domain (Coluccio, 1997). This domain has been shown to

bind to negatively charged phospholipids and protein stripped membranes (Adams and Pollard, 1989; Doberstein and Pollard, 1992; Hayden et al., 1990; Miyata et al., 1989). Class I myosins can be divided into short-tailed and long-tailed. The tail of short-tailed myosins bears only the TH1 domain, while long-tailed myosins comprise a C-terminal extension, which recently has been proven to be involved in the activation of Arp2/3 dependent actin polymerization (Coluccio, 1997; Soldati, 2003). Most lower eukaryotes, e.g. *Acanthamoeba* and yeast, have only long-tailed myosins I (Coluccio, 1997). In mammals, two members of long-tailed and 6 types of short-tailed class I myosins have been described (Berg et al., 2001). The specific properties of the long-tailed myosins will be explained in detail later on in this work.

4.1.1. Class I myosins function in membrane dynamics

Consistent with their potential to translocate actin and to associate with membranes, members of the class I myosins have been implicated in processes that require reshaping or translocation of membranes associated to actin-rearrangements, e.g. endocytic and exocytic processes, cell motility, polarized cell growth and vacuole contraction (for review see (Mermall et al., 1998; Mooseker and Cheney, 1995).

Since class I myosins were first discovered in protozoa, most early studies came from *Acanthamoeba* and *Dictyostelium*. Subcellular localization studies in *Acanthamoeba* and analysis of myosin knockout mutants in *Dictyostelium* demonstrated the involvement of the long-tailed class I myosins in cell motility, phagocytosis and pinocytosis (Baines et al., 1992; Baines et al., 1995; Jung and Hammer, 1990; Novak et al., 1995; Ostap et al., 2003; Temesvari et al., 1996; Titus et al., 1993; Wessels et al., 1991; Wessels et al., 1996). A more detailed study in *Dictyostelium* has recently demonstrated an important role of MyoB in membrane recycling from the endosomes to the plasma membrane (Neuhaus and Soldati, 2000). Finally, early studies using microinjection of antibodies have also demonstrated a role of *Acanthamoeba* myosin-IC in contractile vacuole function (Doberstein et al., 1993).

The best established cellular function of the type I myosins is their role in the uptake step of endocytosis in *Saccharomyces cerevisiae* (Geli and Riezman, 1996), which will be discussed in detail later on in this work. A double knockout mutant of the yeast myosins I Myo3p and Myo5p also shows a strong defect in cell polarity (Goodson et al., 1996). However recent data indicate that the polarity defect is probably installed as a secondary effect of the defect in endocytosis (Valdez-Taubas and Pelham, 2003).

Similar cellular functions have also been described for class I myosins of *Schizosaccharomyces pombe*, *Aspergillus nidulans* and *Candida albicans* (Lee et al.,

2000; McGoldrick et al., 1995; Oberholzer et al., 2004; Sirotkin et al., 2005). In addition, *Aspergillus* MyoA has been implicated in polarized secretion, but also in this case the observed defect might be a consequence of impaired endocytic trafficking (McGoldrick et al., 1995).

In vertebrates, so far, most studies have focused on the short-tailed myosins. The best studied ones are those which participate in specialized functions associated to particular cell types, like Myo1c which is involved in the adaptation of hair cells in the inner ear, and brush-border myosin I (BBMI or Myo1a) which is a cross-linker of actin filaments in microvilli required for structural maintenance (Coluccio, 1997; Gillespie and Cyr, 2004; Tyska et al., 2005). Besides their specialized activities, these myosins also seem to participate in cellular functions associated to membrane traffic in a broader range of cell types. BBMI has been implicated in transcytosis in polarized cells and in the movement of Golgi-derived secretory vesicles to the plasma membrane (Durrbach et al., 2000; Fath et al., 1994). Myo1c promotes the fusion of Glut4-containing vesicles with the plasma membrane after insulin-treatment in adipocytes (Bose et al., 2002). Also, it was recently shown that Myo1c is essential for controlled actin-dynamics which drive compensatory endocytosis in frog oocytes (Sokac et al., 2006).

Another short-tailed myosin, Myo1b, associates with endosomes and lysosomes and the effects observed upon expression of dominant negative mutants indicates that they are involved in membrane traffic between these two compartments (Raposo et al., 1999). Moreover, Myo1b mediates short-range movements of lysosomes on actin-filaments (Cordonnier et al., 2001). Myo1d has been implicated in membrane traffic events between recycling and early endosomes (Huber et al., 2000).

Only recently, a first functional analysis has been made for a long-tailed myosin I in mammalian cells. Myo1f-deficient mice were shown to have neutrophiles with increased adhesion and reduced motility. Exocytosis of β2 integrin-containing granules, induced by integrin ligands, was augmented in Myo1f-knockout cells, suggesting that Myo1f functions as a negative regulator in the process (Kim et al., 2006).

4.1.2. The functional domains of class I myosins

4.1.2.1. The conserved domains characterizing myosins I: the head, the neck and the TH1 domain

Likewise the conventional muscular myosins, the class I myosins are actin-based molecular motors. They can transform the energy derived from ATP hydrolysis in the head domain into mechanical work, as demonstrated by *in vitro* motility assays where the movement of labelled actin filaments can be observed on myosin I coated coverslips in the presence of ATP (Adams and Pollard, 1986; Albanesi et al., 1985; Pollard, 1982).

Small conformational changes which occur in the myosin head as a consequence of the ATPase hydrolysis are transmitted and amplified by the neck towards the tail.

The mechanochemical cycle of class I myosins has been studied in detail in myosins from *Acanthamoeba* and vertebrates (El Mezgueldi et al., 2002; Jontes et al., 1997; Ostap and Pollard, 1996; Pollard and Ostap, 1996; Veigel et al., 1999). The general enzyme mechanism of these myosins is very similar to the mechanism of muscle myosin II (see figure 1). However, in contrast to class II myosins, all characterized class I myosins are low-duty-ratio motors, i.e. they spend a small fraction of their catalytic cycle strongly bound to actin (De La Cruz and Ostap, 2004). Moreover, the weak-binding states have a very low affinity to actin. Therefore, class I myosins cannot achieve processive movement of their cargo unless a high number of motors is concentrated at the sites where they function.

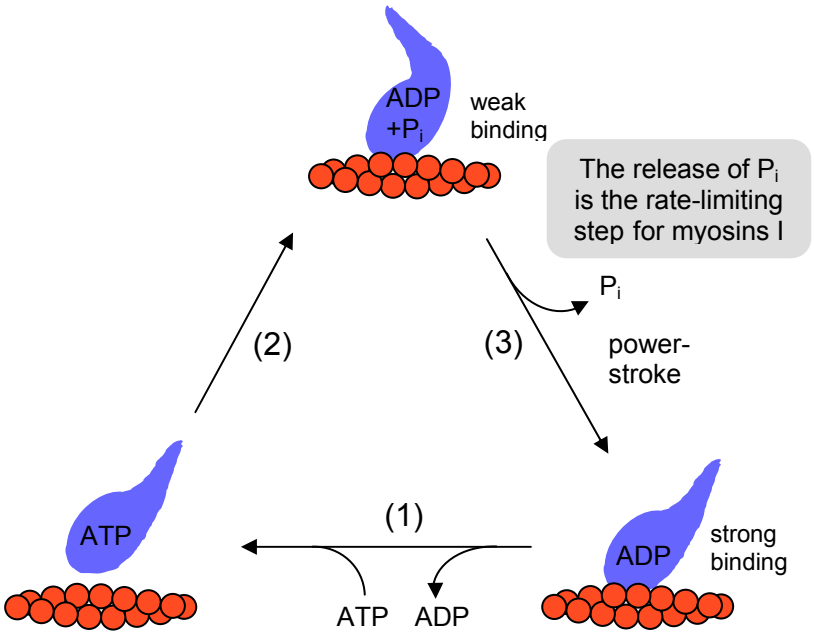

Figure 1. A simplified model for the myosin ATPase cycle. In the absence of ATP the myosin (blue) binds tightly to actin (red). ATP binding induces a conformational change in the myosin that weakens its actin-affinity and causes the release of the myosin from actin (1). ATP-hydrolysis causes a second conformational change allowing actin binding with low affinity (2). After ATP-hydrolysis ADP and P_i stay first bound to the myosin. When P_i is finally released the myosin can bind with high affinity to actin and the force-generating power-stroke is finally generated, which moves the myosin relative to the actin-filament (3). ADP is released and ATP can rebind to repeat the cycle (De La Cruz and Ostap, 2004).

In protozoan and yeast myosins the motor activity of class I myosins is controlled by phosphorylation (Barylko et al., 2000). The phosphorylated site, called TEDS site (since the phosphorylated serine or threonine is replaced by negatively charged aspartic acid or glutamic acid residues in vertebrate myosins) is located in a surface loop that mediates strong hydrophobic bonds with actin. Thus, phosphorylation regulates the productive interaction of the head with actin.

In vitro experiments indicate that the motor activity of class I myosins can also be regulated by Ca^{2+}-triggered release of the calmodulin or calmodulin-like light chains.
The neck region of different class I myosins varies in length. It bears 1 to 6 IQ motifs (α-helical segments with N-terminal isoleucine (I) and glutamine (Q) residues, consensus IQXXXRGXXXR) which bind calmodulin or other members of the EF-hand protein family in the absence of Ca^{2+} (Sellers, 2000; Wolenski, 1995).
In vitro, a rise in Ca^{2+} inhibited motility of class I myosins (Stoffler and Bahler, 1998; Wolenski et al., 1993). However, the influence of an elevated Ca^{2+}-concentration on the ATPase activity was either stimulatory or inhibitory, depending on the myosin studied (Wolenski, 1995). Ca^{2+}-binding might either induce a conformational change in the calmodulin protein associated to the neck or cause dissociation of the light chain from the myosin. Depending on the exact sequence of the IQ motif, calmodulin binding is more or less sensitive to Ca^{2+} (Bahler and Rhoads, 2002). *In vitro*, calmodulin can be removed from some IQ motifs by high Ca^{2+}-concentrations. However, it is not known whether Ca^{2+} can influence calmodulin-binding to the neck under physiological conditions.

The TH1 domain characterizing class I myosins is required for the localization of the motor proteins to their membrane-bound destinations (Lee et al., 2000; Oberholzer et al., 2004; Yamashita et al., 2000). The domain is highly enriched in positively charged amino acids and has been shown to interact *in vitro* with purified protein stripped membranes and with different kinds of negatively charged lipids, e.g. phosphatidylserine, phosphatidic acid and PI(4,5)P2 (Adams and Pollard, 1989; Doberstein and Pollard, 1992; Hayden et al., 1990; Miyata et al., 1989). Thus, it was believed that the TH1 domain of class I myosins interacts with membranes by unspecific electrostatic interactions. However, it was recently shown that the TH1 domain of mammalian Myo1c binds specifically to PI(4,5)P2 in *in vitro* experiments with liposomes (Hokanson and Ostap, 2006). By sequence analysis and structural modelling, the TH1 domains of mammalian Myo1c and *Acanthamoeba* myosin-1C were predicted to exhibit structural homology to PI(4,5)P2-specific pleckstrin homology (PH) domains (Hokanson et al., 2006; Hwang et al., 2007). Thus, for these myosins the TH1 domain might be sufficient for the localization to PI(4,5)P2-enriched membranes or membrane subdomains. However, important residues for PI(4,5)P2 binding are not conserved in the TH1 domain from other class I myosins, suggesting that TH1 domains might mediate different kinds of lipid binding (Hokanson et al., 2006).
Interestingly, recent reports have also suggested a possible role of the myosin I neck in membrane binding. The junction between head and tail domains of class I myosins forms an extended amphipathic alpha-helical structure bearing positively charged residues that could mediate binding to acidic phospholipids (Coluccio, 1997).

Early investigations by Swanljung-Collins and Collins suggested that the neck of the brush-border myosin I might bind to anionic lipids in the absence of associated light chains. They demonstrated that *in vitro* Ca^{2+} can promote dissociation of some calmodulin light chains from the brush-border myosin I and stimulate binding to phosphatidylserine (Swanljung-Collins and Collins, 1992). Consistently, Tang et al. showed that the addition of Ca^{2+} dramatically decreases the dissociation of Myo1c from phosphatidylserine-containing liposomes (Tang et al., 2002). However, these observations could still be explained by an artificial effect of Ca^{2+}, as it is possible that high levels of free Ca^{2+} induce phosphatidylserine to cluster, which could favour an electrostatic interaction via the TH1 domain. Hirono et al. could finally demonstrate that a recombinant neck construct of Myo1c binds to negatively charged lipids and that this interaction is inhibited by the addition of calmodulin, also in the presence of EGTA (Hirono et al., 2004). For Myo1c it was shown that the neck is not required for *in vivo* membrane binding (Hokanson et al., 2006). Since the neck domain alone binds unspecifically anionic lipids with low affinity, it was proposed to function in Myo1c recruitment to certain membrane subdomains, in combination with the TH1 domain (Hokanson et al., 2006). Surprisingly, it was recently shown that a neck-protein interaction might also be involved in the recruitment of Myo1c of the inner ear to the plasma membrane. *In vivo* and *in vitro* data suggest that a specific IQ motif of Myo1c associates with cadherin 23 in a calmodulin-regulated manner (Cyr et al., 2002; Phillips et al., 2006).

4.1.2.2. The C-terminal extension of the long-tailed class I myosins

As mentioned before, the long-tailed class I myosins have a C-terminal extension located downstream of the TH1 domain (see also figure 2). This extension of the tail includes a glycine, alanine and proline or glutamine rich domain (GPA or GPQ domain), also called the tail homology 2 (TH2) domain, and a Src homology (SH3) domain, which mediates protein-protein interactions by binding to proline-rich motifs (consensus PXXP) (Coluccio, 1997; Kuriyan and Cowburn, 1997).

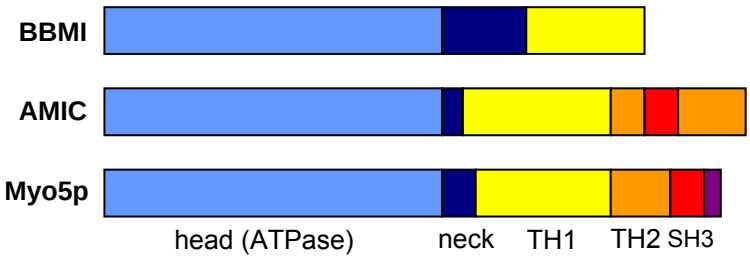

Figure 2. Schematic presentation of the structural organization of some class I myosins. Brush-border myosin I (BBMI) is short-tailed, bearing only the lipid binding tail homology 1 (TH1) domain in the tail. *Acanthamoeba* myosin-IC and Myo5p of *S. cerevisiae* are long-tailed class I myosins. The extension of their tails bears tail homology 2 (TH2; orange) and SH3 domains (red). Myo5p has additionally an acidic motif at the very C-terminus (violet). See text for details.

For long time, the molecular function of the C-terminal extension stayed obscure and hypotheses only derived from *in vitro* experiments whose physiological significance remained elusive. Early *in vitro* experiments demonstrated that the TH2 domain binds filamentous actin (F-actin) *in vitro* (Rosenfeld and Rener, 1994), a property that might also be shared with some of the TH1 domains (Lee et al., 1999). In contrast to the actin binding site of the myosin motor head, the TH2 and the TH1 F-actin binding site is ATP-insensitive. Thus, it was proposed that the TH2 domain may allow the class I myosins to cross-link and contract actin filaments (Fujisaki et al., 1985; Lynch et al., 1986). Alternatively, the TH2 domain could be required to recruit the myosins I onto actin filaments and thereby help to achieve a high local concentration of motor heads at low actin/myosin ratios. As mentioned before, reaching a high local concentration of motor heads might be important for myosin I motor function, since the class I myosins are non-processive, low-duty-ratio motors (De La Cruz and Ostap, 2004).

In addition to the TH2 domain, the long-tailed class I myosins bear an SH3 domain at the C-terminus or within the TH2 domain. The SH3 domain mediates binding to proteins with proline-rich motifs (Kuriyan and Cowburn, 1997). Full function of myosins I was shown to be dependent on this domain, indicating that its interaction with the prolin-rich target protein is important for myosin I activity (Anderson et al., 1998; Novak and Titus, 1998). Since the TH2 domain is rich in proline residues it was proposed that the SH3 domain might control access to the ATP-insensitive actin-binding site by intramolecular interaction with this domain (Goodson et al., 1996). Moreover, proteolytic removal of the SH3 domain from rat myosin I myr3 was shown to activate the ATPase activity *in vitro*, suggesting that the myosin tail folds back and the SH3 domain allosterically inhibits the ATPase (Stoffler and Bahler, 1998). Alternatively, 3D reconstruction analysis of the *Acanthamoeba* myosin-IB suggested that the SH3 domain might form intermolecular bridges with the TH2 domain of adjacent myosin molecules, thus promoting myosin oligomerization (Jontes et al., 1998). The physiological relevance of all these data has not been tested yet.
However, more recent data have established the functional significance of interactions of the C-terminal extension with the machinery involved in Arp2/3 dependent actin polymerization. The SH3 domain of the protozoal class I myosins interacts with CARMIL (capping protein, Arp2/3 and myosin linker), a protein that acts as a molecular linker with the Arp2/3p complex (Jung et al., 2001). Further, the C-terminal extension of the fungal class I myosins bears an acidic domain that directly participates in the activation of the actin nucleating activity of the Arp2/3 complex and their SH3 domains interact with the yeast homologs of WASP (Wiskott-Aldrich syndrome protein) and WIP (WASP interacting

protein), Las17p and Vrp1p, two proteins with a well established function in Arp2/3 dependent actin polymerization (Evangelista et al., 2000; Geli et al., 2000a; Lechler et al., 2000).

4.1.2.1.1. The C-terminal extension of long-tailed class I myosins forms a linkage to the Arp2/3 complex

The highly conserved Arp2/3 protein complex plays a central role in the control of actin dynamics (Goley and Welch, 2006). It consists of 7 proteins of which two, Arp2p and Arp3p, are actin-related. Upon activation of the complex Arp2p and Arp3p can form an actin dimer-like structure which allows the addition of further actin monomers and thus induces actin polymerization. Since the Arp2/3 complex also interacts with the sides of existing actin filaments its activation finally leads to the formation of a network of branched actin filaments (Welch and Mullins, 2002). The Arp2/3 complex alone has low intrinsic actin nucleation activity. For the induction of actin polymerization, activator proteins, e.g proteins of the WASP (Wiskott-Aldrich syndrome protein) family, have to induce the active conformation of the complex (Goley and Welch, 2006).

In the highly homologous class I myosins of *S. cerevisiae*, Myo3p and Myo5p, Evangelista et al. identified an acidic domain at the very C-terminus that shares homology with the acidic C-terminus of WASP proteins and other Arp2/3 activators (Evangelista et al., 2000). The acidic domain of Arp2/3 activators directly binds to the Arp2/3 complex (Mullins, 2000). Consistently, it was also demonstrated for the class I myosins that the acidic domain mediates direct binding to subunits of the complex (Evangelista et al., 2000; Lechler et al., 2000). Moreover, the acidic domain of the myosins was shown to be functionally redundant with the acidic domain of Las17p, the yeast WASP homologue, since the deletion of the acidic region from the class I myosins or Las17p had little effect in living cells, but removal of all acidic domains led to drastic growth and actin organization defects (Evangelista et al., 2000; Lechler et al., 2000). However, the induction of Arp2/3 dependent actin-polymerization by purified class I myosins could not be demonstrated. A direct function of the class I myosins as Arp2/3 activators remained a matter of debate. Up to this point, all strong Arp2/3 activator proteins, e.g. Las17p, had been shown to exhibit actin-binding domains that were structurally different from the TH2 domain (Machesky and Insall, 1999).

Since it was shown that the SH3 domain of the myosins directly interacts with Las17p and Vrp1p, the yeast homologue of WIP (WASP interacting protein), it was suggested that Myo3p and Myo5p work in a complex with these two proteins (Evangelista et al., 2000; Machesky, 2000). Vrp1p bears a binding domain for monomeric actin (the WASP homology 2 domain; WH2) which is homologous to the actin binding domain of Las17p

(Vaduva et al., 1997) Thus, it was proposed that Vrp1p functions together with Myo5p, delivering monomeric actin (G-actin) to the Arp2/3 complex, while the acidic domain of the myosins mediates Arp2/3 binding and induces the structural reorganization of the complex (Machesky, 2000). Consistently, a fusion construct of the Vrp1p WH2 domain and the acidic domain of Myo3p could efficiently activate the Arp2/3 complex *in vitro* (Lechler et al., 2001). Moreover, in a cytosol-dependent *in vitro* assay, Arp2/3 dependent actin polymerization induced by a recombinant tail-construct of Myo5p was shown to depend on Vrp1p but not on Las17p (Geli et al., 2000a; Idrissi et al., 2002).

Only recently, Sun et al. could finally demonstrate in an *in vitro* actin polymerization assay with purified components that Myo5p has Arp2/3 activator activity in combination with Vrp1p (Sun et al., 2006). The capacity of the myosin-Vrp1p complex to activate the Arp2/3 complex was shown to be very similar to purified Las17p, which is considered to be a strong Arp2/3 activator.

Since the acidic domain required for Arp2/3 activation can only be found at the C-terminus of fungal class I myosins (in *S. cerevisiae*, *S. pombe*, *Candida albicans* and *Aspergillus nidulans*) (Soldati, 2003), the generality of the result, that myosins I function in Arp2/3 dependent actin polymerization was doubted. Jung et al. could then demonstrate that also the SH3 domain of *Dictyostelium* myosins I recruits the Arp2/3 complex, although not direct, but via an adaptor protein called CARMIL (for capping protein, Arp2/3 and myosin I linker) (Jung et al., 2001). CARMIL was isolated from cell extracts using GST-tagged constructs of the MyoB and MyoC SH3 domain as baits. The protein was shown to have strong homology to Acan125, a protein which was isolated as a binding partner of the SH3 domain of *Acanthamoeba* class I myosins. CARMIL is a protein of the leucin-rich repeat family of proteins and binds the α-and β-subunits of capping protein to its N-terminus. Besides 2 C-terminal PXXP motifs which mediate the interaction with the class I myosins, CARMIL exhibits 2 domains which can also be found in the Myo5p-Vrp1p complex from *S. cerevisiae*: a G-actin binding WH2 domain and an acidic domain. A protein fragment containing the WH2 domain and the acidic region of CARMIL could activate the Arp2/3 complex in an *in vitro* actin polymerization assay. Moreover, an interaction between CARMIL and the Arp2/3 complex, independent of the class I myosins, was shown in immunoprecipitation experiments. Thus, the CARMIL-myosin I complex seems to function very similar to the myosin I-Vrp1p complex in yeast. Interestingly, CARMIL homologues have been identified in *C. elegans*, *Drosophila*, mouse and human (Jung et al., 2001). This suggests that the long-tailed class I myosins are also linked to the Arp2/3 complex in higher organisms and that the participation in actin polymerization is a general activity of this myosin I subclass.

4.2. Endocytosis in *S. cerevisae*: the assembly of a highly dynamic endocytic patch

Endocytosis is the essential cellular process whereby vesicles are formed at the plasma membrane, which finally detach from the cell surface and travel through the cytosol to fuse with endosomes and enter the endo-lysosomal system. Among many different functions, endocytosis serves for the down-regulation of surface proteins (e.g. receptors and nutrient transporters) and for the uptake of signalling molecules for intracellular communication (Di Fiore and De Camilli, 2001; Mellman, 1996).

In the budding yeast *S. cerevisiae,* a dynamic actin cytoskeleton is essential for the endocytic uptake (Engqvist-Goldstein and Drubin, 2003). A temperature sensitive mutation in the gene encoding actin causes a dramatic defect in the endocytic internalization immediately upon shift to restrictive temperature (Kubler and Riezman, 1993). Further, latrunculin A, a drug that binds to actin monomers and prevents its incorporation into actin filaments, and jasplakinolide, which stabilizes actin filaments, rapidly and potently block endocytosis (Ayscough, 2000; Ayscough et al., 1997). Finally, many endocytic mutants isolated from different screenings bear mutations in genes that encode proteins known to control actin dynamics (Ayscough, 2005).

In *S. cerevisiae,* actin patches associated with the plasma membrane have been described for many years. The observation that many proteins required for endocytosis colocalized with these structures suggested their involvement in the endocytic process (Ayscough, 2005). However, the protein composition of the cortical actin patches seemed heterogeneous (Warren et al., 2002) and their actual involvement in endocytosis remained unproven for many years. Only recently, the matter could be resolved by using real-time, live-cell fluorescence microscopy to analyze the dynamics of the actin patch components tagged with different GFP variants. This technique demonstrated that the different proteins are recruited to and disassemble from cortical patches in a highly defined temporal order and in a partially overlapping manner (Kaksonen et al., 2003; Kaksonen et al., 2005; Kaksonen et al., 2006; Sun et al., 2006). Most importantly, internalization of exogenously added endocytic markers (i.e. the fluorescent lipophilic marker FM4-64 or fluorophor-conjugated alpha factor) together with some patch components was reported, unequivocally demonstrating that the cortical patches constitute sites of endocytosis (Kaksonen et al., 2003; Toshima et al., 2006b). The results revealed that the previously described heterogeneous composition of the cellular cortical patches represented a static view of different maturation stages during the formation of the primary endocytic profile.

When observing several patch components by real-time fluorescence microscopy Kaksonen et al. distinguished 3 different phases of patch behaviour (Kaksonen et al., 2003) (see figure 3). During the first phase, early patch proteins associate to the endocytic site, but the patches remain immotile at the plasma membrane. The second phase is characterized by slow movement (0.05-0.1 µm/sec) of the patch by which the structure moves up to 200 nm away from the plasma membrane. Then, during the third phase, the cortical patch shows rapid, directional movement (0.3 µm/sec) away from the cell cortex. Several studies by the Drubin lab and others suggest that these 3 phases of patch behaviour correspond to coat-assembly, plasma membrane invagination /vesicle scission and vesicle inward movement after scission (Jonsdottir and Li, 2004; Kaksonen et al., 2003; Kaksonen et al., 2005; Sun et al., 2006).

While coat proteins assemble in the absence of actin, actin polymerization seems to be required for membrane invagination and the formation of the endocytic vesicle, as indicated by real-time fluorescence microscopy of cells treated with latrunculin A (Kaksonen et al., 2003). Consistently, actin and the Arp2/3 complex can be observed at the patch just at the onset of slow movement and disappear during the fast motility phase (Kaksonen et al., 2003; Kaksonen et al., 2005).

Besides actin and the Arp2/3 complex, several Arp2/3 activators, coat proteins, endocytic adaptors, scaffold proteins and proteins regulating actin dynamics have been observed on the endocytic patches (see table I). Based on their time of arrival at the endocytic site and their motiliy behaviour, patch components have been grouped into 4 different modules: the coat module, the Las17p/Myo5p module, the actin module, and the amphiphysin module (Kaksonen et al., 2005) (see figure 4 and table I).

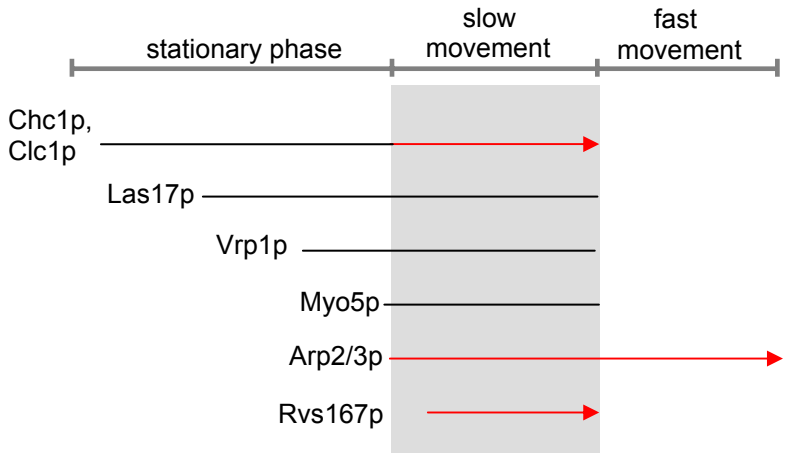

Figure 3. Endocytic proteins show different kinds of behaviour at the endocytic patch. Proteins arrive at different time points during patch formation and either stay stationary or show movement away from the plasma membrane. Stationary behaviour is indicated by black lines and movement is indicated by red arrows.

The coat module includes coat proteins, endocytic adaptors and scaffold proteins like clathrin, Sla1p, Sla2p, Ede1p, End3p and Pan1p. These proteins arrive early to the endocytic patch, during the immotile phase, and then internalize with the forming vesicle (during the slow motility phase) before disassembling (Kaksonen et al., 2003; Kaksonen et al., 2005; Sun et al., 2006; Toshima et al., 2006b). Coat module proteins function not only in cargo recruitment, but some of them also regulate actin-dynamics. For example, Sla1p and Sla2 act as negative regulators of Arp2/3p dependent actin polymerization and Pan1p is itself an Arp2/3 activator (Duncan et al., 2001; Rodal et al., 2003; Toshima et al., 2006a).

Some proteins of the second module, like the Arp2/3 activator Las17p and its binding partners Vrp1p and Bzz1p, also arrive early at the endocytic site, however, they do not move with the vesicle. Together with Myo5p and Bbc1p which arrive just before actin and the initiation of slow movement, these proteins remain in an immotile complex at the plasma membrane until the scission of the endocytic vesicle (Jonsdottir and Li, 2004; Kaksonen et al., 2003; Kaksonen et al., 2005; Sun et al., 2006). The Arp2/3 activators Las17p and the class I myosins are thought to act in concert to promote actin polymerization at the plasma membrane that drives the invagination of the membrane (Sun et al., 2006). Thus, proteins of this module probably stay at the rim of the coated pit while the coat module moves inward with the growing vesicle.

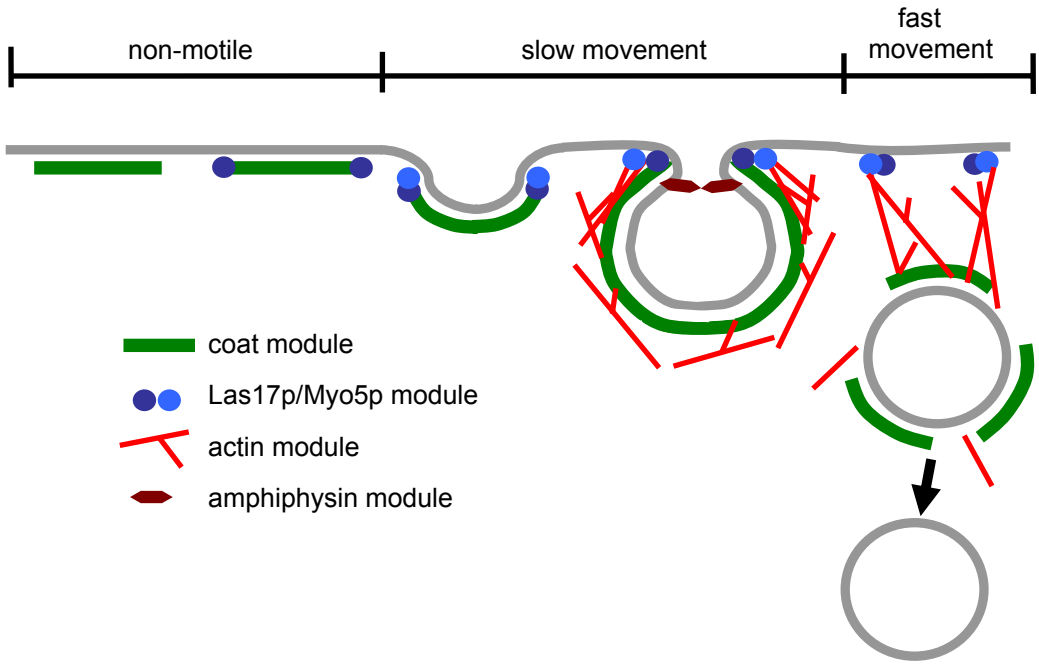

Figure 4. The modular organization of the endocytic patch. Based on their time of arrival at the endocytic site and their motiliy behaviour, patch components have been grouped into 4 different modules: the coat module, the Las17p/Myo5p module, the actin module, and the amphiphysin module. The figure was adopted from Kaksonen et al., 2003, and Kaksonen et al., 2005. See text for details.

The actin module arrives to the endocytic patch when the membrane starts to invaginate and moves with the patch also after the transition from slow to fast motility. It includes actin, the Arp2/3 complex and other proteins involved in the regulation of actin-polymerization, like actin-binding protein Abp1p, capping protein (Cap1/2p) and the yeast fimbrin Sac6p (Kaksonen et al., 2003; Kaksonen et al., 2005). These proteins are thought to work together to form the complex cone-like actin meshwork surrounding the endocytic vesicle (Rodal et al., 2005; Young et al., 2004). Although Abp1p activates the Arp2/3 complex *in vitro*, it is now thought to restrain Arp2/3 activity, limiting actin polymerization via the strong activators Las17p and Myo5p by competing for binding sites in the Arp2/3 complex (Goode et al., 2001; Sun et al., 2006). Moreover, Abp1p acts in vesicle uncoating, as it has been shown to recruit proteins involved in the disassembly of the coat, like the kinases Prk1p/Ark1p and the phosphatidyl-inositol-(4,5)-bisphosphate-(5)-phosphatase Sjl2p (Fazi et al., 2002; Stefan et al., 2005).

The fourth protein module of the endocytic patch consists of the two yeast amphiphysin proteins Rvs161p and Rvs167p. The 2 proteins form a complex that appears very transiently at the endocytic patch, arriving after the onset of actin-polymerization and disappearing before the fast movement starts (Kaksonen et al., 2005). Rvs161p and Rvs167p contain N-BAR domains which are known to induce membrane curvature (Dawson et al., 2006). A yeast strain deficient in the 2 proteins shows endocytic patches that first move away from the cortex and then retract towards the cell surface (Kaksonen et al., 2005). This striking phenotype together with the time of patch association of Rvs161p and Rvs167p suggests that the amphiphysin proteins function in vesicle scission. However, scission can still occur without Rvs161p and Rvs167p, indicating that other factors are also involved in the process.

Endocytic modules are not independent molecular machineries but they influence each other's activity. The Arp2/3 complex can not only be activated by proteins present in different modules (Pan1p, Las17p, Myo5p and Abp1p), but also the Arp2/3 activators themselves are regulated by interactions with proteins in their own or in other protein modules. For example, the activity of Las17p is negatively regulated by interactions with Sla1p, a member of the coat module, whereas Bzz1p, a member of the Las17p/Myo5p module relieves this inhibition (Rodal et al., 2003; Sun et al., 2006). Bbc1p blocks the Arp2/3 activator activity of Las17p and Myo5p (Sun et al., 2006), and Pan1p seems to be negatively regulated by Sla2p (Toshima et al., 2006a).

The molecular mechanisms that control the extremely transient and precise association and dissociation between the different components of the endocytic patch are far from being understood. Endocytic modules do not seem to be pre-assembled in the cytosol, but rather, within a time window of a few seconds, each single protein associates and

dissociates to the patch in a precise and ordered manner, which can hardly be explained by single protein-protein interactions. Molecular mechanisms that intersect multiple synergistic protein-protein and protein-lipid contacts and postranslational modifications such as ubiquitination or phosphorylation, which modify the affinity between the different components, are surely involved.

***Saccharomyces cerevisiae* protein**	**Function**	**References**
Chc1p, Clc1p	vesicle coat component, initiation of patch formation	(Kaksonen et al., 2005; Newpher et al., 2005)
End3p	scaffold protein	(Tang et al., 1997)
Pan1p	Arp2/3 activator, scaffold protein	(Duncan et al., 2001; Tang et al., 1997)
Sla1p	endocytic adaptor (binds NPF-motif), regulator of actin dynamics (inhibits Las17p)	(Howard et al., 2002; Rodal et al., 2003)
Sla2p	scaffold between endocytic coat and actin machinery, binds PI(4,5)P2, negatively regulates Pan1p	(Sun et al., 2005; Toshima et al., 2006a; Wesp et al., 1997)
Ent1p, Ent2p*	endocytic adaptors, bind ubiquitin, bind $PI(4,5)P_2$	(Shih et al., 2002; Wendland et al., 1999)
Ede1p	coat component, binds ubiquitin	(Shih et al., 2002; Toshima et al., 2006b)
Las17p	Arp2/3 activator, recruits Vrp1p	(Sun et al., 2006; Winter et al., 1999)
Vrp1p	binds Las17p and Myo5p, required for Myo5p activity as Arp2/3 activator	(Evangelista et al., 2000; Geli et al., 2000a; Lechler et al., 2001; Lechler et al., 2000; Sun et al., 2006)
Myo5p, Myo3p	motor proteins, Arp2/3 activators together with Vrp1p	(Evangelista et al., 2000; Geli et al., 2000a; Lechler et al., 2000; Sun et al., 2006)
Bbc1p	negatively regulates Las17p and Myo5p	(Rodal et al., 2003; Sun et al., 2006)
Bzz1p	binds and regulates Las17p (relieves inhibition by Sla1p)	(Soulard et al., 2002; Sun et al., 2006)
Arp2/3 complex	actin nucleator, promotes filament branching	(Goley and Welch, 2006)
Abp1p	Arp2/3 activator, regulator of actin polymerrization (inhibits Las17p and Myo5p), recruits Ark1p/Prk1p kinases and Sjl2p	(Fazi et al., 2002; Goode et al., 2001; Stefan et al., 2005; Sun et al., 2006)
Cap1p, Cap2p	barbed-end actin filament capping protein	(Kim et al., 2004)
Sac6p	yeast fimbrin, bundles and stabilizes actin filaments	(Adams et al., 1991)
Rvs161p, Rvs167p	curvutare sensing and membrane bending via N-BAR domain, involved in scission	(Kaksonen et al., 2005; Lombardi and Riezman, 2001)

Table I. Endocytic patch components. The table is giving an overview about the molecular function of proteins which localize to the endocytic patch and which have been grouped into the different protein modules: the coat module (green), the actin module (red), the Las17p/Myo5p module (blue) and the amphiphysin module (brown).
* For Ent1p and Ent2p the exact behaviour at the endocytic patch has not been determined, but due to their molecular function and binding characteristics they can be grouped into the coat module.

4.3. The *S. cerevisiae* class I myosins in the endocytic uptake step

Two highly homologous type I myosins exist in *S. cerevisiae*. Myo5p and Myo3p belong to the long-tailed class I myosins and bear a TH1, a TH2 and an SH3 domain in the tail (Brown, 1997). The neck domain of these myosins bears two IQ motifs that bind calmodulin (Geli et al., 1998).

The strong requirement for actin in the endocytic uptake early suggested that an actin dependent motor might be involved in the process and provide the force necessary to bend the lipid bilayer (Kubler and Riezman, 1993). The hypothesis was also supported by the early observation for a calcium-independent requirement of calmodulin in the endocytic uptake (Kubler et al., 1994).

Consistent with the idea, Geli and Riezman demonstrated the direct involvement of Myo5p and Myo3p in the uptake step of receptor-mediated endocytosis (Geli and Riezman, 1996), using an assay that specifically measures the kinetics of membrane budding from the plasma membrane *in vivo* (α-factor uptake assay). When expressing a temperature sensitive allele of Myo5p in a *myo3*Δ*myo5*Δ strain they could observe a strong defect in the uptake of radioactive alpha-factor after a shift to restrictive temperature. Despite the functional redundancy of Myo5p and Myo3p, Myo5p seems to be the prevalent type I myosin for receptor-mediated endocytosis, since a *myo5*Δ strain is defective in alpha-factor uptake at 37°C, while a *myo3*Δ strain shows normal uptake kinetics under the same conditions (Geli and Riezman, 1996). Besides their function in receptor-mediated endocytosis, Myo5p and Myo3p have also been shown to exhibit a redundant function in the constitutive fluid-phase uptake (Goodson et al., 1996). Shortly after the identification of the yeast class I myosins as essential factors for endocytosis, findings from several groups led to the discovery that Myo5p and Myo3p can function as activators of the Arp2/3 complex (see section 4.1.2.1.1.). As explained before, an acidic domain was identified at the C-terminus of the myosins that mediates direct interaction with subunits of the Arp2/3 complex (Evangelista et al., 2000). In combination with Vrp1p-binding to the SH3 domain of the myosin this interaction was shown to induce actin polymerization (Evangelista et al., 2000; Geli et al., 2000a; Lechler et al., 2001; Lechler et al., 2000). Overexpression of Vrp1p partially rescues the endocytic uptake defect of a *myo5*Δ strain (Geli et al., 2000a). This observation demonstrates that Vrp1p and Myo5p exhibit overlapping functions in endocytosis and suggests that the uptake defect of the *myo5*Δ mutant is at least partially reflecting impaired actin-polymerization via Myo5p-Vrp1p. Besides the activity of the class I myosins as Arp2/3 activators, also the motor function of Myo5p and Myo3p has been shown to be important for endocytosis. Mutation of a serine-residue in the motor head of Myo5p, which has to be phosphorylated for

efficient actin binding and motor activity, led to a striking defect in endocytosis in a *myo3*Δ strain (Grosshans et al., 2006).

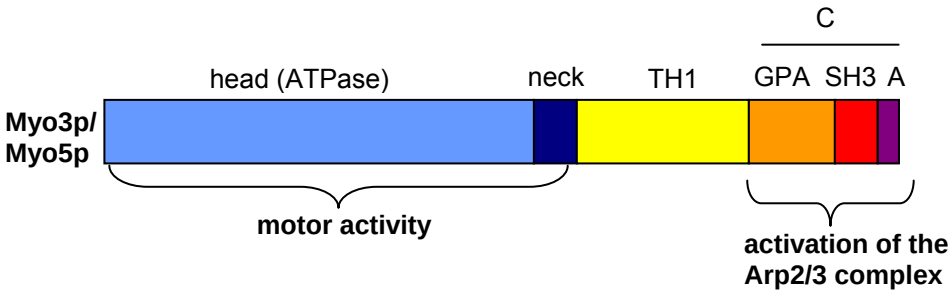

Figure 5. Endocytic functions of class I myosins. The motor activity via the head and neck domains and the Arp2/3 activator activity via the C-terminal part of the tail (C) bearing the GPA domain, the SH3 domain and the acidic peptide have been shown to be important for endocytosis.

How the two activities of the class I myosins, motor function and Arp2/3 activator function (see figure 5), participate on the molecular level in endocytosis remains to be understood. Only recently, Sun et al. presented important insights regarding this question by analyzing the contribution of the two myosin I activities to endocytic patch dynamics (Sun et al., 2006).

Arp2/3 dependent actin polymerization has been proposed to function in membrane invagination, vesicle constriction, scission or vesicle movement after scission during endocytosis (Kaksonen et al., 2006). Sun et al. performed photobleaching experiments in *bbc1*Δ *sla1*Δ cells that carry out endocytosis but have highly enlarged endocytic actin structures (Sun et al., 2006). The experiments demonstrated that actin-monomers are added next to the plasma membrane. Moreover, slow inward-movement of cortical patch components was observed at the same speed as actin-protrusions grew. This suggests that actin polymerization at the plasma membrane is generated for plasma membrane invagination, implicating the plasma membrane-based Arp2/3 activators Myo5p/Vrp1p and Las17p in these processess. Moreover, deleting the Myo5p acidic domain required for Arp2/3 activation caused a significant reduction of the frequency of Sla1-GFP slow inward movement (in a *myo3*Δ background), while similar truncations in the other Arp2/3 activator proteins had no or very little effect. This observation suggests that the Arp2/3 activator activity of Myo5p is especially important for membrane invagination during endocytosis.

By analyzing Myo5p mutants mutated in important sites of the motor head, Sun et al. demonstrated that, independent of the Myo5p function as Arp2/3 activator, also the myosin I motor activity plays an important role for the slow motility phase of cortical patch components. Myo5p mutants with blocked motor activity could still polymerize actin at

endocytic sites, but were strikingly impaired in the slow endocytic inward-movement of Sla1-GFP (Sun et al., 2006). This suggests that the myosin I motor activity is required for membrane invagination and/or scission. The idea that Myo5p functions in membrane scission is supported by the observation that a temperature sensitive *myo5* mutant exhibits cortical patches with a prolonged slow-movement phase at semipermissive temperature (Jonsdottir and Li, 2004). The ts mutant was also shown to exhibit an increased number of plasma membrane invaginations, but the endocytic origin of these membrane invaginations was not demonstrated.

It remains to be answered how the myosin I motor activity participates exactly in endocytosis. On the molecular level the motor could participate in the generation of membrane tension by moving the membrane along actin filaments or in the organization of actin filaments, i.e. their correct orientation and movement away from the plasma membrane.

4.3.1. Mechanisms of Myo5p regulation

As mentioned before, the complex formation of the endocytic vesicle can be controlled by sharply limiting the activity and the time interval of appearance of the endocytic proteins at the endocytic patch. One of the proteins that might integrate a major number of inputs that modulate its presence and activity is the unconventional class I myosin Myo5p. Myo5p has a complex domain structure and directly interacts with a number of proteins involved in endocytosis, which include not only components of the hard core machinery required for the formation of vesicles but also some signalling molecules, i.e. kinases, phosphatases and calmodulin (Evangelista et al., 2000; Geli et al., 2000a; Geli et al., 1998; Grosshans et al., 2006; Lechler et al., 2000)(and our unpublished data).

As explained before, Myo5p exhibits two activities that are important for the formation of the endocytic vesicle: Arp2/3 activator function and molecular motor activity. Both activities seem to be independently regulated.

Since binding of the Myo5p SH3 domain to Vrp1p is essential for the Myo5p activity as Arp2/3 activator (Geli et al., 2000a; Lechler et al., 2000; Sun et al., 2006), actin polymerization via Myo5p can be controlled by mechanisms affecting the interaction with Vrp1p. The protein Bbc1p has been shown to inhibit the Arp2/3 activator function of Myo5p/Vrp1p *in vitro* (Sun et al., 2006). Since Bbc1p binds to the Myo5p SH3 domain via a proline-rich region it most likely negatively regulates Myo5p by competing with Vrp1p for myosin binding (Mochida et al., 2002; Tong et al., 2002).

The motor activity of class I myosins from lower organisms can be controlled by phosphorylation of a single site in an actin-binding loop (Barylko et al., 2000).

Phosphorylation of the corresponding residue was shown to be required for Myo5p motor activity during fast, ligand-induced endocytosis (Grosshans et al., 2006)

Besides the regulatory mechanisms affecting Myo5p activities, also the recruitment of Myo5p to the endocytic patch seems to be sharply regulated.

Myo5p appears at the endocytic patch during an extremely short time interval (15 to 20 seconds), which probably precedes vesicle scission from the plasma membrane (Jonsdottir and Li, 2004; Sun et al., 2006). Consistent with an important role of the SH3 domain in Myo5p recruitment, a Myo5p mutant with a mutated SH3 domain appears partially delocalized (Sun et al., 2006). However, while Bbc1p arrives together with Myo5p at the endocytic site, two binding partners of the Myo5p SH3 domain, Las17p and Vrp1p, arrive significantly earlier (Jonsdottir and Li, 2004; Kaksonen et al., 2003; Kaksonen et al., 2005; Sun et al., 2006). Las17p association precedes the recruitment of Myo5p about 20 seconds and Vrp1p arrives about 10 seconds earlier than the myosin.

So far, direct evidence for a role in Myo5p recruitment has been only shown for Vrp1p, since the myosin appears partially delocalized in a *vrp1*Δ yeast strain (Sun et al., 2006). Las17p binds to the SH3 domain of Myo5p and also to Vrp1p (Evangelista et al., 2000; Naqvi et al., 1998). Thus, a direct and indirect implication of Las17p in Myo5p recruitment has been proposed. The observation that Las17p and Vrp1p associate to the endocytic sites significantly earlier than Myo5p suggests that their interaction with the myosin might be regulated. Moreover, other Myo5p domains and Myo5p interactions should necessarily be involved in the recruitment of the myosin to the cortical patches, because the SH3 domain is not sufficient to target Myo5p to these structures and the effects of deleting the SH3 domain are only partial (Anderson et al., 1998; Sun et al., 2006).

Since Myo5p bears a TH1 domain that for other class I myosins has been shown to interact with negatively charged lipids (see 4.1.2.1.) it seems to be likely that also the binding to certain lipids might influence Myo5p behaviour at the endocytic patch. Moreover, as it was demonstrated that the interaction between Cmd1p and the Myo5p neck is important for the endocytic uptake step (Geli et al., 1998), a Cmd1p-dependent regulation of Myo5p might be required for the formation of the primary endocytic profile.

5. Objectives

Recently, real-time microscopy of fluorescently labelled proteins required for the uptake step of endocytosis has allowed defining the temporal sequence of recruitment of the different elements of the budding machinery. This kind of analysis has demonstrated that association and dissociation between the different cortical patch components has to be exquisitely regulated within a time frame of seconds. The molecular mechanisms regulating this highly dynamic process are largely unknown.

As previously discussed, one of the proteins that might integrate a major number of inputs that modulate its presence at the endocytic patch is the unconventional type I myosin Myo5p. Therefore, we decided to investigate the *cis* and *trans* elements required for the Myo5p recruitment to the endocytic patch and the mechanisms that precisely modulate this process. The specific aims of our work are:

1) Define the Myo5p domains necessary and sufficient to target the type I myosin to the cortical endocytic patch.
2) Identify protein-protein or lipid-protein interactions that might contribute to the localization of Myo5p to the cortical endocytic patch with a special focus in the components that are present at the cortical patch before Myo5p.
3) Investigate the molecular mechanisms that regulate the transient nature of these interactions.

6. Results

6.1. Analysis of Myo5p recruitment to endocytic patches

Recently, real-time fluorescence microscopy has allowed observing the sequential recruitment of endocytic proteins to cortical patches (Kaksonen et al., 2003; Kaksonen et al., 2005; Sun et al., 2006). In these studies it was shown that Myo5p localizes to the endocytic patch about 20 seconds after the recruitment of Las17p and about 10 seconds after the recruitment of Vrp1p, two proteins that are known to bind to the Myo5p tail via its SH3 domain (Evangelista et al., 2000; Sun et al., 2006). The observation that Myo5p and its known binding partners arrive at different stages during the formation of the endocytic patch and the fact that they remain there during overlapping but still different time windows, suggests that their interaction might be regulated. Further, the observation that the Myo5p SH3 domain, which mediates the interaction with Las17p and Vrp1p, is not sufficient for Myo5p patch localization (Anderson et al., 1998) suggests that other factors might be involved in the recruitment of Myo5p to the endocytic site.
Myo5p has a complex domain organization that could integrate a number of different cellular signals. Thus, in order to look for the molecular mechanisms regulating the cortical patch recruitment of the myosin, first, we decided to analyze the contribution of the different Myo5p domains to the cortical patch localization.

6.1.1. An interaction between different Myo5p tail domains regulates the recruitment of Myo5p to cortical patches

6.1.1.1. The cellular localization of GFP-Myo5p constructs bearing different truncations suggests that an interaction between the TH1 domain and the Myo5p C-terminus prevents Myo5p recruitment to cortical patches

In order to analyze the role of the different Myo5p tail domains in the recruitment to cortical patches, we expressed GFP-fusion proteins of full-length Myo5p or different truncations under the control of the native *MYO5* promoter in *myo5*Δ cells (figure 6). The full-length fusion protein (GFP-Myo5p) showed localization to cortical patches, as it has been described before. Moreover, a diffuse localization at the plasma membrane and some cytosolic expression could be observed.
When visualizing GFP-Myo5p constructs with C-terminal truncations, a construct missing only the Myo5p domains required for Arp2/3 activation (GFP-HnT) failed to concentrate at cortical patches. Thus, the Myo5p C-terminus including the GPA domain, the SH3 domain and the acidic peptide seemed to be required for patch localization. Not surprisingly then, also the constructs with bigger C-terminal truncations showed only diffuse cytoplasmic fluorescence (GFP-Hn and GFP-H).

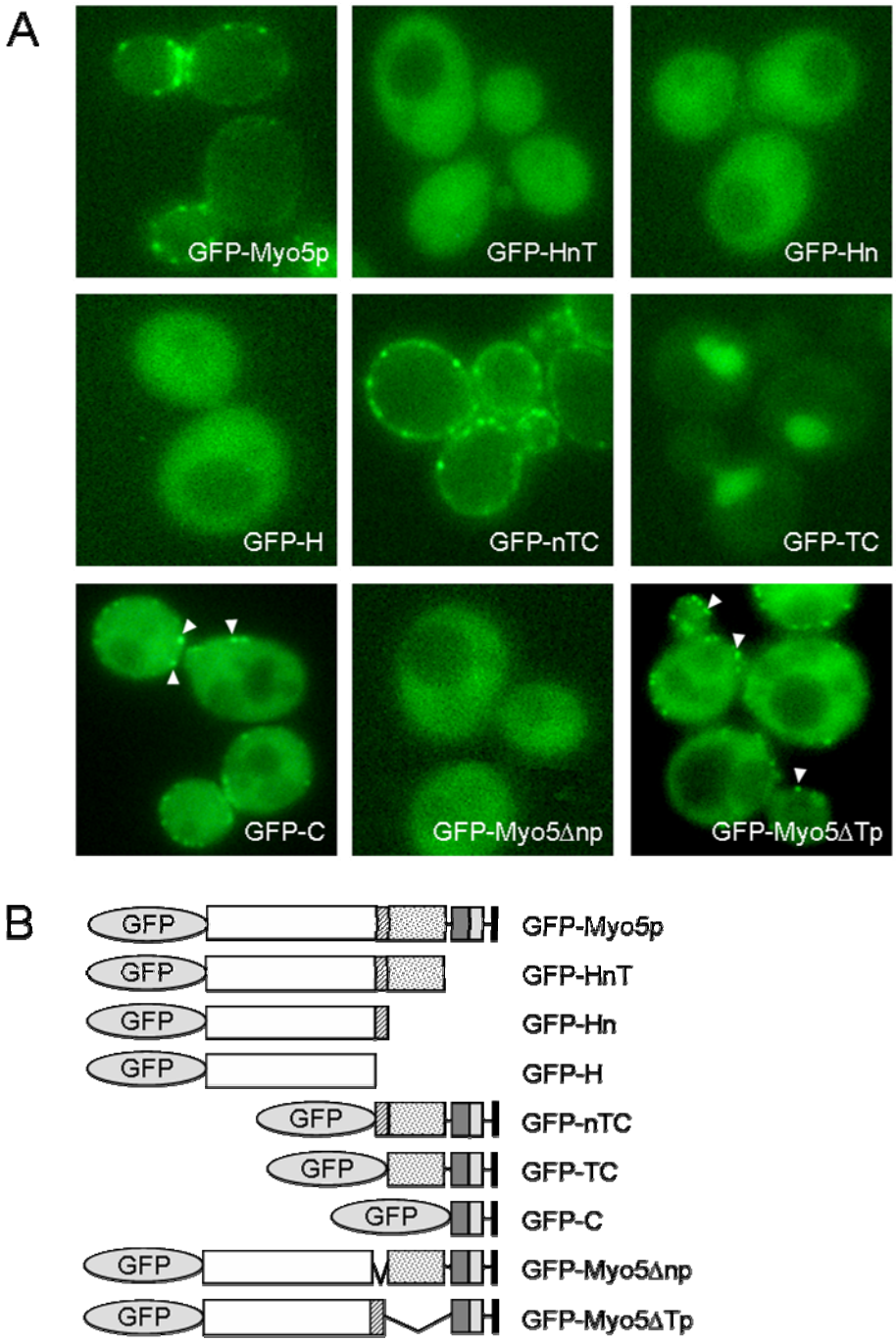

Figure 6. Localization of Myo5p constructs fused to GFP. A. Fluorescence micrographs of live *myo5*Δ cells (SCMIG275) expressing the indicated constructs represented in **B** from centromeric plasmids under the control of the *MYO5* promoter. Cells were grown to mid-log phase at 25°C and directly observed by conventional fluorescence microscopy. Arrowheads indicate cortical patches.

Visualization of GFP constructs with N-terminal truncations demonstrated that a construct missing just the head domain (GFP-nTC) exhibited a cellular localization nearly indistinguishable from the full-length protein. In contrast, a GFP fusion protein bearing the

Myo5p-tail without the neck (GFP-TC) appeared exclusively localized to the nucleus, suggesting that the Myo5p neck was required for Myo5p localization to the cortical patch. Surprisingly though, a construct bearing only the Myo5p C-terminal domains required for Arp2/3 activation (GFP-C) partially recovered the cortical patch localization. These observations suggested that an intra- or intermolecular interaction occurs between the Myo5p TH1 domain and the C-terminus, which blocks Myo5p recruitment to cortical patches via its C-terminal domain. On the other hand, since the construct missing just the head domain (GFP-nTC) was localized normally, the neck seemed to be required to release the Myo5p C-terminus / TH1 domain interaction.

For further analysis of these hypotheses, we expressed GFP fusion proteins missing only the neck (GFP-Myo5Δnp) or only the TH1 domain (GFP-Myo5ΔTp). As expected, the construct missing the neck could not localize to cortical patches, implying that also in this construct the interaction of the Myo5p C-terminus with patch components was blocked by the TH1 domain. The fusion protein missing only the TH1 domain was recruited to patches, supporting the idea that the C-terminus alone is sufficient for patch localization.

Nevertheless, it should be noticed that besides their cortical patch localization, the GFP-C and GFP-Myo5ΔTp constructs, missing the TH1 domain, showed strong cytosolic localization when compared with the full-length GFP-Myo5p or with the construct missing the motor head (GFP-nTC). This suggests that the lipid binding TH1 domain contributes to the efficient localization of Myo5p.

6.1.1.2. The Myo5p neck and TH1 domains directly interact with a C-terminal Myo5p fragment containing the GPA domain, the SH3 domain and the acidic peptide in *in vitro* binding assays

Since visualization of the GFP-Myo5p constructs suggested that an intra- or intermolecular interaction may occur between the Myo5p TH1 domain and the C-terminus, we next decided to test this interaction *in vitro* using purified components.

A GST-fusion protein bearing the Myo5p C-terminus (GST-C) was purified from bacteria and incubated with a construct bearing two Protein A IgG-binding domains fused to the neck and TH1 domains of Myo5p (ProtA-nT), which was purified from yeast. Unfortunately, we could not purify a construct bearing the TH1 domain alone, since significant amounts of the protein could not be expressed in yeast or in bacteria.

As shown in figure 7A, glutathion-Sepharose beads coated with GST-C could efficiently pull down purified ProtA-nT (approximately 50 % of the total input), while beads coated with GST alone could not, suggesting a direct interaction between the Myo5p neck and TH1 domains and the Myo5p C-terminus.

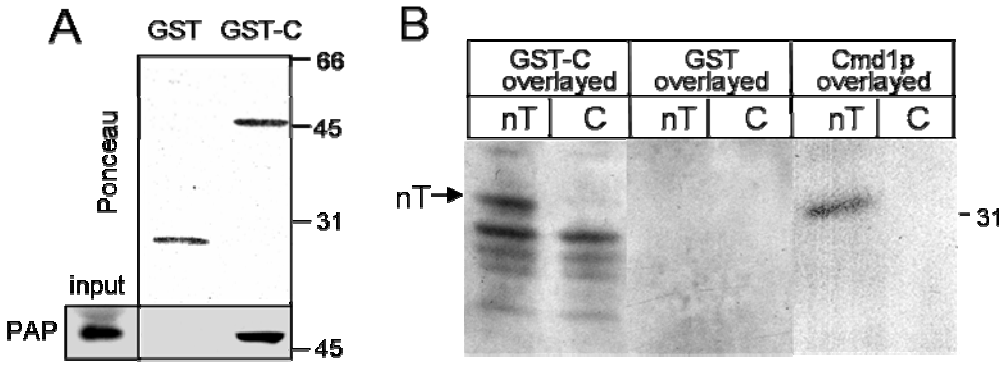

Figure 7. A Myo5p fragment bearing the neck and TH1 domains directly binds to the Myo5p C-terminus. A. Immunoblot (lower panel) of glutathion-Sepharose pull-downs of 3 µg of a recombinant purified C-terminal fragment of Myo5p bearing the GPA, SH3 and acidic domains fused to GST (GST- C) or GST, incubated with 0.01 µg of a Protein A-tagged Myo5p fragment bearing the neck and TH1 domains (ProtA-nT) purified from yeast. *Ponceau* red staining was used to detect the GST and the GST- C proteins (upper panel). PAP was used to decorate the ProtA-nT construct (lower panel). 5 % of the total input and 10 % of the precipitate were loaded.
B. Overlay assay of 0.15 µg of a Myo5p fragment bearing the neck and TH1 domain (nT) purified from yeast overlayed with 20 mM GST or the C-terminal fragment of Myo5p bearing the GPA, SH3 and acidic domains fused to GST (GST-C) or 60 mM calmodulin (Cmd1p). An α-GST antibody was used to detect GST and the GST-C construct and an α-Cmd1p antibody was used for detection of calmodulin. Control assays were performed starting from a yeast strain that did not express the nT-protein (C).

Although the ProtA-nT construct purified from yeast appeared at least 90% pure by SDS-PAGE and Coomassie staining, and about 50 % of the ProtA-nT input was associating to the GST-C construct, copurifying yeast proteins could still mediate binding between the different Myo5p domains. Thus, in order to test if the interaction between the Myo5p C-terminus and the neck and TH1 domains was really direct, we performed a protein overlay assay (figure 7B). ProtA-nT bound to IgG-Sepharose beads was purified from yeast and the Myo5p fragment containing the neck and TH1 domains was stripped from the ProtA-tag using the TEV (tobacco etch virus) protease. The polypeptide was subjected to SDS-PAGE, transferred to nitrocellulose and finally overlayed with GST-C, GST alone or recombinant Cmd1p as a positive control, all of them purified from *E. coli*. As expected, binding to the fragment containing the Myo5p neck and TH1 domains could be detected for GST-C and for Cmd1p, but not for GST alone. Thus, the interaction between the Myo5p C-terminus and the Myo5p neck and TH1 domains seemed to be direct.

6.1.1.3. The TH1 domain blocks the interaction of the Myo5p C-terminus with Verprolin *in cis* and *in trans*

Visualization of the GFP-Myo5p constructs suggested that the interaction between the TH1 domain and the Myo5p C-terminus might inhibit the recruitment of Myo5p to cortical patches mediated by the C-terminus. An interaction between the Myo5p SH3 domain (included in the C-terminal portion of the protein) and the endocytic protein Verprolin

(Vrp1p) has been shown to be essential for Myo5p function (Anderson et al., 1998; Geli et al., 2000b). Moreover, an involvement of Vrp1p in Myo5p patch recruitment has been suggested (Sun et al., 2006). Thus, we decided to analyze if the Myo5p-Vrp1p interaction could be blocked by the Myo5p TH1 domain. Extracts of yeast cells expressing ProtA-tagged Myo5p constructs and HA-tagged Vrp1p (Vrp1-HAp) were subjected to IgG pull-downs (precipitating mainly cytosolic ProtA-Myo5p, see methods) and coprecipitating Vrp1-HAp was detected by immunoblot.

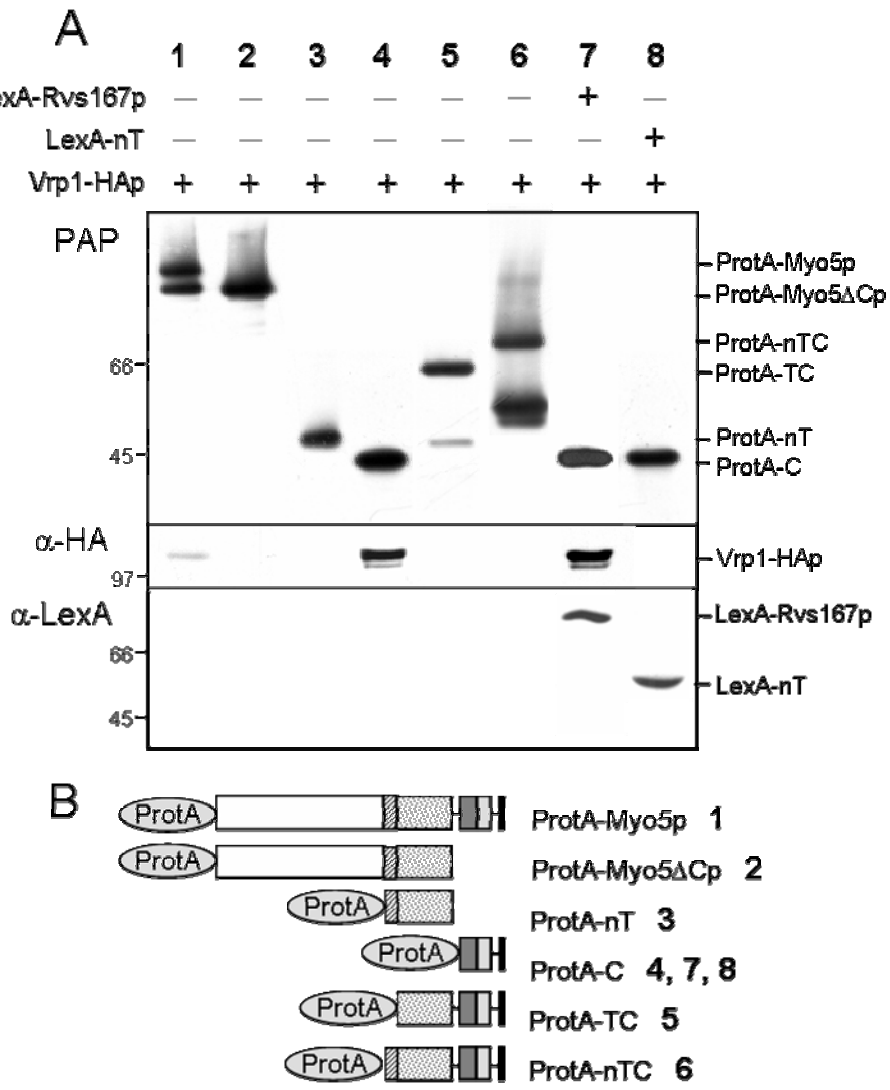

Figure 8. The Myo5p TH1 domain blocks the interaction of the Myo5p C-terminus with verprolin *in cis* and *in trans*. Immunoblots of IgG-Sepharose pull-downs of *myo5*Δ *vrp1*Δ cells (SCMIG304) expressing the Protein A-tagged Myo5p constructs represented in **B** and HA-tagged Verprolin (Vrp1-HAp) from centromeric plasmids under the control of the *MYO5* and *VRP1* promoters, respectively, in the absence or in the presence of LexA-fusion proteins of Rvs167p (LexA-Rvs167p) or the Myo5p neck and TH1 domains (LexA-nT), both overexpressed under the control of the constitutive ADH promoter. Cells were lysed and proteins were precipitated with IgG-Sepharose. IgG-precipitated proteins were analyzed by immunoblot using PAP for detection of the Myo5p constructs, and α-HA or α-LexA antibodies for detection of Vrp1-HAp and the LexA fusion constructs, respectively.

As shown in figure 8, a ProtA-construct bearing the Myo5p C-terminus (ProtA-C) showed strong interaction with Vrp1-HAp when compared with the full-length Myo5p. Adding back the TH1 domain to the C-terminus (ProtA-TC and ProtA-nTC) completely blocked the interaction with Vrp1p. In addition, coexpression of a LexA-fusion protein bearing the neck and TH1 domains (LexA-nT) clearly diminished the Myo5p C-terminus / Vrp1p interaction *in trans*, while coexpression of LexA fused to Rvs167p did not have this effect. Interestingly, LexA-Rvs167p and LexA-nTH1 were both pulled down by ProtA-C. Thus, although both LexA fusion proteins interacted with the Myo5p C-terminal extension, only the neck-TH1 fragment was competing for binding with Vrp1p.

6.1.2. Calmodulin regulates the recruitment of Myo5p to endocytic patches at the plasma membrane

Visualization of the GFP-constructs indicated that the Myo5p neck is essential for Myo5p localization in the presence of the TH1 domain. This result suggested that a molecular mechanism that involves the Myo5p neck might be involved in the release of the inhibitory interaction between the TH1 domain and the C-terminal extension, allowing Vrp1p binding and Myo5p patch recruitment.

Interestingly, it has been demonstrated before that calmodulin dissociation from the neck of mammalian Myo1c promotes association of this short tailed myosin to phopholipids *in vitro*, suggesting that under certain circumstances calmodulin dissociation could contribute to membrane targeting of the unconventional class I myosins (Hirono et al., 2004). Thus, we wondered if calmodulin release from the Myo5p neck could also promote lipid binding through the neck and TH1 domains and concomitantly trigger the dissociation of these domains from the Myo5p C-terminus.

6.1.2.1. Calmodulin dissociation promotes efficient lipid binding of Myo5p

Since the lipid binding properties of the Myo5p neck and TH1 domains have never been investigated we decided to analyze if these domains bind specifically to certain lipids and if this interaction can be modulated by Cmd1p dissociation. Unfortunately, the lipid binding properties of the TH1 domain or the neck alone could not be analyzed, since tagged constructs bearing these domains were not expressed in sufficient amounts in yeast or bacteria. Thus, we purified a Protein A-tagged fragment bearing the neck and TH1 domains together (ProtA-nT) or the Myo5p C-terminus (ProtA-C, as negative control) from yeast, and we overlayed lipid-strips bearing spots of different phospholipids with the proteins. As expected, only ProtA-nT, but not ProtA-C could bind to acidic phospholipids (figure 9A). ProtA-nT was interacting to a much stronger extent with phosphatidic acid and

especially with PI(4,5)P2 and PI(3,5)P2 than with the other phospholipids. Remarkably, some lipids bearing the same or even more negative charge than PI(4,5)P2 and PI(3,5)P2 bound much less ProtA-nT. This suggests that Myo5p lipid binding is not merely mediated by electrostatic interactions.

Consistent with the results described for the mammalian Myo1c, we also found that the nTH1 phopholipid binding was clearly enhanced by calmodulin dissociation. It has been shown that 5 mM Ca^{2+} induces Cmd1p dissociation from Myo5p (Geli et al., 1998). When we added 5 mM $CaCl_2$ to the lipid binding assay the interaction of the ProtA-nT construct with acidic lipids was clearly enhanced (figure 9A). The addition of 5 mM $MgCl_2$ did not have this effect (data not shown). The association of ProtA-nT with phosphatidic acid seemed to be most strikingly influenced by the addition of calcium.

Next, we also checked the effect of adding recombinant purified Cmd1p to Cmd1p-stripped ProtA-nT in the absence of Ca^{2+}. As shown in figure 9B, the addition of Cmd1p clearly diminished binding of the Myo5p fragment to the acidic lipids.

These results strongly suggest that calmodulin dissociation from the Myo5p neck domain promotes phospholipid binding of Myo5p.

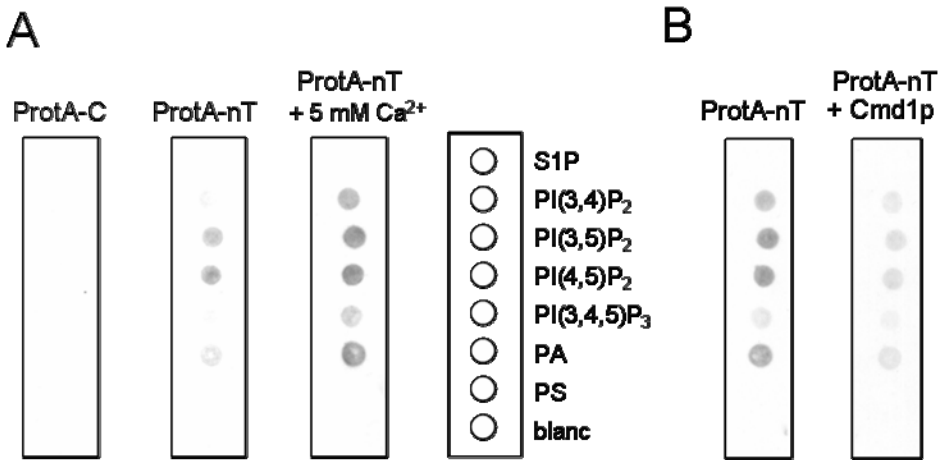

Figure 9. Calmodulin dissociation from a Myo5p fragment bearing the neck and TH1 domains promotes phospholipid binding *in vitro.* A. Commercially available PIP strips (Echelon) bearing dot spots of immobilized sphingosine-1-phosphate (S1P), the indicated phosphoinositides (PI(3,4)P2; PI(3,5)P2; PI(4,5)P2; PI(3,4,5)P3)), phosphatidic acid (PA) and phosphatidyl serine (PS) overlaid with 0.5 nM of Protein A-tagged Myo5p fragments bearing either the neck and TH1 domains (ProtA-nT) or the C-terminal portion containing the GPA, SH3 and the acidic domains (ProtA-C). The constructs were purified from yeast in the absence of Ca^{2+} to preserve calmodulin binding to the Myo5p neck and the incubation was performed either in the absence or in the presence of 5 mM Ca^{2+}. PAP was used to detect the ProtA fusion proteins. **B.** PIP strips overlaid with 0.5 nM of the ProtA-nT construct purified from yeast in the presence of Ca^{2+} to dissociate calmodulin from the Myo5p neck. Overlay assays were performed in the absence of Ca^{2+} and in the absence or in the presence (+ Cmd1p) of 14 nM calmodulin. PAP was used to detect the Protein A-tagged constructs.

6.1.2.2. Cmd1p dissociation from the Myo5p neck releases the interaction of the neck and TH1 domains with the Myo5p C-terminus *in vitro*

Next, we wanted to investigate if Cmd1p dissociation can also release the inhibitory interaction in the Myo5p tail. Thus, we analyzed if Cmd1p dissociation affects the *in vitro* interaction between the Myo5p tail domains observed previously (figure 7). As before, a GST-fusion protein bearing the Myo5p C-terminus (GST-C) purified from bacteria was used to pull down a ProtA-construct bearing the neck and TH1 domains (ProtA-nT) purified from yeast. Cmd1p copurified with the ProtA-nT construct.

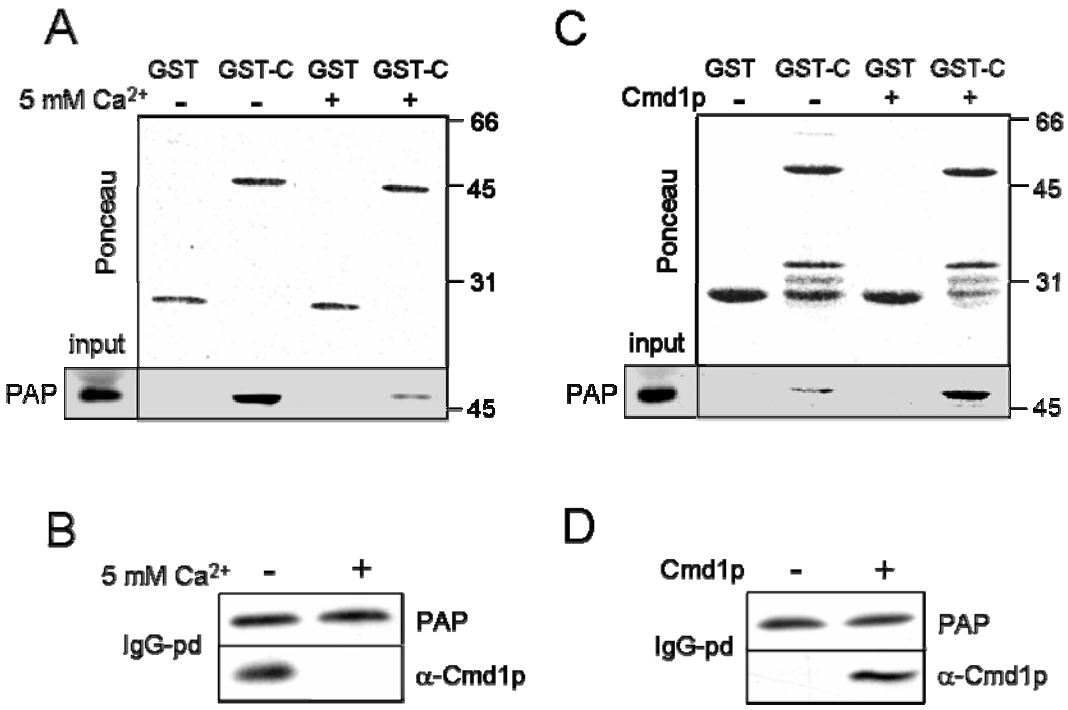

Figure 10. Calmodulin dissociation releases the interaction between a Myo5p fragment containing the neck and TH1 domains and the Myo5p C-terminus. A. Immunoblot (lower panel) of gluthation-Sepharose pull-downs of 3 µg of a recombinant purified C-terminal fragment of Myo5p bearing the GPA, SH3 and acidic domains fused to GST (GST-C) or GST, incubated with 0.01 µg of a Protein A-tagged Myo5p fragment bearing the neck and TH1 domains (ProtA-nT) purified from yeast in the absence of Ca^{2+} to preserve the calmodulin association to the Myo5p neck. Pull downs were performed in the absence (-) or in the presence (+) of 5 mM Ca^{2+}. Ponceau red staining was used to detect the GST and the GST-C proteins (upper panel). PAP was used to decorate the ProtA-nT construct (lower panel). 5 % of the total input and 10 % of the precipitate were loaded. **B.** Immunoblot of IgG-Sepharose pull-downs (IgG-pd) from a *myo5*Δ strain (SCMIG 275) expressing the ProtA-nT construct under the promoter of *MYO5* in the absence (-) or in the presence (+) of 5 mM Ca^{2+} to demonstrate calmodulin dissociation from the Myo5p neck in the presence of calcium. An antibody against Cmd1p (α-Cmd1p) and PAP were used for detection of calmodulin and the Protein A-tagged construct, respectively. **C.** Immunoblot (lower panel) of gluthation-Sepharose pull downs of 3 µg of the recombinant purified C-terminal fragment of Myo5p fused to GST (GST-C) or GST incubated with 0.04 µg of purified calmodulin-free Protein A-tagged Myo5p fragment bearing the neck and TH1 domains (ProtA-nT), in the absence (-) or in the presence (+) of 50 nM calmodulin. Ponceau red staining was used to detect the GST and GST-C proteins (upper panel). PAP was used for detection of ProtA-nT. 5 % of the total input and 10 % of the precipitate were loaded. **D.** Immunoblot of IgG-Sepharose pull-downs (IgG-pd) from a *myo5*Δ strain (SCMIG275) expressing the ProtA-nT construct performed in the presence of 5 mM Ca^{2+} to dissociate calmodulin from the Myo5p neck. The IgG-Sepharose beads were washed in the absence of Ca^{2+} and further incubated in the absence (-) or in the presence (-) of 14 nM calmodulin. Cmd1p and the Protein A-tagged construct were detected as described in B.

Addition of 5 mM $CaCl_2$ (but not addition of 5 mM $MgCl_2$, data not shown) induced dissociation of Cmd1p from the ProtA-nT construct (figure 10B) and triggered the dissociation of the ProtA-nT fusion protein from the Myo5p C-terminus (figure 10A).
Next, the experiment was performed with Cmd1p-stripped ProtA-nT and in the absence of calcium. Recombinant Cmd1p purified from *E. coli* was added to analyze the effect of Cmd1p-binding to the Myo5p neck. As expected, the addition of Cmd1p significantly increased binding of ProtA-nT to GST-C (figure 10C). An IgG pull-down experiment was performed in parallel, demonstrating that the recombinant Cmd1p could efficiently bind to ProtA-nT (figure 10D). Altogether, the results supported the view that the interaction between the neck and TH1 domains and the Myo5p C-terminus is released by dissociation of Cmd1p from the Myo5p neck.

6.1.2.3. Cmd1p dissociation from the Myo5p neck promotes Myo5p binding to Vrp1p

The previous results indicated that Cmd1p dissociation from the Myo5p neck promotes phospholipid binding through the neck and TH1 domains and releases the inhibitory interaction affecting the C-terminal fragment. From our observations we could predict that Cmd1p dissociation promotes binding of Myo5p to Vrp1p. To verify this point, Protein A fusion proteins of full-length Myo5p (ProtA-Myo5p), a Myo5p construct missing the Cmd1p binding sites (ProtA-Myo5ΔIQp) or Myo5p lacking the C-terminus (ProtA-Myo5ΔCp) were coexpressed with Vrp1-HAp in yeast cells. The ProtA-tagged proteins were then precipitated from cell extracts with IgG-Sepharose, in the presence or absence of 5 mM $CaCl_2$. As shown in figure 11A, the addition of calcium strongly reduced Cmd1p binding to Myo5p. Under these conditions, the full length Myo5p precipitated significantly more Vrp1-HAp than in the absence of calcium. In contrast, the interaction of the Myo5p construct missing the Cmd1p binding sites (IQ motifs) was not affected by the addition of calcium, demonstrating that the observed effect was dependent on the Cmd1p association to Myo5p. Further, the detected interactions between Myo5p and Vrp1-HAp in the presence or absence of calcium were both mediated by the C-terminus, since the Myo5p construct missing the C-terminus did not coprecipitate Vrp1-HAp at all in any condition.
To confirm that Cmd1p dissociation from Myo5p promotes the Myo5p-Vrp1p interaction, coimmunoprecipitation experiments were performed with extracts of a *cmd1-226* mutant specifically impaired in the Myo5p-Cmd1p interaction (Geli et al., 1998). As a control, the same experiment was performed with extracts of a calmodulin mutant (*cmd1-231)* in which the interaction between Cmd1p and Myo5p is not affected (Geli et al., 1998).
ProtA-Myo5p and Vrp1-HAp were coexpressed in the *cmd1-226 and cmd1-231* mutants or in a *CMD1* wild-type strain. When precipitating ProtA-Myo5p with IgG-Sepharose from

the cell extracts, significantly more Vrp1-HAp coprecipitated in the *cmd1-226* strain, when compared with the *cmd1-231* mutant or the wild-type strain (figure 11B).

Thus, also this experiment indicates that the dissociation of Cmd1p is a prerequisite for efficient binding of Vrp1p to the Myo5p C-terminus.

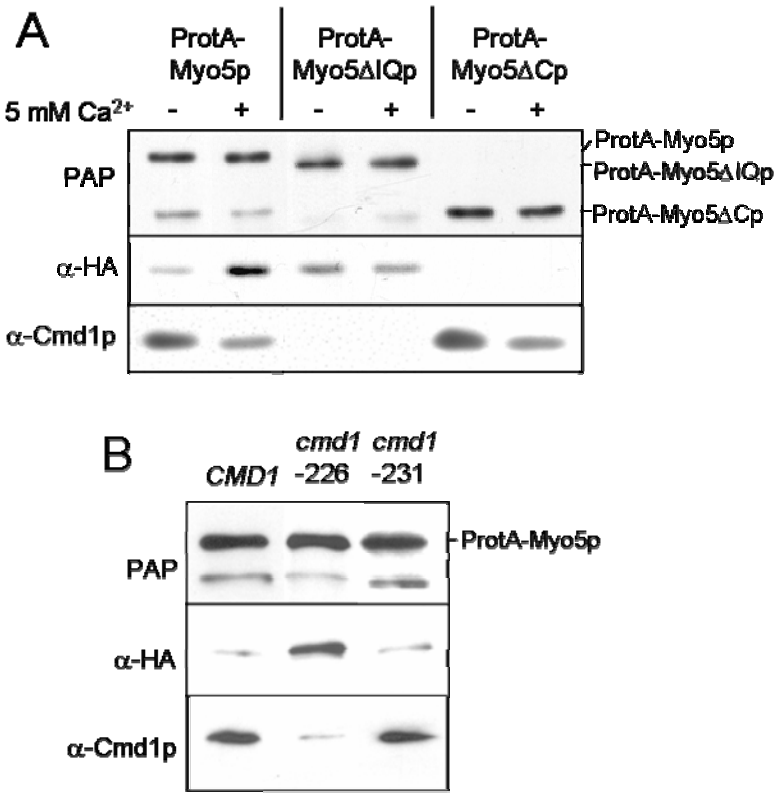

Figure 11. Calmodulin dissociation promotes Myo5p binding to Vrp1p. A. Immunoblots of IgG-Sepharose pull-downs of *myo5Δ vrp1Δ* cells (SCMIG304) expressing Protein A-tagged constructs of full-length Myo5p (ProtA-Myo5p), or mutant Myo5p proteins either lacking the IQ motifs (GFP-Myo5ΔIQp) or the C-terminus including GPA, SH3 and acidic domains (ProtA-Myo5ΔCp) together with HA-tagged verprolin (Vrp1-HAp), all expressed from centromeric plasmids under control of the *MYO5* and VRP1 promoters, respectively. Cells were lysed and proteins were precipitated with IgG-Sepharose in the absence (-) or in the presence (+) of 5 mM Ca^{2+}. Precipitates were analyzed by immunoblot using PAP for detection of the Myo5p constructs, and α-HA or α-Cmd1p antibodies for detection of Vrp1-HAp and Cmd1p, respectively. **B.** Immunoblots of IgG-Sepharose pull-downs from wild-type cells (*CMD1*, SCMIG947) or the temperature sensitive calmodulin mutants *cmd1-226* (SCMIG182) or *cmd1-231* (SCMIG187) expressing Protein A-tagged constructs of full-length Myo5p (ProtA-Myo5p) and HA tagged Verprolin (Vrp1-HAp) from centromeric plasmids under the control of the *MYO5* and *VRP1* promoters, respectively. Cells were lysed and proteins were precipitated with IgG-Sepharose. Precipitated proteins were analyzed by immunoblot, using PAP for detection of the Myo5p constructs and α-HA and α-Cmd1p antibodies for detection of Vrp1-HAp and Cmd1p, respectively. Note that disruption of the Myo5p-Cmd1p interaction by the *cmd1-226* mutation promotes Myo5p association with Vrp1p.

6.1.2.4. At the plasma membrane, Myo5p releases Cmd1p and binds to Vrp1p

If Cmd1p dissociation from the neck domain was required to promote the interaction of Myo5p with plasma membrane phospholipids and with the cortical patch component Vrp1p, one would predict that cytosolic Myo5p should have much more Cmd1p bound than plasma membrane associated Myo5p. Moreover, only the plasma membrane fraction of Myo5p should be able to interact with Vrp1p. To test these predictions, we established a protocol for the purification of highly enriched plasma membrane and cytosolic fractions. After preparing the plasma membrane and cytosolic fractions from yeast expressing ProtA-Myo5p, we subjected them to IgG pull-downs and detected coprecipitating Cmd1p by immunoblot. As shown in figure 12, the plasma membrane associated Myo5p clearly coprecipitated much less Cmd1p than the cytosolic Myo5p. The detected Cmd1p binding to Myo5p was specific, since it disappeared when a ProtA-Myo5p mutant lacking the two Cmd1p-binding sites (ProtA-Myo5ΔIQp) was used instead of the wild-type protein (figure 12).

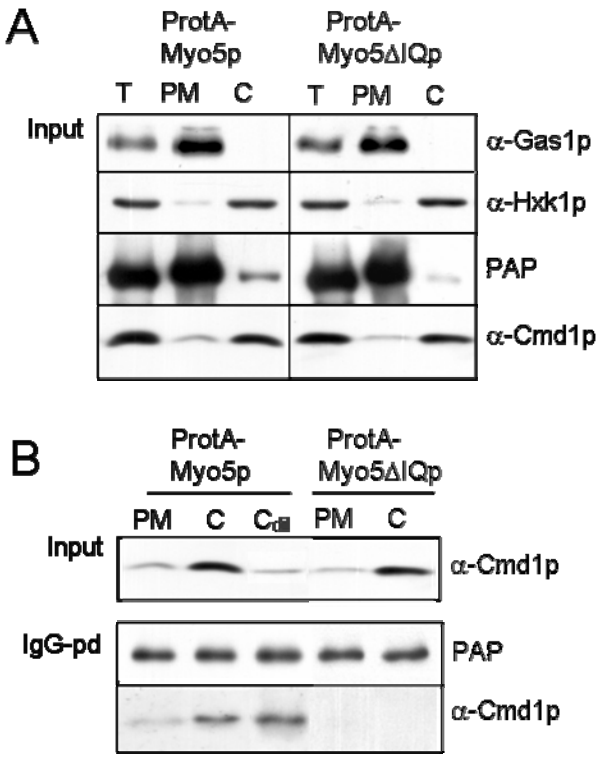

Figure 12. Calmodulin dissociates from Myo5p at the plasma membrane. A. Immunoblot of 10 μg of total yeast protein extract (T) or of yeast plasma membrane (PM) or cytosolic (C) fractions prepared from *myo5*Δ cells (SCMIG275) expressing Protein A-tagged constructs of full-length Myo5p (ProtA-Myo5p) or a mutant Myo5p lacking the IQ motifs (GFP-Myo5ΔIQp) from centromeric plasmids under the control of the *MYO5* promoter. Nitrocellulose membranes were decorated with antibodies against the plasma membrane marker Gas1p (α-Gas1p), the cytosolic marker hexokinase (α-Hxk1p) or calmodulin (α-Cmd1p). PAP was used for detection of the ProtA-Myo5p constructs. **B.** Immunoblots of IgG pull-downs (IgG-pd) from yeast plasma membrane (PM) and cytosolic (C) fractions of the strains described in A. ProtA-Myo5p constructs and calmodulin were detected as described in A. 10% of the total inputs was loaded to control the calmodulin concentration in the pull-down mixture. Diluting the cytosolic fraction 1 to 10 (C_{dil}) did not alter the result.

Since the cytosolic fraction used for the pull-down experiments had a much higher concentration of Cmd1p than the plasma membrane fraction (figure 12A), we had to rule out that the different amounts of coprecipitating Cmd1p only reflected the differences in the Cmd1p concentration in the reaction mixtures. For this purpose, the cytosol preparation was diluted (1:10) until the Cmd1p concentration was similar to that in the plasma membrane fraction and ProtA-Myo5p was pulled down with IgG-sepharose as before. As shown in figure 12B, ProtA-Myo5p of non-diluted or diluted cytosol coprecipitated the same amount of Cmd1p, and strikingly more than ProtA-Myo5p from the plasma membrane. Thus, in our experiments the Myo5p pool associated with the plasma membrane had less Cmd1p bound than the cytosolic Myo5p.

To check the hypothesis that only plasma membrane associated Myo5p binds to Vrp1p, coimmunoprecipitation experiments were performed with plasma membrane and cytosolic fractions prepared from yeast expressing ProtA-Myo5p and HA-tagged Vrp1p (Vrp1-HAp). ProtA-Myo5p was precipitated with IgG-Sepharose and copurifying Vrp1p-HA was detected by immunoblot. As shown in figure 13, the plasma membrane associated Myo5p clearly coprecipitated much more Vrp1-HAp than the cytosolic Myo5p. To demonstrate the specificity of the interaction, the same experiment was performed with a ProtA-Myo5p construct missing the C-terminus (ProtA-Myo5ΔCp), a protein which does not interact with Vrp1p. ProtA-Myo5ΔCp did not pull down significant amounts of Vrp1-HAp (figure 13).

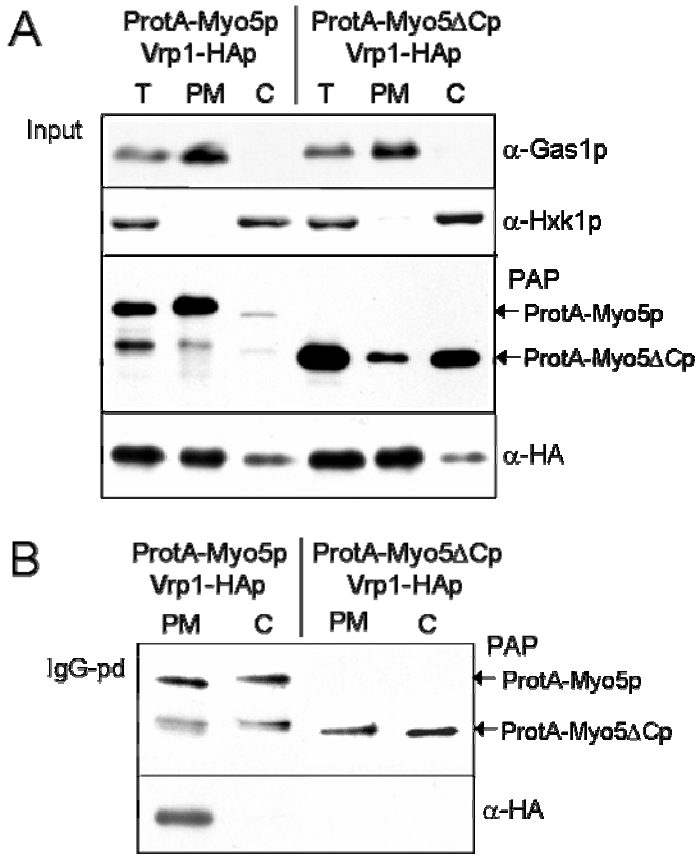

Figure 13. Myo5p interacts with Vrp1p mostly at the plasma membrane. Immunoblot of 10 μg of protein from a total yeast extract (T) or of yeast plasma membrane (PM) or cytosolic (C) fractions prepared from *myo5Δ vrp1Δ* strains (SCMIG304) expressing Protein A-tagged constructs of full-length Myo5p (ProtA-Myo5p) or a mutant Myo5p missing the C-terminus including GPA, SH3 and acidic domains, (ProtA-Myo5ΔCp) together with HA-tagged verprolin (Vrp1-HAp), all expressed from centromeric plasmids under control of the *MYO5* and *VRP1* promoters, respectively. Nitrocellulose membranes were decorated with antibodies against the plasma membrane marker Gas1p (α-Gas1p) and the cytosolic marker hexokinase (α-Hxk1p). Vrp1-HAp was detected with an α-HA antibody and PAP was used for detection of the ProtA-Myo5p constructs. **B.** Immunoblots of IgG pull-downs (IgG-pd) from yeast plasma membrane (PM) and cytosolic (C) fractions from the strains described in A. ProtA-Myo5p constructs and Vrp1-HAp were detected as described before.

6.1.2.5. No evidence for homo-oligomerization of the cytosolic or plasma membrane associated Myo5p

Cryo-electron microscopy studies have indicated an extended intramolecular interaction between the TH1 domain and the C-terminal extension of the *Acanthamoeba* myosin-IB (Jontes et al., 1998). This observation and our previous results suggest a model for the regulated recruitment of Myo5p to cortical endocytic patches. Cytosolic Myo5p in complex with calmodulin might exhibit a "closed" conformation, in which the TH1 domain interacts with the Myo5p C-terminus and prevents binding with other cortical patch components, which are also present in the cytosol. Only at the plasma membrane, an unknown signal might induce Cmd1p dissociation from Myo5p, thus promoting phospholipid and Vrp1p binding. However, with the experiments performed, we did not investigate if an intermolecular interaction between the TH1 and the C-terminal extension of cytosolic Myo5p could account for the observed inhibition of the interaction with Vrp1p.

To investigate if oligomerization of Myo5p might occur, cytosol and plasma membrane fractions were purified from yeast expressing myc-tagged Myo5p (myc-Myo5p) and Myo5p bearing an HA-tag (Myo5-HAp), and myc-Myo5p was precipitated with α–myc agarose beads. As shown in figure 14, no coprecipitating Myo5-HAp could be detected in the immunoprecipitates from the different fractions.

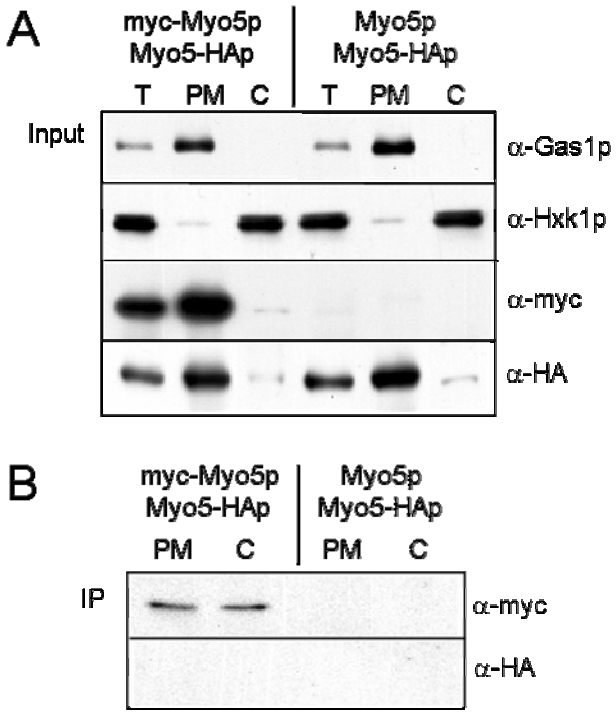

Figure 14. An intermolecular interaction of Myo5p molecules cannot be detected in plasma membrane or cytosolic fractions. Immunoblot of 10 μg of a total protein yeast extract (T) or of yeast plasma membrane (PM) or cytosolic (C) fractions prepared from *myo5*Δ strains (SCMIG275) expressing myc-tagged Myo5p (myc-Myo5p) or wild-type Myo5p (Myo5p) together with HA-tagged Myo5p (Myo5-HAp), all from centromeric plasmids under the control of the *MYO5* promoter. Nitrocellulose membranes were decorated with antibodies against the plasma membrane marker Gas1p (α-Gas1p) and the cytosolic marker hexokinase (α-Hxk1p). Myc-Myo5p and Myo5-HAp were detected with α-myc or α-HA antibodies, respectively. **B.** Immunoblots of immunoprecipitations (IP) with anti-myc agarose beads from yeast plasma membrane (PM) and cytosolic (C) fractions of the strains described in A. Myc-Myo5p and Myo5-HAp were detected as described in A.

6.1.2.6. Cmd1p binding to Myo5p influences the average lifespan of Myo5p at cortical patches *in vivo*

Recently, real-time fluorescence microscopy has allowed measuring the life time of different endocytic proteins at the cortical patches. Since our model predicted that Cmd1p regulates patch recruitment of Myo5p, we decided to analyze *in vivo* if Cmd1p binding influences the life time of Myo5p at the cortical patches. GFP-Myo5p was expressed in a yeast strain bearing a *cmd1* mutation (*cmd1-226*) which has been shown to specifically impair the interaction of Cmd1p with Myo5p. In collaboration with the laboratory of Prof. Sandra K. Lemmon (University of Miami), the lifetime of GFP-Myo5p patches was analyzed in wild type and mutant cells. As shown in figure 15, the *cmd1* mutant exhibited more GFP-Myo5p patches at the plasma membrane than wild-type cells. Moreover, the Myo5p patches in the *cmd1-226* mutant had an average life span which was extended for about 4 seconds when compared with the patches of the wild-type cell. These observations support the view that Cmd1p dissociation from Myo5p promotes its association with the cortical patch.

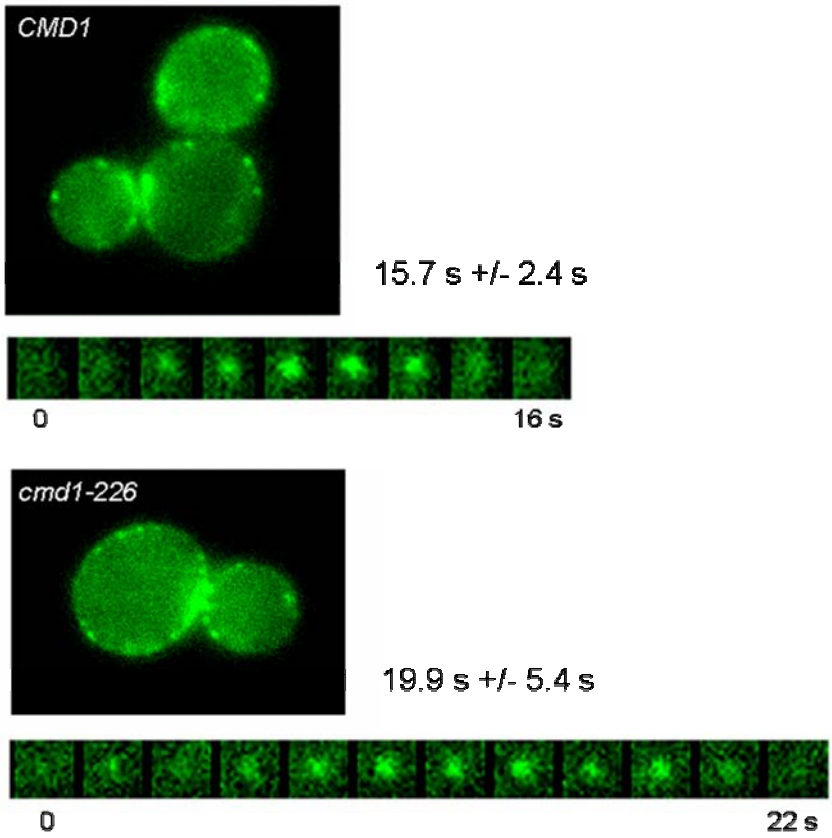

Figure 15. GFP-Myo5p cortical patches exhibit a prolonged lifespan in a yeast strain specifically impaired in the Myo5p-Cmd1p interaction. Time lapse fluorescence microscopy of live *CMD1* wild-type (SCMIG947) or *cmd1-226* mutant (SCMIG182) cells expressing GFP-tagged Myo5p (GFP-Myo5p) from a centromeric plasmid under the control of the *MYO5* promoter. For each strain a representative cell and the time series of an invidual patch from a time lapse movie is shown. Cells were grown to mid-log phase, incubated at 37°C and images were taken every 2 seconds. Values indicate the average lifespan of GFP-Myo5p patches in the yeast strains, which was estimated from 30 independent GFP-Myo5p cortical patches.

6.2. Screening for factors *in trans* involved in Myo5p localization

The results presented so far strongly indicated that Cmd1p regulates Myo5p recruitment to the cortical patch via the C-terminal domain and phospholipid association of Myo5p via the TH1 domain and possibly the neck. However, the signal triggering Cmd1p release from the Myo5p neck at the plasma membrane was not identified. Also, depletion of cellular Vrp1p only causes a partial defect in Myo5p recruitment to the cortical patches (Kaksonen et al., 2003; Kaksonen et al., 2005; Sun et al., 2006), suggesting that other proteins might also interact with the Myo5p C-terminus and contribute to the recruitment of the myosin. In order to look for more factors *in trans* involved in Myo5p localization, we followed two different strategies: a visual screening for localization defects of GFP-Myo5p in yeast mutants and a genetic screening based on the Plasma Membrane Recruitment System (a system that Helga Grötsch started to establish during her diploma thesis).

6.2.1. Visual screening for factors *in trans* required for Myo5p localization

6.2.1.1. Las17p might share a redundant function with Vrp1p in Myo5p patch recruitment

In order to look for mutants with a defect in Myo5p localization, GFP-Myo5p under the control of the Myo5p promoter was expressed in different mutant strains. Mutants deficient in several endocytic patch components were analyzed (figure 16A). Although "early patch components" would most likely affect Myo5p recruitment, we also checked mutants defective in "late components" of the endocytic patch, since such proteins could participate in earlier processes before accumulating at the patch for a later function.

As previouslly explained, the endocytic patch components can be grouped into 4 different protein modules, depending on their time of recruitment and motile behaviour at the endocytic site (see introduction and table I for a short description of the function of the endocytic proteins). Concerning the coat module, we analyzed *chc1*Δ, *pan1-4*, *sla1*Δ, *sla2*Δ and *end3*Δ mutants. Moreover, GFP-Myo5p was expressed in an *ent1-UIM*Δ *ent2*Δ *ede1*Δ strain (*uim*Δ). Ent1p, Ent2p and Ede1p are considered to be endocytic adaptors for ubiquitinated cargo and it has been shown that Ede1p arrives very early during the formation of the endocytic patch (Shih et al., 2002; Toshima et al., 2006b).

GFP-Myo5p localization was also observed in *bbc1*Δ, *las17*Δ and *vrp1*Δ mutants affecting proteins of the Las17p/Myo5p module and in *abp1*Δ, *arp2-2* and *sac6*Δ mutants deficient in proteins of the actin module. Concerning the amphiphysin protein module, we analyzed an *rvs167* knockout strain that has been shown to be also defective in Rvs161p expression (Lombardi and Riezman, 2001).

All knockout strains and mutants missing essential parts of endocytic proteins (*pan1-4*, *uim*Δ) were observed at room temperature. The temperature sensitive *arp2-2* strain was analyzed additionally after incubation at 37°C for 30 min.

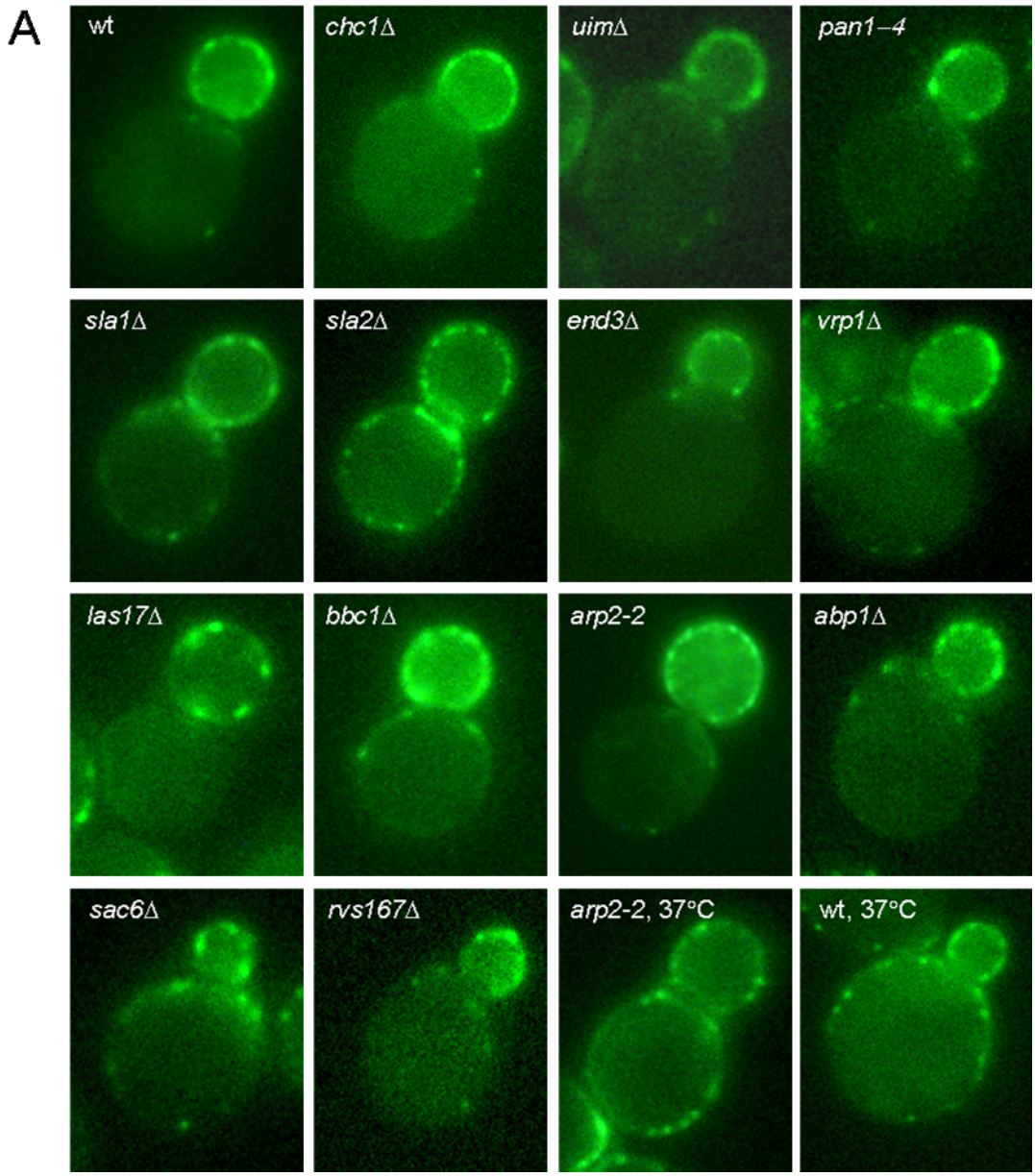

Figure 16A. GFP-Myo5p localization in yeast mutants affecting the coat, Las17p/Myo5p, amphiphysin and actin modules. Representative fluorescence micrographs of wild-type cells (SCMIG19; wt) and different yeast mutants affecting the endocytic coat (*chc1*Δ (SCMIG754), *chc1*Δ (SCMIG754), *ent1*Δ *ent2*Δ *ede1*Δ *pent1-UIM*Δ (=*uim*Δ; SCMIG806), *pan1-4* (SCMIG392), *sla1*Δ (SCMIG391), *sla2*Δ (SCMIG669), *end3*Δ (SCMIG55)), the Las17p/Myo5p module (*vrp1*Δ (SCMIG57), *las17*Δ (SCMIG273), *bbc1*Δ (SCMIG553)), the amphiphysin module (*rvs167*Δ (SCMIG59)) and the actin module (*arp2-2*Δ (SCMIG229), *abp1*Δ (SCMIG458)) expressing GFP-tagged Myo5p from pGFP-*MYO5* under the control of the *MYO5* promoter. Cells were grown to mid-log phase at 25°C and directly observed by conventional fluorescence microscopy. The temperature-sensitive *arp2-2* mutant (SCMIG229) and a wild-type strain (wt, SCMIG19) expressing GFP-Myo5p were also observed after a shift to 37°C for 30 min (30' 37°C). Note that GFP-Myo5p appears mislocalized in the *las17*Δ mutant

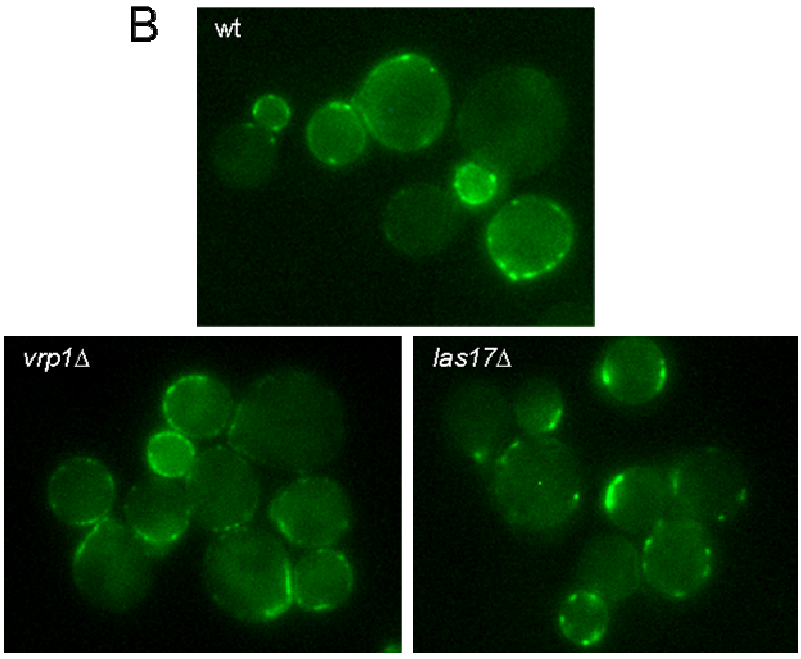

Figure 16B. GFP-Myo5p localization in a wild-type strain, a *vrp1*Δ mutant and a *las17*Δ mutant. Fluorescence micrographs of wild-type cells (SCMIG19; wt), *vrp1*Δ (SCMIG57) or *las17*Δ (SCMIG273) mutants expressing GFP-Myo5p under the control of the Myo5p promoter. Note that GFP-Myo5p appears mislocalized in the *las17*Δ mutant.

After repetitive visualization of GFP-Myo5p in the different mutants, comparing with the phenotype of a wild-type strain, we concluded that only the *las17*Δ strain was showing a clear defect in GFP-Myo5p localization (see figure 16B). We could observe abnormal big patches that accumulated at certain sites in the cell.

Surprisingly, in contrast to other authors, we did not detect a clear delocalization of GFP-Myo5p in the *vrp1*Δ strain (figure 16B). Sun et al. have observed that a *vrp1*Δ strain exhibits strongly enhanced cytosolic localization of Myo5-GFPp (Sun et al., 2006). In our strain we could not detect this phenotype; just the cortical patches appeared slightly smaller than in the wild-type strain. The variation of Myo5p localization in the different *vrp1*Δ strains might be due to the different genomic backgrounds of the strains and/or differences in the expression of the GFP-tagged Myo5p constructs.

Las17p is known to be required for Vrp1p localization and it has also been shown to bind to the SH3 domain of Myo5p independent of Vrp1p (Duncan et al., 2001; Evangelista et al., 2000; Geli et al., 2000b; Lechler et al., 2000; Madania et al., 1999). Thus, it already has been suggested that Las17p might share a redundant function with Vrp1p in Myo5p recruitment. Our results support this idea.

6.2.1.2. PI(4,5)P2 might be involved in Myo5p recruitment to the plasma membrane

So far, we analyzed mutants that affect proteins directly participating in endocytic vesicle formation. Next, we observed the localization of GFP-Myo5p in different mutants affecting the synthesis (*erg2*Δ, *mss4-2*) or the turnover (*sjl1*Δ *sjl2*Δ) of lipids which have been implicated in endocytosis, namely, PI(4,5)P2 and the yeast cholesterol analog ergosterol.
Erg2p is an enzyme participating in the synthesis of ergosterol, the main sterol of yeast (Pichler and Riezman, 2004). Mss4p is the phosphatidylinositol-4-phosphate-5-kinase that converts PI(4)P into PI(4,5)P2 (Desrivieres et al., 1998). The synapatojanins Sjl1p and Sjl2p catalyze the opposite reaction. They are phosphatidylinositol-bisphosphate-5-phosphatases, required for the dephosphorylation of PI(4,5)P2 to PI(4)P (Singer-Kruger et al., 1998). The *erg2*Δ and *sjl1*Δ *sjl2*Δ mutants have been shown to be defective in receptor-mediated endocytosis (Munn et al., 1999; Singer-Kruger et al., 1998).
First, we analyzed the localization of GFP-Myo5p in the knockout strains (*erg2*Δ and *sjl1*Δ *sjl2*Δ) at room temperature (figure 17A, B). The *erg2*Δ mutant showed the same phenotype as a wild-type strain, but the *sjl1*Δ *sjl2*Δ cells exhibited abnormal GFP-Myo5p localization with fuzzy cortical patches, enhanced cytosolic expression and abnormal intracellular structures bearing GFP-Myo5p. This phenotype of the *sjl1*Δ *sjl2*Δ mutant was clearly pronounced after incubation at 37°C for 30 minutes (figure 17B), a treatment which is known to increase PI(4,5)P2 production in yeast (Desrivieres et al., 1998).
In order to check if the *sjl1*Δ *sjl2*Δ mutation was specifically affecting Myo5p localization, we also expressed GFP-Abp1p (under control of the *ABP1* promoter) in the *sjl1*Δ *sjl2*Δ mutant. Similar to GFP-Myo5p, GFP-Abp1p appeared mislocalized at room temperature and even stronger after incubation at 37°C for 30 minutes (figure 17B). When compared with the wild-type, the cytosolic expression of GFP-Abp1p was clearly enhanced in the *sjl1*Δ *sjl2*Δ strain. Moreover, the Abp1p-patches appeared fuzzy and were not restricted to the cell cortex. Thus, Myo5p is not the only delocalized patch component in the *sjl1*Δ *sjl2*Δ strain.

The temperature sensitive *mss4-2* mutant was also observed at room temperature and after incubation at 37°C for 30 minutes. Moreover, since it has been described for the *mss4*-2 strain that the concentration of PI(4,5)P2 changes more dramatically after longer exposure to 37°C, we also observed this mutant after 2 hours at restrictive temperature.
The *mss4-2* strain, which was compared with its specific wild-type strain (*MSS4*), was undistinguishable from the wild-type at room temperature and after 30 min at 37°C (see figure 17C).

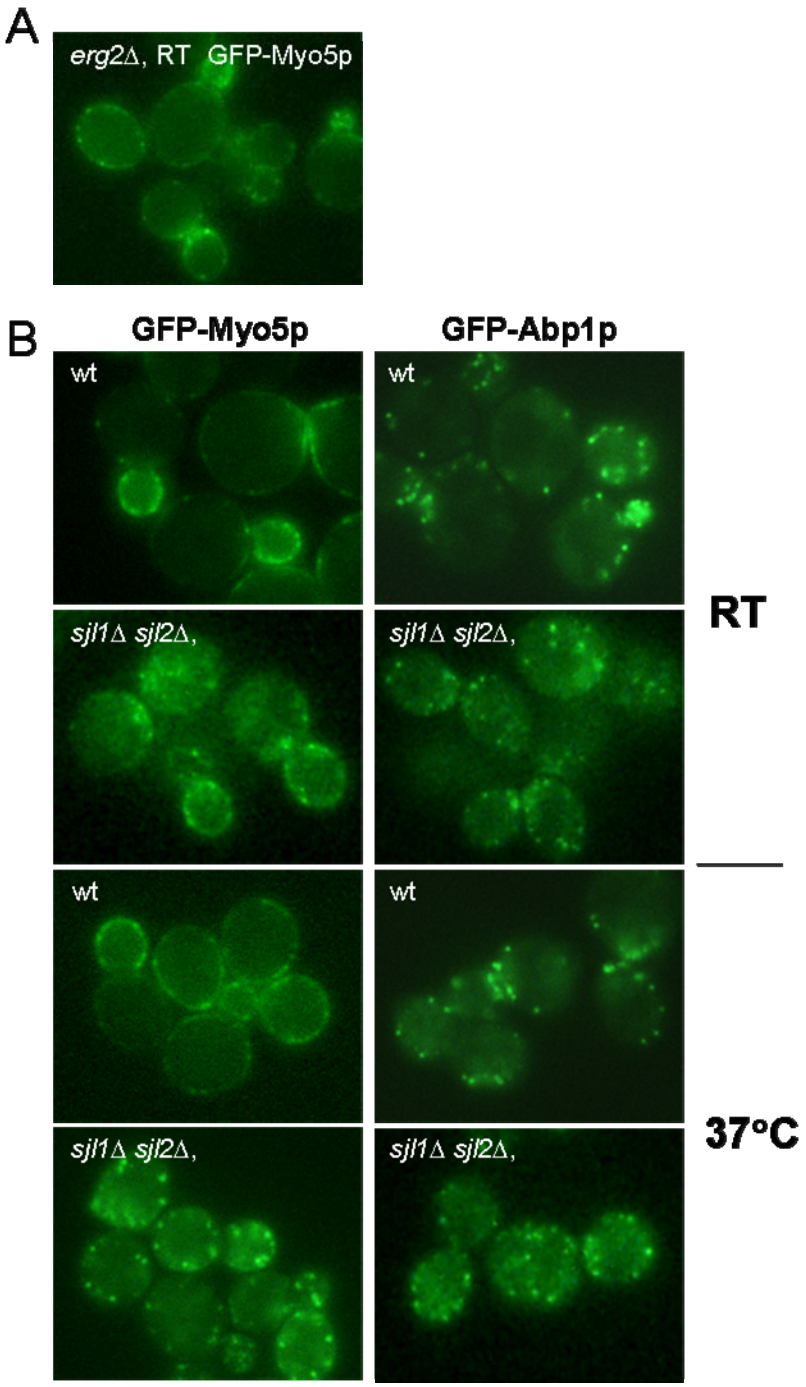

Figure 17. GFP-Myo5p localization in yeast mutants affecting the synthesis and turnover of lipids with a relevant endocytic function A. Fluorescence micrographs of an *erg2*Δ mutant (SCMIG61) defective in the synthesis of ergosterol expressing GFP-tagged Myo5p from plasmid pGFP-*MYO5* under the control of the *MYO5* promoter. Cells were grown to mid-log phase at 25°C and directly observed by conventional fluorescence microscopy. **B.** Fluorescence micrographs of a wild-type strain (SCMIG19; wt) or a *sjl1*Δ *sjl2*Δ mutant (SCMIG958) defective in the PI(4,5)P2 hydrolysis, expressing GFP-fusion constructs of Myo5p or Abp1p from centromeric plasmids under the control of the *MYO5 or ABP1* promoter, respectively. Cells were grown to mid-log phase at 25°C and visualized with a conventional fluorescence microscope, either directly (RT) or after a shift to 37°C for 30 min before visualization (37°C) to enhance the PI(4,5)P2 production.

However, after 2 hours at 37°C, a treatment that is known to deplete almost completely PI(4,5)P2 from the *mss4-2* strain (Desrivieres et al., 1998), GFP-Myo5p looked clearly mislocalized in the *mss4*-2 mutant when compared with the isogenic wild-type. GFP-Myo5p appeared strongly localized to the cytosol, but cortical patches disappeared nearly totally. This phenotype could also be an indirect defect due to the general sickness of the strain after long exposure at 37°C. Therefore, we also expressed GFP-tagged Abp1p in the *mss4-2* mutant and wild-type strain. After 2 hours at 37°C, GFP-Abp1p appeared equally localized in both strains (figure 17C).

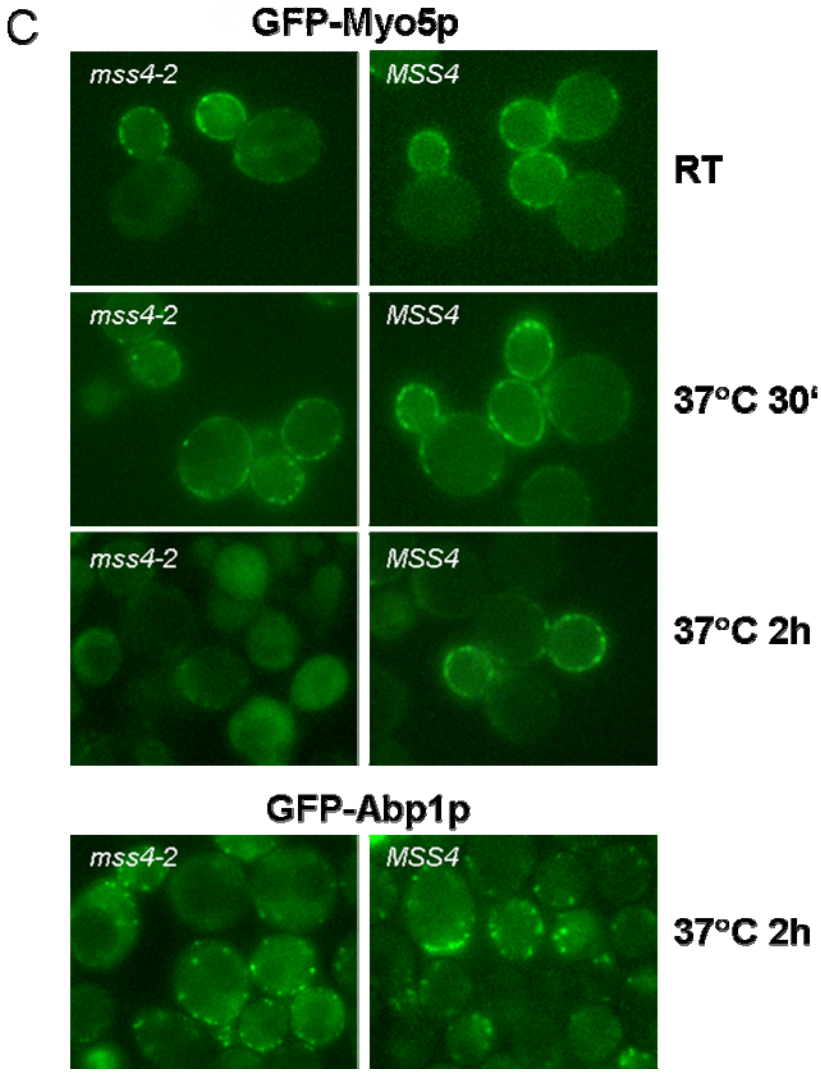

Figure 17C. GFP-Myo5p localization in wild-type and *mss4-2* cells. Fluorescence micrographs of a *MSS4* wild-type strain (SCMIG 729) or a *mss4-2* mutant (SCMIG730) expressing GFP-tagged Myo5p or Abp1p from centromeric plasmids under the control of the *MYO5* or *ABP1* promoter, respectively. Cells were grown to mid-log phase at 25°C and either directly visualized (RT) or shifted to 37°C for 30 min (37°C 30') or 2 h (37°C 2h) before visualization with a conventional fluorescence microscope.

We could see abnormal GFP-Myo5p localization in 2 different strains affecting PI(4,5)P2 (*sjl1*Δ *sjl2*Δ and *mss4-2*). The observation that the *sjl1*Δ *sjl2*Δ mutant is also defective in the localization of the patch component Abp1p does not exclude that PI(4,5)P2 is involved in Myo5p localization. Several endocytic patch proteins can interact with PI(4,5)P2 (see table I) and their mislocalization could indirectly effect the recruitment of the later patch component Abp1p. Since the mislocalization of GFP-Myo5p in the *mss4-2* strain appeared more specific and in previous experiments we had observed *in vitro* binding of Myo5p domains to PI(4,5)P2 (see section 6.1.2.1), an involvement of this specific lipid in Myo5p recruitment seems likely. Future experiments will further analyze the role of PI(4,5)P2 in Myo5p localization.

6.2.2. The Plasma Membrane Recruitment System (PRS): a reporter system to investigate the close association of proteins with the plasma membrane *in vivo*

For the genetic analysis of the Myo5p localization at the plasma membrane we established a reporter system that we called Plasma membrane Recruitment System (PRS). This work was started during the diploma thesis of Helga Grötsch.

The PRS is based on the observation that the human protein Sos (a guanyl nucleotide exchange factor (GEF) of Ras) can bypass the requirement for a functional Cdc25p (the yeast GEF of Ras) in *S.cerevisiae*, only when it is closely associated with the plasma membrane (Broder et al., 1998). We reasoned that a truncated form of human Sos (5'Sos) lacking the plasma membrane localization signal could therefore be used as a reporter gene in a *cdc25* temperature sensitive (ts) mutant background, to investigate whether a given protein interacts with the plasma membrane. Expression of a construct of 5'Sos fused to the protein of interest should only rescue the ts growth defect of the *cdc25-2* strain if the protein of interest would localize to the plasma membrane (see figure 18A, B).

Expression of the 5'Sos-fusion protein could be controlled by coexpression of the human protein Rin fused to a myristoylation site (myrRin). The human Rin protein has been observed to interact with 5'Sos (A. Aronheim, personal communication). As a myristoylated protein myrRin is localized to the plasma membrane and recruits any 5'Sos fusion protein expressed in the cell to this membrane. Thus, co-expression of myrRin allows growth of the *cdc25-2* strain at restrictive temperature if any Sos-protein is expressed (A. Aronheim, personal communication) (see figure 18C).

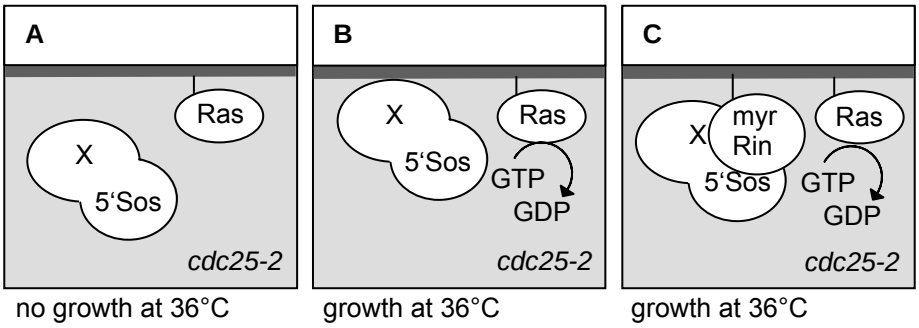

Figure 18. The plasma membrane recruitment system (PRS). A./B. The PRS is based on the observation that human Sos, a GEF for Ras, can rescue a temperature sensitive *cdc25-2* mutant only if Sos is localized to the plasma membrane. A construct of Sos missing its plasma membrane localization signal (5'Sos) can therefore be fused to a protein of interest (X) to monitor plasma membrane localization. Only if the fusion protein 5'Sos-X is localized to the plasma membrane the Ras-pathway can be activated and the cells can grow at restrictive temperature (36°C). **C.** The human protein Rin bearing a myristoylation motif (myrRin) interacts with 5'Sos and recruits it to the plasma membrane. Thus, expression of myrRin will allow growth at restrictive temperature (36°C) if any functional 5'Sos-protein is expressed.

6.2.2.1. The PRS can monitor the plasma membrane localization of Myo5p

In order to investigate whether the PRS could be used to monitor the Myo5p plasma membrane recruitment *in vivo*, the entire coding sequence of *MYO5* was fused to the truncated form of human Sos (5'Sos). The temperature sensitive *cdc25-2* strain (SCMIG271) was transformed with the plasmid encoding the 5'Sos-Myo5p fusion protein (pYX5'SOS-*MYO5*) or with pYX5'SOS encoding 5'Sos alone. Cells were streaked on selective medium containing 2% galactose for the induction of the GAL1-promoter of the constructs and growth was monitored after incubation for 3-4 days at restrictive temperature (36°C).

Cells carrying the plasmid pYX5'SOS-*MYO5* were able to grow at restrictive temperature while cells carrying pYX5'SOS could not grow (figure 19). Coexpression of myrRin rescued the ts growth defect of both strains, indicating that 5'Sos and 5'Sos-Myo5p were expressed.

These results strongly suggested that Myo5p was indeed recruiting the truncated Sos protein to the plasma membrane. However, to rule out that Myo5p overexpression alone or in combination with 5'Sos expression was rescuing the ts phenotype of the *cdc25-2* cells, Myo5p alone or Myo5p and 5'Sos separated on 2 different plasmids were expressed in the *cdc25-2* cells. Cells expressing these proteins were not able to grow at restricitive temperature (figure 19). Overexpression of Myo5p was even blocking growth, since cells that expressed 5'Sos and Myo5p from 2 different plasmids or Myo5p alone could not be rescued by coexpression of myrRin. Thus, the fusion between 5'Sos and Myo5p was necessary for complementation of the *cdc25-2* ts phenotype, suggesting that

Myo5p localization to the plasma membrane recruited 5'Sos and induced activation of the Ras-pathway.

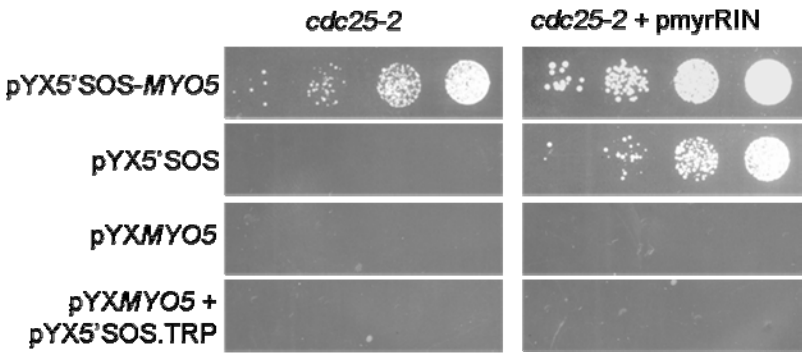

Figure 19. A 5'Sos-Myo5p fusion protein can rescue the temperature sensitive growth defect of a *cdc25-2* strain. Dot spots of *cdc25-2* cells (SCMIG271) bearing plasmids encoding 5'Sos fused to Myo5p (pYX5'SOS-*MYO5*), 5'Sos alone (pYX5'SOS), Myo5p alone (pYX*MYO5*) or 5'Sos and Myo5p on two different plasmids (pYX5'SOS.TRP and pYX*MYO5*), with or without a plasmid encoding myrRin (pmyrRin), all under the control of the GAL1-promoter, were grown on SGC-Leu-Trp-Ura at 36°C for 3-4 days. To allow growth on the selective medium, cells carrying only one or two plasmids were transformed additionally with empty vectors (Ycplac22 and Ycplac33).

6.2.2.2. The PRS monitors close plasma membrane association, but not cortical patch localization of proteins

To further control the applicability of the PRS we also fused the truncated Sos protein to two different yeast proteins which localize to endocytic cortical patches: the yeast epsin Ent1p, a protein which is known to bind to plasma membrane lipids via an ENTH (epsin N-terminal homology) domain (Wendland et al., 1999), and to the yeast actin-binding protein Abp1p, which has no membrane interacting domain but still localizes to cortical patches. As expected, expression of 5'Sos-Ent1p rescued the ts growth defect of the *cdc25-2* strain while expression of 5'Sos-Abp1p did not complement the ts phenotype (see figure 20A). These results strongly support the view that the PRS only monitors close association of proteins to the plasma membrane (most likely, interaction with the lipid bilayer). Since Ent1p and Abp1p both localize to cortical patches (figure 20B), we could rule out that cortical patch localization alone, without membrane binding, would be monitored by our system.

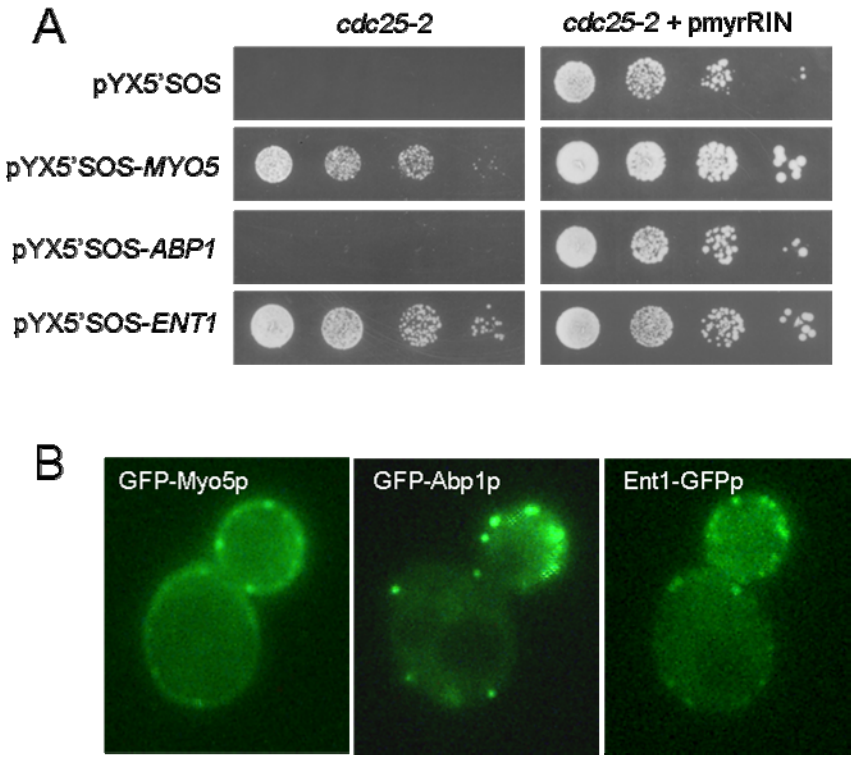

Figure 20. The PRS monitors plasma membrane association but not cortical patch localization of proteins. Dot spots of *cdc25-2* cells (SCMIG271) bearing plasmids encoding 5'Sos alone (pYX5'SOS) or 5'Sos fused to Myo5p (pYX5'SOS-*MYO5*), to Abp1p (pYX5'SOS-*ABP1*) or to Ent1p (pYX5'SOS-*ENT1*), with or without a plasmid encoding myrRin (pmyrRin), all under the control of the GAL1-promoter, were grown on SGC-Leu-Ura at 36°C for 3-4 days. To allow growth on the selective medium, cells carrying only one plasmid were transformed additionally with the empty vector Ycplac33. **B.** Fluorescence micrographs of a *myo5*Δ strain (SCMIG275) expressing GFP-tagged Myo5p (GFP-Myo5p), an *abp1*Δ strain (SCMIG458) expressing GFP-tagged Abp1p (GFP-Abp1p) or an *ent1*Δ strain (SCMIG459) expressing GFP-tagged Ent1p, all from centromeric plasmids under the control of their own promoters. Cells were grown to mid-log phase at 25°C and directly observed by conventional fluorescence microscopy.

6.2.2.3. The Myo5p domains mediating lipid binding (the neck and TH1 domains) allow growth of the 5'Sos fusion construct in the PRS.

The results described before indicated that the PRS can be used to monitor close interaction of Myo5p with the plasma membrane (probably with the phospholipid bilayer). From previous experiments and the available literature we knew that the neck and TH1 domains participate in association of Myo5p to the lipid bilayer. Thus, we predicted that these domians would allow growth of 5'Sos constructs in the PRS. To test this hypothesis several constructs of Myo5p with truncations at the N- or the C-terminus were fused to 5'Sos and expressed in the *cdc25-2* strain. As before, growth of the cells was monitored after incubation for 3-4 days at restrictive temperature and expression of the constructs was controlled by coexpression of myrRin.

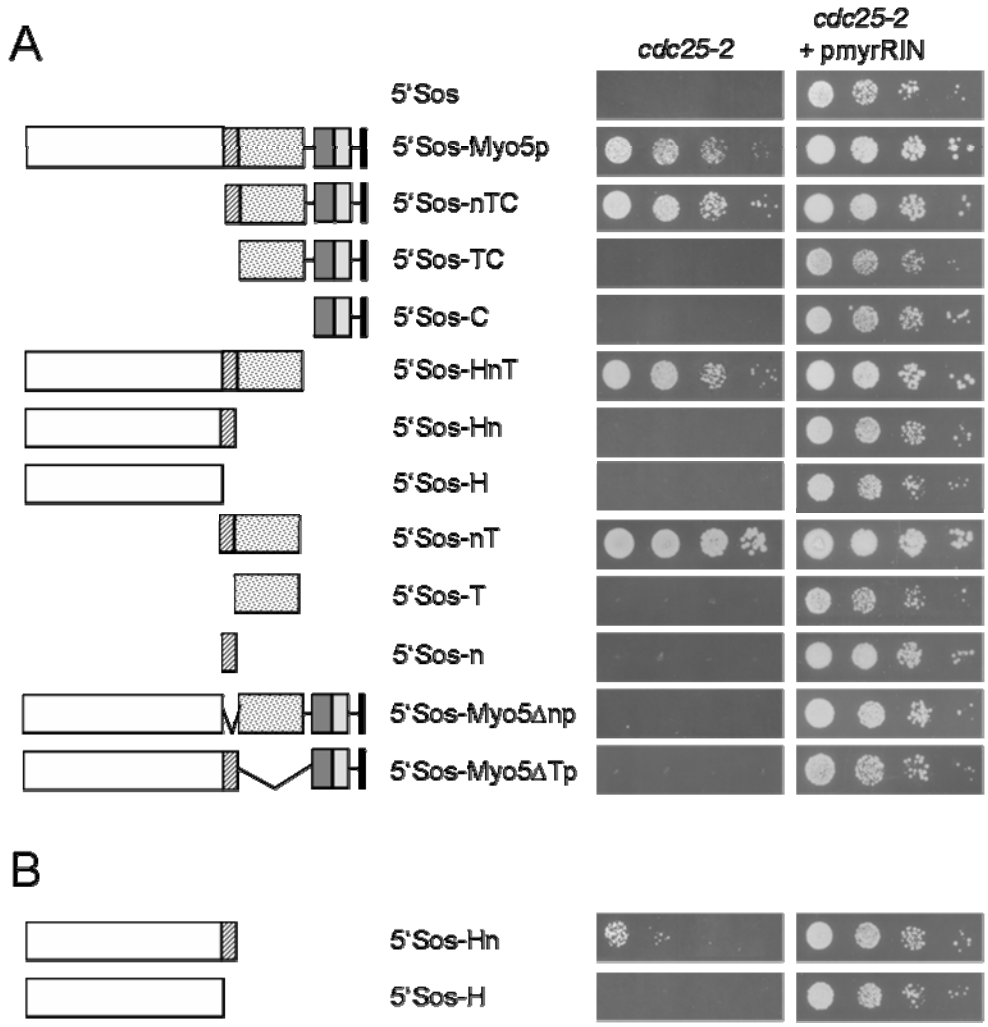

Figure 21. The neck and TH1 domain of Myo5p are necessary and sufficient to allow growth of a 5'Sos fusion construct in the PRS. Dot spots of *cdc25-2* cells (SCMIG271) bearing plasmids encoding 5'Sos alone (pYX5'SOS) or the represented 5'Sos-fusion constructs of Myo5p, with or without a plasmid encoding myrRin expression (pmyrRin), all under the control of the GAL1-promoter, were grown on SGC-Leu-Ura at 36°C for 3-4 days (**A**) or for 10 days (**B**). To allow growth on the selective medium, cells carrying only one plasmid were transformed additionally with the empty vector Ycplac33.

Expression of the Myo5p C-terminus which we had previously identified as sufficient for Myo5p patch localization was not rescuing growth of the *cdc25-2* cells at high temperature, indicating once again that the PRS does not monitor patch association.

Generally, constructs missing either the neck or the TH1 domain of Myo5p could not rescue the ts growth defect of the *cdc25-2* mutant (figure 21A), suggesting that both domains are required for Myo5p plasma membrane recruitment.

To further analyze the implication of the neck and TH1 domain in the plasma membrane recruitment of Myo5p, both domains together, the neck alone or the TH1 domain alone were fused to 5'Sos and analyzed for complementation of the *cdc25-2* ts growth defect. Also, Myo5p-constructs missing only one domain, either the neck or the TH1 domain,

were analyzed. While 5'Sos-fusions of the single domains or 5'Sos-Myo5p constructs missing single domains could not rescue growth at restrictive temperature, the construct bearing the neck and TH1 domains together allowed growth at 36°C.

The data indicated that the neck and the TH1 domains together are required to achieve a strong association of Myo5p with the phospholipid bilayer. The observations are in agreement with the knowledge about other class I myosins, since both domains have been implicated in membrane binding (see introduction, section 4.1.2.1.).

Nevertheless, it should be mentioned that when incubating the cells for a much longer time period (up to 10 days) at restrictive temperature, some growth for the 5'Sos-construct bearing the head and the neck domains could be observed, whereas no growth could be observed for a construct bearing the head alone (figure 21B). Thus, the neck alone could perhaps mediate some plasma membrane interaction, although with much less affinity than the neck and TH1 together. However, it has to be taken into account that differences in expression of the constructs are not tightly controlled in this assay. Coexpression of myrRin allows a qualitative, but not an exact quantitative control of expression.

6.2.2.4. A genetic screen to search for factors *in trans* required for neck and TH1 domain-mediated Myo5p recruitment to the plasma membrane.

The Plasma Membrane Recruitment System (PRS) was developed to design a genetic screen based on the system to look for factors *in trans* involved in Myo5p plasma membrane localization. Since the previous results indicated that the PRS monitors close plasma membrane association of Myo5p via the neck and TH1 domain, such a screen would in theory allow the identification of the enzymes that produce the physiological phospholipid that binds to the TH1 domain in vivo. Also, the screen might lead to the identification of a signal which causes dissociation of Cmd1p from the neck.

As described before, the temperature sensitive *cdc25-2* strain could grow at restrictive temperature if a construct of human 5'Sos fused to Myo5p was expressed (see section 6.2.2.1.). Since Myo5p was able to bring 5'Sos to the plasma membrane, we supposed that a mutation affecting an essential factor for Myo5p cortical recruitment would prevent this growth of the *cdc25-2* strain (see figure 22A, B). Growth of the mutant in the presence of myrRin would be a control for the specificity of the mutation on the Myo5p recruitment, since it would discard mutations affecting the Sos construct, the reporter system (the Ras-pathway) or essential genes (see figure 22C).

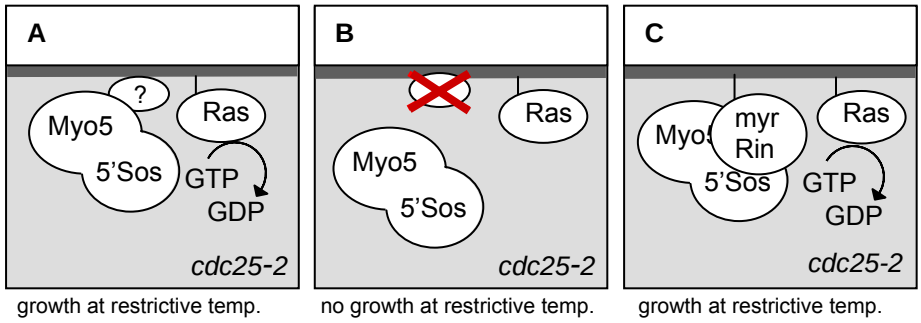

Figure 22. A PRS-based screen for extragenic mutations that prevent plasma membrane recruitment of Myo5p A. As indicated by our results, Myo5p is able to bring 5'Sos to the plasma membrane, allowing growth of the *cdc25-2* mutant at restrictive temperature. **B.** A mutation affecting an essential factor for Myo5p cortical recruitment would prevent this growth. **C.** Growth of the mutant in the presence of myrRin would be a control for the specificity of the mutation on the Myo5p recruitment, since it would discard mutations affecting the 5'Sos construct, the Ras-pathway or essential genes.

Before actually starting with the screen, we looked for conditions to make the system as sensitive as possible. The 5'Sos-Myo5p construct was expressed under the control of the GAL1-promoter. Thus, we sought for the lowest galactose concentration which allowed complementation of the *cdc25-2* growth defect by 5'Sos-Myo5p. A very low expression level of 5'Sos-Myo5p should facilitate selection of mutants that cause only partial delocalization of Myo5p.

Next, we looked for the lowest temperature at which the *cdc25-2* mutant was still defective for growth. Choosing the lowest temperature for the screen should make it more likely to find also ts mutants in essential genes affecting Myo5p localization.

6.2.2.4.1. Screening for *mpr* (*M*yo5p plasma membrane recruitment) mutants

Having defined the optimal conditions for the screen, the actual screening procedure was performed as summarized in figure 23. All steps of the screen were performed with medium containing 0.1% galactose.

C*dc25-2* cells bearing the plasmid for 5'Sos-Myo5p expression (pYX5'SOS-*MYO5*) and the plasmid of myrRin (pmyrRin) were grown in SGC-Leu-Ura liquid medium. Cells were chemically mutagenized with ethylmethane sulfonate, plated on solid medium selecting again for the 2 plasmids and incubated for 3 days at 24°C, until clear colonies were visible. Colonies were then replica-plated on SGC-Leu medium selecting only for the plasmid for 5'Sos-Myo5p expression and incubated at 24°C. Under these conditions cells were allowed to loose the myrRin plasmid bearing the URA3 marker. After 2 days of growth, the colonies were plated on SGC-Leu medium containing 5'-fluoroorotic acid

(FOA) that contraselects cells still bearing the URA3 marker. When transferring the colonies to the FOA-containing plates, the original plates of the screening were also replica-plated, again on SGC-Leu-Ura medium selecting for the 2 plasmids. Both types of replicas (SGC-Leu+FOA plates and SGC-Leu-Ura plates) were incubated at 31°C and the following 2-4 days growth of corresponding colonies was observed. Colonies that clearly showed better growth on the SGC-Leu-Ura medium than on the FOA-medium were selected (see methods, section 9.2.3. for more details of the screening procedure).

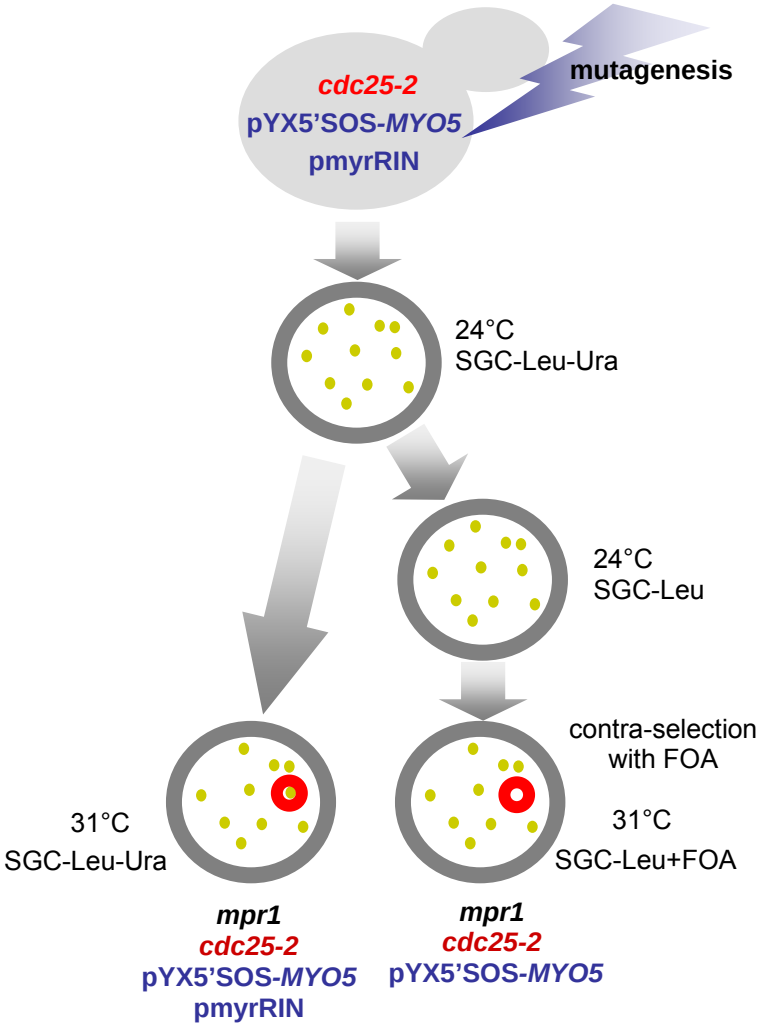

Figure 23. Scheme of the PRS screening procedure. C*dc25-2* cells (SCMIG271) bearing the plasmid for 5'Sos-Myo5p expression (pYX5'SOS-*MYO5*) and the plasmid encoding myrRin (pmyrRin) were chemically mutagenized with ethylmethane sulfonate, plated on SGC-Leu-Ura and incubated for 3 days at 24°C, until clear colonies were visible. Colonies were then replica-plated on SGC-Leu medium and incubated at 24°C. After 2 days of growth, the colonies were plated on SGC-Leu medium containing 5'-fluoroorotic acid (FOA), contraselecting cells still bearing the URA3 marker of the myrRIN plasmid. When transferring the colonies to the FOA-containing plates, the original plates of the screening were also replica-plated, again on SGC-Leu-Ura medium. Both types of replicas (SGC-Leu+FOA plates and SGC-Leu-Ura plates) were incubated at 31°C and after 2-4 days, colonies clearly showing better growth on the SGC-Leu-Ura medium than on the FOA-medium were selected.

Putative candidates growing on FOA-plates at 24°C were discarded to avoid selection of false positives bearing mutations causing hypersensitivity to FOA. Putative candidates that did not grow on FOA at 31°C in the presence of a non-contra-selectable plasmid bearing myrRin were also discarded to avoid selection of false positives that were only temperature sensitive in the presence of FOA.

Overall 21540 colonies were screened and finally **6** mutants were selected, which showed the expected phenotype (see figure 24). These mutants were called *mpr* mutants, for *Myo5p plasma membrane recruitment* mutants. At 31°C the mutants *mpr1*, *mpr2* and *mpr3* showed no growth at all without the plasmid bearing myrRin, while *mpr4*, *mpr5* and *mpr6* were growing without pmyrRin but strikingly less than with the plasmid.

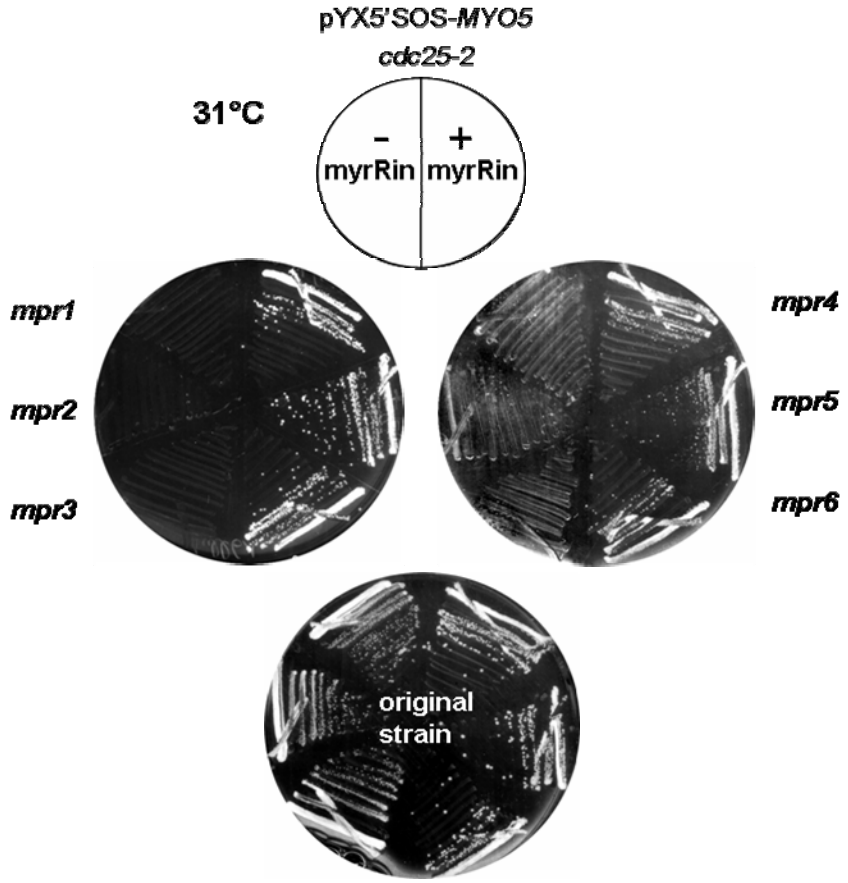

Figure 24. *Myo5p plasma membrane recruitment* mutants (*mpr*) isolated from the PRS screening. The 6 selected mutants (*mpr1, mpr2, mpr3, mpr4, mpr5* and *mpr6*) bearing the plasmid for 5'Sos-Myo5p expression (pYX5'SOS-*MYO5*) were grown on SGC-Leu for 3 days at 31°C, with or without the plasmid for myrRin expression (pmyrRin).

6.2.2.4.2. Identification of genes bearing the *mpr* mutations

The 6 *mpr* mutants, expressing 5'Sos-Myo5p and myrRin were incubated at 37°C to check if they beard temperature sensitive mutations. Three mutants (*mpr1*, *mpr2* and *mpr3*) were temperature sensitive while the other three (*mpr4*, *mpr5* and *mpr6*) were not.

It would be difficult to purify and clone the non-ts mutants. Thus, we decided to continue the work first with the temperature sensitive *mpr* mutants.

In order to check if the 3 ts *mpr* mutants were affected in different genes, the mutants were crossed to each other and the resulting diploids, carrying the plasmids for 5'Sos-Myo5p and myrRin expression, were incubated at 37°C. All diploids could grow at restrictive temperature, demonstrating that the 3 mutants were bearing mutations in different genes.

To segregate the *mpr* mutations from the *cdc25-2* mutation, the temperature sensitive *mpr cdc25-2* mutants were crossed to a wild-type strain (SCMIG19). After tetrade dissection and sporulation, those spores were selected which beard the *mpr* mutation alone (see methods, section 9.2.3.3., for the detailed description of the identification of the single mutants). The *mpr* mutants were then crossed again to the wild-type strain, further isolating the mutation causing the *mpr* phenotype from other mutations that the EMS mutagenesis could have produced.

Finally, the *mpr* mutations were identified by complementation of the ts growth defect with a genomic plasmid library (see methods, section 9.2.3.4. for details).

6.2.2.4.3. *Mpr* mutants bear mutations in Class C VPS genes

All 3 temperature sensitive *mpr* mutants (*mpr1*, *mpr2* and *mpr3*) could be complemented by plasmids of the genomic library. The genomic fragments in the corresponding plasmids were identified by sequencing both ends of the inserts. Surprisingly, the 3 inserts contained sequence of 3 different class C *VPS* genes: *VPS16*, *VPS18* and *VPS33* (see figure 25). The corresponding proteins form together with Vps11p the class C Vps protein complex, a complex which has been implicated in vacuole fusion, Golgi-to-vacuole protein transport, endosome to vacuole transport and the recycling pathway from endosomes to the plasma membrane (Bugnicourt et al., 2004; Peterson and Emr, 2001; Rieder and Emr, 1997; Sato et al., 2000).

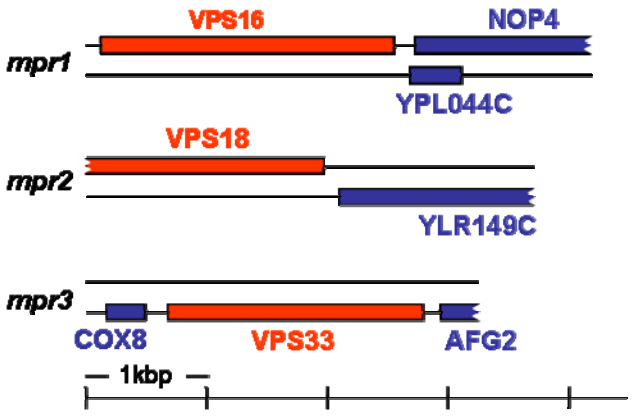

Figure 25. Scheme of the genomic DNA fragments that rescued the ts growth-defects of the *mpr* mutants. Open reading frames are indicated.

Since *mpr1*, *mpr2* and mpr3 were temperature sensitive and showed strongly fragmented vacuoles, like it has been described for class C *vps* knockout mutants (Rieder and Emr, 1997), we could guess that other genes or gene fragments on the identified inserts were not responsible for the complementation.

However, for the unequivocal identification of the *mpr* mutations, the mutants were crossed to knockout strains of the class C *VPS* genes and the resulting diploids were checked for a temperature sensitive phenotype. Diploids could not grow at restrictive temperature if both alleles of the same gene were affected. This analysis confirmed that *mpr1*, *mpr2* and *mpr3* were bearing mutations in *VPS16*, *VPS18* and *VPS33*, respectively (see figure 26).

The VPS18 sequence of the plasmid that was complementing *mpr2* was missing the first 768 bp of the ORF. Thus, a protein fragment of Vps18p probably using the methionine of amino acid 280 as a start codon was sufficient to rescue the ts growth defect of the *mpr2* mutant.

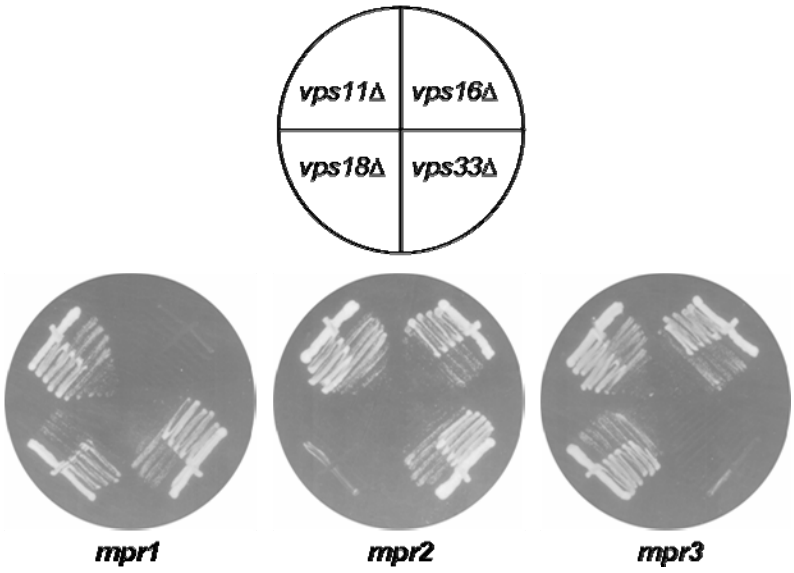

Figure 26. The *mpr1*, *mpr2* and *mpr3* mutants bear mutations in the *VPS16*, *VPS18* and *VPS33* genes, respectively. The *mpr1*, *mpr2* and *mpr3* mutants obtained from the PRS screening were crossed to *vps11*Δ, *vps16*Δ, *vps18*Δ and *vps33*Δ deletion mutants and diploids were grown on YPD medium for 2 days at 36°C. Lack of complementation in the diploids indicates that the parental haploid strains bear mutations in the same gene.

6.2.2.4.4. The *vps* mutants identified in the screening show no delocalization of Myo5p

Since the aim of the screening was to find proteins involved in Myo5p plasma membrane recruitment, next, we analyzed the localization of Myo5p in the *mpr* mutants we had identified. The Plasma Membrane Recruitment System (PRS) applied for the screening was sensing the close association of Myo5p with the plasma membrane, but not Myo5p

patch localization (see section 6.2.2.2.). Thus, to facilitate the identification of the plasma membrane, we stained the membrane of the cells with the lipophilic dye FM4-64 and observed cells expressing Myo5-YFPp under a confocal microscope.

When comparing the Myo5-YFPp localization in the *vps* mutants with a wild type strain, no difference in Myo5p plasma membrane localization could be detected (see figure 27). Like the wild-type, the mutants showed Myo5-YFPp imbedded in the plasma membrane, insight and outsight of patch-like structures. Also, the amount or intensity of Myo5p patches was not reduced in the mutants. These results suggested that the class C vps proteins are not essential factors of Myo5p localization. However, a partial delocalization of Myo5p could perhaps be detected by the PRS and not by fluorescent microscopy. As explained before, we had performed the screening with the lowest expression level of 5'Sos-Myo5p, in order to make it more likely to detect mutants that show only a minor defect in Myo5p localization.

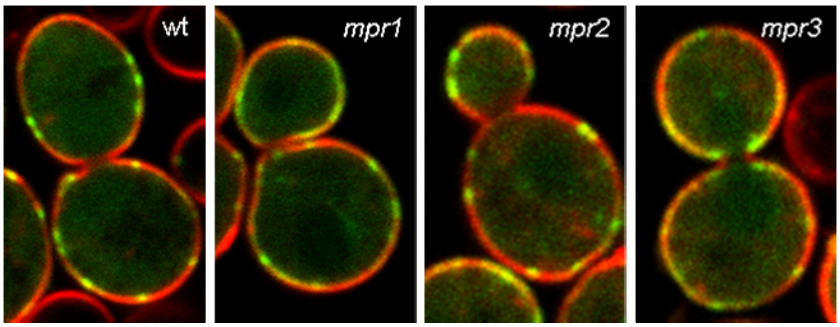

Figure 27. No delocalization of YFP-tagged Myo5p can be observed in the *vps* mutants identified from the PRS screening. Representative confocal fluorescence micrographs of wild-type (SCMIG19) cells or *vps16*Δ, *vps18*Δ or *vps33*Δ mutants identified from the PRS screening expressing a YFP-tagged Myo5p construct from p*MYO5*-YFP. Cells were grown to mid-log phase at 25°C and the plasma membrane was stained with the red lipophilic dye FM4-64.

6.2.2.4.5. The *vps* mutants identified in the screening exhibit a slight defect in the uptake step of endocytosis.

So far, we could not exclude a partial delocalization of Myo5p in the *vps* mutants. Next, we decided to analyze the alpha-factor uptake kinetics in the mutants. Since the class I myosins are essential for the endocytic uptake step (Geli and Riezman, 1996) and the α-factor uptake assay is a very sensitive, quantitative method, a partial delocalization of Myo5p should be reflected by a defect in the α-factor uptake.

Indeed, in comparison to a wild-type strain, all 3 *vps* mutants showed slightly defective uptake kinetics (see figure 28). The *vps16* mutant exhibited the strongest defect, while the

vps18 and *vps33* mutants showed nearly identical uptake kinetics, ranging between those of the *vps16* and the wild-type strain.

These results were in agreement with the idea that the *vps* mutants could exhibit a partial delocalization of Myo5p. However, further experiments will be necessary to proof this idea.

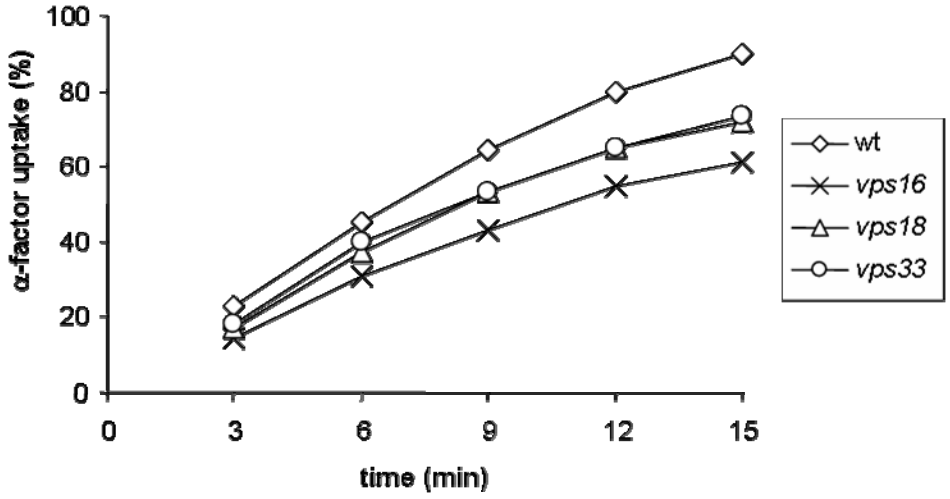

Figure 28. The *vps* mutants identified in the PRS screening are slightly defective in the uptake step of endocytosis. Wild-type cells (wt; SCMIG19) or *vps16*, *vps18* or *vps33* mutants identified from the PRS screening were grown to early log-phase and tested for ^{35}S-radiolabelled α-factor internalization at 25°C.

7. Supplementary data

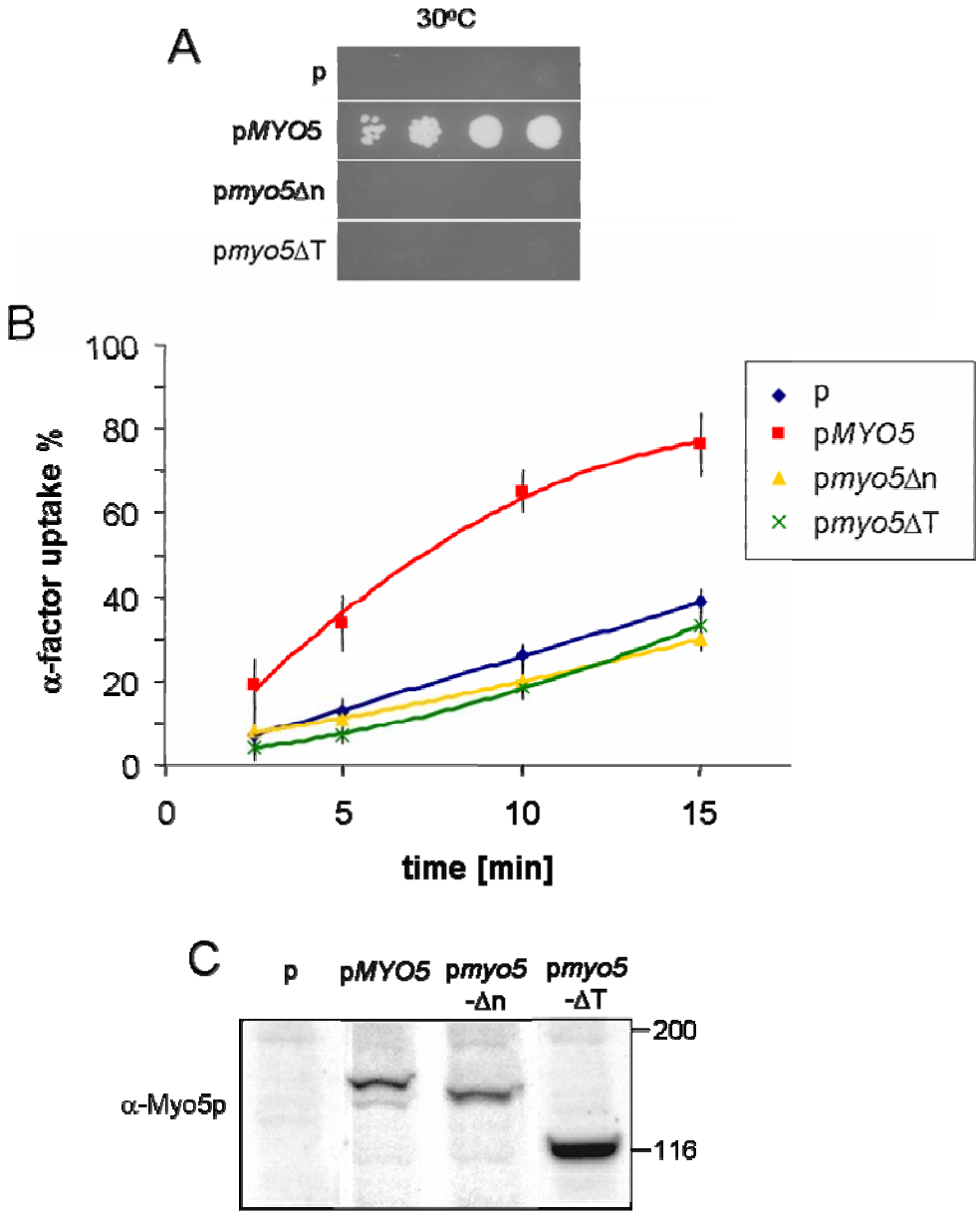

Figure 29. The membrane binding domains of Myo5p are important for Myo5p function and the endocytic uptake step. A. Dot spots of *myo3*Δ *myo5*Δ cells (SCMIG590) complemented with *MYO5* expressed from a centromeric plasmid (p33*MYO5*) with a contraselectable marker (URA3) bearing an empty plasmid (p; Ycplac111) or plasmids for the expression of full-length Myo5p (p*MYO5*), Myo5p missing the neck domain (p*myo5*Δn) or Myo5p missing the TH1 domain (p*myo5*ΔT), grown on SDC-Leu medium with FOA (for contraselection of p33*MYO5*) at 30°C for 3 days. **B.** *myo5*Δ cells (SCMIG275) bearing an empty plasmid (p; Ycplac111) or plasmids for the expression of full-length Myo5p (p*MYO5*), Myo5p missing the neck domain (p*myo5*Δn) or Myo5p missing the TH1 domain (p*myo5*ΔT), were grown to early log-phase, preincubated for 30 min at 37°C and tested for ^{35}S-radiolabelled α-factor internalization at 37°C. **C.** Immunoblot analysis of protein extracts from *myo5*Δ cells (SCMIG275) bearing an empty plasmid (p; Ycplac111) or plasmids for the expression of full-length Myo5p (p*MYO5*), Myo5p missing the neck domain (p*myo5*Δn) or Myo5p missing the TH1 domain (p*myo5*ΔT). Nitrocellulose membranes were decorated with a rabbit polyclonal antibody against the C-terminal domain of Myo5p (α-Myo5p). 20 µg protein were loaded per lane.

8. Discussion

8.1. Cmd1p regulates the Myo5p-Vrp1p interaction and the association of Myo5p to the endocytic patch

In order to identify domains required for proper recruitment of Myo5p to the endocytic patch, we analyzed the localization of GFP-Myo5p constructs bearing different truncations by fluorescence microscopy in living yeast cells. The observations strongly suggested that the Myo5p C-terminus bearing the GPA domain, the SH3 domain and the acidic peptide is sufficient for localization of the myosin to cortical patches. This observation is consistent with previous results suggesting that the protein Vrp1p, which directly binds to the Myo5p SH3 domain, plays an important role in the recruitment of Myo5p (Anderson et al., 1998; Sun et al., 2006). Nevertheless, it should be mentioned that in contrast to what Sun et al observed, GFP-Myo5p did not appear significantly delocalized in our *vrp1*Δ background. On the contrary, a clear Myo5p localization defect was observed in the *las17*Δ strain. Las17p interacts both with Vrp1p and with the Myo5p SH3 domain and Las17p is clearly important for the recruitment of Vrp1p to the endocytic patch (Sun et al., 2006). Therefore, we hypothesize that Las17p participates in endocytic patch localization of Myo5p, either directly or by an indirect interaction bridged by Vrp1p. In addition to the Las17p/Vrp1p-SH3 interaction, the association of the acidic domain to the Arp2/3 complex and the interaction of the TH2 domain with filamentous actin might contribute to stabilize the Myo5p localization at the endocytic patch, since the SH3 alone is not localized to cortical patches (Anderson et al., 1998). Indeed, previous reports have suggested the Myo5p localization is at least partially sensitive to treatment with Latrunculin A (Anderson et al., 1998; Sun et al., 2006).

An unexpected observation from our experiments was that the presence of the TH1 domain seemed to block Myo5p patch recruitment via the C-terminus. Since these results indicated a possible interaction between the Myo5p C-terminus and the TH1 domain, we decided to analyze if this interaction occurred *in vitro*. In an *in vitro* binding assay with purified proteins and in a protein overlay assay, a construct bearing the neck and the TH1 domains could bind to the Myo5p C-terminus, indicating that the interaction between the different tail domains might be direct. Moreover, in immunoprecipitation experiments using whole cell extracts, we could show that the TH1 domain can bind to the Myo5p C-terminus and block the interaction of the SH3 domain with Vrp1p *in cis* and *in trans*.

An *in vitro* interaction between these myosin I tail domains has already been reported for myosin-IA of *Acanthamoeba castellani*, which is closely related to Myo5p (Lee et al., 1999). Consistent with our results, purified TH1 domain was shown to interact with high affinity to a construct bearing the TH2 and SH3 domains.

So far, little structural information exists about class I myosin tails with a domain organization similar to Myo5p. In a study by Jontes et al., the tail of *Acanthamoeba castellanii* myosin-IB was analyzed by cryo-electron microscopy and shown to exhibit a surprisingly globular structure (Jontes et al., 1998). Similar studies on *Acanthamoeba* myosin-IC, which bears the SH3 domain flanked by two TH2 (GPA) domains, indicated that the very C-terminus of the tail, bearing the GPA and SH3 domains, folds back to anneal side by side with the TH1 domain (Ishikawa et al., 2004). Recently, Hwang et al. presented additional NMR data that provide evidence for an intramolecular interaction between the TH1 domain and the SH3 domain in myosin-IC (Hwang et al., 2007).
These studies on different long-tailed class I myosins strongly support our model that the Myo5p tail domains interact intramolecularly with each other. Moreover, when precipitating cytosolic Myo5p under the same conditions which allowed us to observe the nTH1-mediated inhibition of the Myo5p C-terminus (blocking the interaction with Vrp1p), we could not detect any oligomerization of Myo5p. Thus, most likely, an intermolecular interaction does not occur or if at all, in cellular fractions others than the cytosol.

When expressing the GFP-Myo5p constructs with different truncations, we observed that the TH1 domain can only block the C-terminus for patch localization if the neck domain is not present, suggesting that in the full-length protein the neck might regulate the interaction between the tail domains.
The Myo5p neck is known to bind 2 calmodulin (Cmd1p) molecules, and the functional requirement of this interaction for endocytosis has been described (Geli et al., 1998). Moreover, it has been shown for the mammalian brush-border myosin I, that calmodulin release from the neck domain can induce a big conformational change in the tail (Whittaker and Milligan, 1997). Thus, we speculated that Cmd1p association to Myo5p could regulate the intramolecular interaction of the different tail domains and as a result, the interaction of Myo5p with some components of the endocytic patch.
Indeed, Cmd1p binding clearly stabilized the interaction between a construct bearing the neck and TH1 domains and the Myo5p C-terminus in *in vitro* binding experiments, using purified components. Consistently, in immunoprecipitation assays from total yeast extracts the interaction of Myo5p with Vrp1p was strongly enhanced under conditions that cause dissociation of Cmd1p from the myosin. Moreover, in a *cmd1* mutant with impaired Cmd1p-Myo5p interaction much more Vrp1p appeared associated to Myo5p than in a wild-type strain. These results suggested that Cmd1p dissociation at the plasma membrane might release the intramolecular interaction between the tail domains and favour the interaction of the Myo5p C-terminus with Vrp1p, leading to cortical patch association of Myo5p.

If our hypothesis would have a physiological relevance for the endocytic patch recruitment of Myo5p, one would expect that Cmd1p interacts to a less extent with Myo5p at the plasma membrane than in the cytosol. It should be mentioned that dissociation of calmodulin from the class I myosins has never been demonstrated under physiological conditions and thus, a role for calmodulin in the regulation of these motors has only been suggested based on *in vitro* experiments using purified components. To test our hypothesis, we purified plasma membrane and cytosolic fractions from yeast cells and performed immunoprecipitation experiments. Cmd1p clearly appeared more associated with cytosolic Myo5p than with Myo5p from the plasma membrane, indicating that indeed Cmd1p might dissociate from Myo5p to promote Vrp1p-binding and localization of the myosin to endocytic patches. Consistent with this interpretation, immunoprecipitation experiments showed only association of Myo5p with Vrp1p in a plasma membrane fraction but not in the cytosol.

Further underlying the physiological relevance of calmodulin dissociation for Myo5p patch association, we also observed that a *cmd1* mutant specifically impaired in the Cmd1p-Myo5p interaction showed more GFP-Myo5p patches at the plasma membrane than wild-type cells. Moreover, the lifespan of individual GFP-Myo5p patches was prolonged. Also these *in vivo* observations support our model that Cmd1p-binding to the Myo5p neck domain negatively regulates patch association of the myosin.

Finally, a role of Cmd1p as a negative regulator of Myo5p function is supported by earlier observations in which the deletion of the Cmd1p binding sites in Myo5p only slightly affected Myo5p endocytic function at low temperatures (Geli et al., 1998). The strong uptake defects observed at 37°C in *cmd1* and *myo5* mutants specifically impaired in the Cmd1p-Myo5p interaction might be a consequence of the precipitation of the cytosolic myosin upon exposure of the naked neck.

Although studies from different class I myosins have indicated an intramolecular interaction of the tail, our data suggest for the first time a regulatory function of this interaction. Moreover, we present for the first time evidence that Cmd1p dissociates from a myosin I under physiological conditions, modulating myosin association with lipids and with the actin polymerization machinery.

An important prediction of our observations is that calmodulin release from Myo5p might also regulate the myosin function as an activator of the Arp2/3 complex, since it has been demonstrated that Myo5p binding to Vrp1p is essential to induce Arp2/3 dependent actin polymerization (Geli et al., 2000a; Sun et al., 2006). Further experiments are now required to address this matter.

8.2. Phospholipid binding of Myo5p

It has been shown for class I myosins others than Myo5p that the TH1 domain, which bears many positively charged amino acids, interacts *in vitro* with purified membranes and with different kinds of negatively charged lipids (Adams and Pollard, 1989; Doberstein and Pollard, 1992; Hayden et al., 1990; Miyata et al., 1989). Thus, it was believed that the TH1 domain of class I myosins interacts with membranes by unspecific electrostatic interactions. In comparison to other intracellular domains, the plasma membrane has a unique anionic character that has been shown to be sufficient to direct basic proteins specifically to this membrane (Okeley and Gelb, 2004). Thus, an unspecific interaction via the TH1 domain could serve to concentrate Myo5p at the plasma membrane, facilitating the interaction with binding partners at the cortical patches. Consistent with this idea, when expressing GFP-Myo5p under the *MYO5* promoter in living cells, sometimes we could observe a diffuse staining of the plasma membrane outside of the cortical patches, which was stronger than the cytosolic staining. Moreover, GFP-Myo5p constructs lacking the TH1 domain but bearing the C-terminal fragment (GFP-C and GFP-Myo5ΔTp) showed a strong cytosolic expression in addition to the localization to cortical patches, suggesting that the TH1 domain might contribute to the efficient localization of Myo5p to the endocytic patches.

Using commercially available lipid strips, we made a first approximation to analyze the lipid binding properties of Myo5p. Since a construct of the TH1 domain alone could not be expressed in sufficient amounts, we purified a construct bearing the Myo5p neck and TH1 domains from yeast and we overlayed the lipid strips with the protein. The construct bound to different negatively charged lipids, consistent with the described binding properties of TH1 domains. However, the neck domain could also participate in the observed lipid binding. The neck domain of class I myosins forms an amphipathic helix and its involvement in membrane binding has been suggested for many years. Only recently, it was shown that the neck of mammalian Myo1c binds to anionic lipids *in vitro* and that this interaction can be blocked by Cmd1p (Hirono et al., 2004). Therefore, we decided to analyze the effect of Cmd1p on the lipid binding properties of Myo5p, using again a purified construct of Myo5p bearing the neck and TH1 domains and commercial lipid strips. Cmd1p clearly diminished binding of the construct to acidic lipids, suggesting that either the neck participates in lipid binding upon Cmd1p dissociation or the release of Cmd1p might induce a conformational change in the TH1 domain. Both possibilities might also work together.

In our experiments with the PRS (plasma membrane rescruitment system) a 5'Sos-construct bearing the head and neck domains could restore slow growth of the *cdc25-2*

mutant while a construct of the head alone could not, suggesting that the Myo5p neck alone has membrane binding capacity *in vivo*. However, the neck and TH1 domains were both required to rescue efficient growth of the *cdc25-2* strain. This might indicate that a strong interaction with the lipid bilayer only occurs upon cooperative neck and TH1 binding to phospholipids. The observation is also supporting the idea that the neck promotes a conformational change in the TH1 domain which allows efficient membrane binding. Interestingly, using cryoelectron microscopy it has been demonstrated for the short-tailed brush-border myosin I that Cmd1p dissociation causes a major conformational change in the TH1 domain (Whittaker and Milligan, 1997).
Since our results indicate that a Cmd1p-dependent intramolecular interaction occurs between the TH1 domain and the C-terminus of Myo5p, it would also be possible that the TH1 domain can only bind to lipids upon Cmd1p dissociation and the release of the C-terminus from the TH1 domain. Further experiments are necessary to discriminate between these hypotheses.

The TH1 domain of several myosins has been shown to bind to different negatively charged lipids (Adams and Pollard, 1989; Doberstein and Pollard, 1992; Hayden et al., 1990). However, recent results indicate that the TH1 domain might mediate more specific lipid interactions. Hokanson and Ostap have demonstrated that the TH1 domain of mammalian Myo1c binds specifically to PI(4,5)P2 in in vitro experiments with liposomes (Hokanson and Ostap, 2006). Moreover, it has been shown that the TH1 domains of Myo1c and *Acanthamoeba* myosin-IC reveal structural homology to PI(4,5)P2-specific PH-domains (Hokanson et al., 2006; Hwang et al., 2007).
Consistent with these results, when using commercial lipid strips to analyze the lipid binding properties of Myo5p, PI(4,5)P2 was one of the lipids to which a construct of the neck and TH1 domains preferentially bound. The binding to PI(4,5)P2 was stronger than to other phospholipids with the same or even higher negative charge, suggesting that Myo5p lipid binding domains mediate not only electrostatic interactions. However, based on our binding assay we cannot decide which influence the neck domain or the TH1 domain have on Myo5p binding to lipids. On the other hand, we also observed that the neck-TH1 construct binds with high affinity to PI(3,5)P2 and phosphatidic acid. Phosphatidic acid can be produced at the plasma membrane by the activity of phospholipase D and the lipid has been implicated in endocytosis (Jenkins and Frohman, 2005). An involvement of PI(3,5)P2 in Myo5p recruitment to cortical endocytic patches appears unlikely, as this phospholipid is found mainly on the outer membrane of multivesicular bodies and not on the plasma membrane (Di Paolo and De Camilli, 2006; Odorizzi et al., 1998).

Even though the experiments using lipid strips are not conclusive regarding the affinity of Myo5p for the different lipids and further analysis with liposomes should be carried out to address this matter, our *in vivo* data also suggest a role of PI(4,5)P2 in Myo5p localization. When we expressed GFP-Myo5p in mutants affecting PI(4,5)P2 synthesis (*mss4-2*) or turnover (*sjl1*Δ *sjl2*Δ), mislocalization of the myosin was observed. The *sjl1*Δ *sjl2*Δ mutant has been shown to exhibit long plasma membrane invaginations which might present endocytic invaginations unable to bud off from the plasma membrane (Singer-Kruger et al., 1998). Consistently, we could observe that not only Myo5p but also Abp1p localization was affected in the *sjl1*Δ *sjl2*Δ strain. However, the mislocalization of Myo5p in the *mss4-2* strain appeared more specific, as Abp1p was normally localized in this mutant.

Besides the described results, also the observation that a *mss4* ts mutant is synthetical lethal with a *myo5*Δ strain suggests an important role of PI(4,5)P2 for Myo5p function (Audhya et al., 2004).

Studies from mammalian cells indicate that PI(4,5)P2 might be produced locally at sites of endocytosis, and the lipid is important for the localization of several endocytic proteins (Haucke, 2005; Krauss et al., 2003; Krauss et al., 2006). Therefore, a specific interaction of the TH1 domain with PI(4,5)P2 could be involved in the endocytic patch recruitment of Myo5p.

As mentioned before, our experiments also suggest a direct participation of the neck in Myo5p membrane binding. As the neck domain forms an amphipathic helix it might mediate unspecific electrostatic interactions with lipids. Consistent with this idea, *in vitro* experiments with a head-neck construct of mammalian Myo1c showed only weak, unspecific binding of the neck to negatively charged phospholipids (Hokanson et al., 2006). Moreover, it was demonstrated that the neck is not required for membrane association of a Myo1c-tail construct in living cells (Hokanson et al., 2006). This suggest that the TH1 domain alone localizes Myo1c to the plasma membrane and the neck might then participate in the targeting to specific subdomains, e.g. membrane regions especially enriched in PI(4,5)P2.

The amphipathic character of the neck could not only promote the localization of class I myosins to membrane regions especially enriched in negatively charged phospholipids. After membrane binding via the TH1 domain, the neck could be inserted into the phospholipid bilayer, where hydrophobic amino acids would interact with the lipid acyl chains and the positively charged amino acids would interact with negatively charged lipid head groups. Such a membrane insertion of an amphipathic helix might be important for

Myo5p function by inducing stronger anchoring of Myo5p to the plasma membrane. Moreover, proteins bearing N-BAR domains (e.g. amphiphysin) and the COPII coat protein Sar1p have been shown to promote membrane curvature by the insertion of an amphipathic helix into the lipid bilayer (Lee et al., 2005; Peter et al., 2004). *In vitro* experiments with Sar1p and liposomes also suggest that the accumulation of inserted helices at the bud neck promotes vesicle scission (Antonny, 2006; Lee et al., 2005). Interestingly, Myo5p appears localized to the neck of endocytic vesicles in electron micrographs (F. Idrissi, unpublished data). The participation of Myo5p in the scission of endocytic vesicles has been proposed, since a temperature sensitive *myo5* mutant exhibits cortical patches with a prolonged slow-movement phase at semipermissive temperature (Jonsdottir and Li, 2004). Moreover, a *myo5*Δ mutation is synthetical lethal with a rvs167Δ mutation, suggesting that Myo5p and the amphiphysin-like protein Rvs167p might share a redundant function in endocytosis (Tong et al., 2004).
Besides PI(4,5)P2, phosphatidic acid (PA) was also preferentially bound by the nTH1 construct in the lipid binding assays and the association of the Myo5p fragment to this lipid appeared especially elevated after the addition of 5 mM Ca^{2+} (to induce Cmd1p dissociation). Thus, even though we still need to confirm this result using liposomes, PA could also specifically bind to the neck and/or the TH1 domain. Interestingly, PA has been implicated in endocytosis and vesicle fission (Jenkins and Frohman, 2005). Because of its biophysical properties, PA might induce negative curvature in the inner leaflet of the lipid bilayer and thus may be directly involved in the closure of the vesicle neck for scission (Kooijman et al., 2003). Alternatively, clusters of PA have been proposed to function as platforms for the insertion of fissiogenic proteins. Thus, the lipid might be enriched at the neck of the forming endocytic vesicle, where also Myo5p appears to concentrate. Moreover, a number of observations indicate that PI(4,5)P2 and PA positively regulate each others synthesis, making a model of a synchronic PI(4,5)P2 and PA binding by the Myo5p TH1 domain and neck domain, respectively, very attractive (Jenkins and Frohman, 2005; Powner and Wakelam, 2002). The role of phospholipase D in the uptake step of endocytosis and in the patch recruitment of Myo5p will now be investigated to address the possible role of PA in the process.

The importance of phospholipid binding for Myo5p function and endocytosis is reflected by the strong growth and uptake defects of yeast strains expressing Myo5p constructs lacking the lipid-binding domains (Myo5-ΔTp or Myo5-Δnp). The *myo3*Δ *myo5*Δ strain used in our lab cannot grow at all at 30°C. This growth defect can not be rescued by the expression of a Myo5 construct missing the TH1 domain or the neck (see supplementary

data, page 56, figure 29A). Moreover, the endocytic uptake defect of a *myo5*Δ strain is also not suppressed at all by expression of the corresponding constructs (supplementary data, figure 29B).

Since we have observed that the GFP-Myo5ΔTp construct localizes to endocytic patches, patch recruitment of the Myo5p motor-head and the C-terminus does not seem to be sufficient for Myo5p function. Probably, the motor protein function and/or Arp2/3 activator activity have to be tightly bound to the plasma membrane (e.g. to translocate the phospholipid bilayer with respect to the actin cytoskeleton) or the TH1 domain might have an active role in membrane bending.

8.3. A model for Cmd1p-regulated recruitment of Myo5p to endocytic patches

Our results allow us to propose a model for regulated patch recruitment of Myo5p (see figure 30).

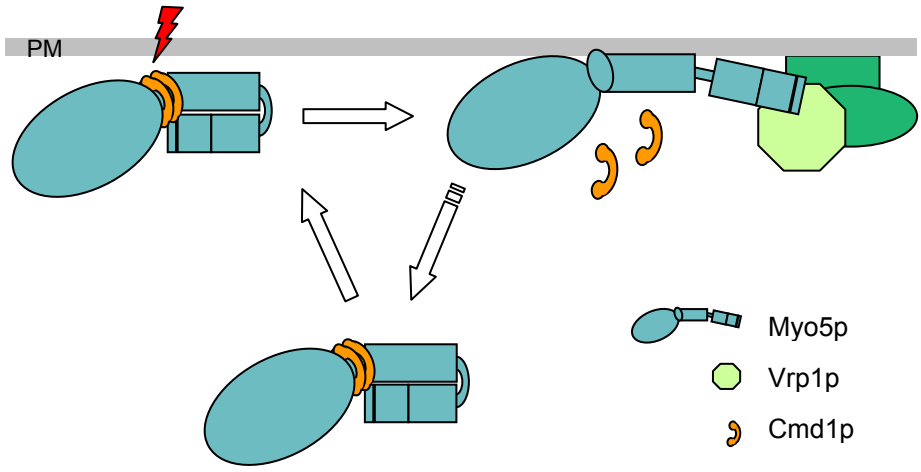

Figure 30. Model of Myo5p recruitment to cortical patches (see text for details)

In the cytosol, Myo5p with Cmd1p associated to the neck might exhibit a “closed” conformation, in which the TH1 domain interacts with the Myo5p C-terminus and prevents binding with other cortical patch components such as Vrp1p, which are also present in the cytosol. Only at the plasma membrane, an unknown signal might induce Cmd1p dissociation from Myo5p. The dissociation of Cmd1p would then favour an “open” conformation of the tail in which the TH1 domain does not interact with the Myo5p C-terminus anymore. This would then allow the interaction of the Myo5p SH3 domain with Vrp1p and Myo5p function as an Arp2/3 complex activator. Moreover, Cmd1p release would allow efficient binding to plasma membrane lipids. After fulfilling its function in

endocytosis, Myo5p might rebind Cmd1p, promoting Myo5p dissociation from the endocytic vesicle.

Interestingly, an intramolecular interaction which regulates protein localization and function has been described for other actin-regulating proteins. For the mammalian formin FRLalpha (formin-related gene in leukocytes alpha) is has been described that autoinhibition via an interaction between the N- and C-terminus regulates its plasma membrane localization and actin assembly activity for phagocytosis. In this case, release of the intramolecular interaction is induced by the activated form of the RhoGTPase Cdc42 (Seth et al., 2006).

Also the actin-regulating activity of the mammalian homologue of Las17p, N-WASP (neuronal Wiskott-Aldrich Syndrome protein), has been shown to be autoinhibited by an interaction between the N- and C-terminus. Simultaneous binding of PI(4,5)P2 and activated Cdc42 to a central region of the protein reduces the affinity between the N- and C-terminal domains, allowing the interaction of the C-terminus with the Arp2/3 complex (Rohatgi et al., 2000).

A number of points need to be analyzed to further refine our model of Myo5p patch recruitment. First, we can not conclude from our results if Myo5p is already associated to the plasma membrane via the TH1 before Cmd1p dissociation is induced or if membrane association also requires Cmd1p dissociation. The results with the lipid strips and with the PRS only indicate that the neck is essential to mediate tight association with the lipid bilayer and Cmd1p release increases phospholipid association of Myo5p.

However, some specific Cmd1p-Myo5p interaction could still be observed in the immunoprecipitation experiments from plasma membrane fraction. Further, a diffuse plasma membrane localization of GFP-Myo5p, in addition to the endocytic patch localization, could sometimes be observed in fluorescence microscopy of living cells. Thus, our preferred hypothesis would propose that a loose TH1-mediated Myo5p association with the plasma membrane occurs in the closed, Cmd1p-bound state of Myo5p. This kind of membrane association might serve to concentrate the motor at the plasma membrane plane and might already reduce the strong affinity of Cmd1p for the Myo5p neck. Only at the cortical patch, a still unknown signal would trigger the release of Cmd1p. As a consequence, the interaction of Myo5p with the lipid bilayer would be strengthened and the inhibitory intramolecular interaction on the C-terminal extension would be loosed, allowing the interaction of Myo5p with Vrp1p, and, in turn, Myo5p function as activator of the Arp2/3 complex.

A major question derived from our results is why Cmd1p is released from Myo5p at the plasma membrane.

An obvious possibility would be that a phospholipid produced at endocytic sites (e.g. PI(4,5)P2 or phosphatidic acid) directly competes with Cmd1p for binding to the neck domain. PI(4,5)P2 degradation after vesicle formation might then allow Cmd1p rebinding. However, we do not favour this hypothesis unless other molecular mechanisms participate in lowering the strong affinity of Cmd1p for the IQ motifs (Kd values of 2-4 μM were measured for Myo1c)(Gillespie and Cyr, 2002). An interesting possibility would be that binding of PI(4,5)P2 via the TH1 domain induces a conformational change in the adjacent neck and reduces the affinity to Cmd1p. Only then, a high local concentration of PA or PI(4,5)P2 could displace Cmd1p from the Myo5p neck.

Likely, the Myo5p-Cmd1p interaction could also be affected by phosphorylation. Phosphorylation of rat liver myosin by protein kinase C (PKC) has been shown to reduce Cmd1p binding *in vitro* (Williams and Coluccio, 1995). Interestingly, the neck domain of Myo5p and adjacent sequences of the TH1 domain bear possible phosphorylation sites for the PKC. Further, a role for PKC in the uptake step of endocytosis has been demonstrated (Friant et al., 2001).

Finally, since Ca^{2+} is known to inhibit Cmd1p binding to Myo5p, a local gradient of Ca^{2+} could induce Cmd1p release from the myosin. In mammalian cells, a local elevation of Ca^{2+} next to the plasma membrane seems to be important for the regulation of plasma membrane associated processes (Barritt, 1999). However, since it has been shown that a *cmd1* mutant impaired in Ca^{2+} binding has normal endocytic uptake kinetics, a Ca^{2+}-dependent regulation of the Cmd1p-Myo5p interaction appears less likely (Kubler et al., 1994).

Future experiments are now being designed to identify the molecular mechanism that triggers Cmd1p dissociation from Myo5p at the plasma membrane.

8.4. The PRS screening

In this work we present a genetic screen, which could theoretically be useful for the identification of factors involved in Cmd1p dissociation from Myo5p. The plasma membrane recruitment system (PRS) seems to monitor the close interaction of the neck and TH1 domains with the plasma membrane, probably with the lipid bilayer. Thus, by a screening based on the PRS we expected to identify enzymes involved in the production or the turn over of certain lipids or proteins with the capacity to modify the lipid binding affinity of the neck or the TH1 domains of Myo5p.

So far, the PRS screening led to the identification of 3 different genes which encode proteins of the same complex, namely *VPS16*, *VPS18* and *VPS33*. The corresponding proteins form together with Vps11p the class C Vps protein complex, a complex which has been implicated in Golgi-to-vacuole protein transport, vacuole fusion, endosome to vacuole transport and the recycling pathway from endosomes to the plasma membrane (Bugnicourt et al., 2004; Peterson and Emr, 2001; Rieder and Emr, 1997; Sato et al., 2000).

Since the class C Vps proteins have not been described to be localized at the plasma membrane, their direct involvement in Myo5p recruitment seems to be unlikely. The class C Vps complex functions in more than one important transport route in the yeast cell. Thus, the identification of the *vps* mutants by the screening could indicate that the strains exhibit an abnormal composition of the plasma membrane as a secondary effect of the disturbed intracellular transport. The abnormal plasma membrane composition could then affect Myo5p recruitment. However, Myo5-YFPp localization at the plasma membrane seemed to be unaffected in the *vps* mutants, when analyzed by confocal microscopy.

Nevertheless, the low resolution of the fluorescence microscopy could still prevent detection of minor defects in Myo5p localization. Since we detected a slight endocytic uptake defect in all mutants identified, a defect in Myo5p plasma membrane recruitment in the strains appears still possible. As previously discussed, Myo5p could localize to the plasma membrane before Cmd1p dissociates and the release of Cmd1p might then lead to a tighter or closer interaction with the lipid bilayer. If only this last step would be affected in the *vps* mutants, quantitative biochemical experiments would be required to resolve the differences to a wild-type background.

Another less appealing but still more likely possibility came out recently with the observation that in class C *vps* mutants Ras2p is delocalized from the plasma membrane, mainly to mitochondria (Wang and Deschenes, 2006). Thus, signalling through the Ras-pathway might actually be impaired in the *vps* mutants. In principle, our screening was designed to discard mutants affecting the reporter system using the myrRIN control. However, we cannot rule out that myrRIN recruits more 5'Sos-Myo5p (compared with the 5'Sos construct alone), sufficient to activate residual amounts of Ras2p which reach the plasma membrane in the *vps* mutants. Further experiments are necessary to analyze the credibility of the myrRin control for the *vps* mutants and the screening in general.

8.5. Outlook

For the verification and extension of our model for Cmd1p-regulated patch recruitment of Myo5p we are planning several experiments.

To verify our result from the immunoprecipitation experiments that Vrp1p and the neck and TH1 domains can compete for binding with the Myo5p C-terminus, we will perform *in vitro* binding assays with purified components. Binding of purified Vrp1-HAp to GST-C (bearing the Myo5p C-terminus) will be analyzed, in the presence or absence of ProtA-nT (bearing the Myo5p neck and TH1 domains). The same experiments will also be performed with Cmd1p-free ProtA-nT and in the presence or absence of purified Cmd1p, to demonstrate *in vitro* that the interactions are regulated by Cmd1p.

To investigate the influence of calmodulin on the capacity of Myo5p to induce Arp2/3p dependent actin polymerization, *in vitro* actin polymerization assays will be performed. Full length Myo5p or a construct bearing the neck and tail domains will be analyzed with and without associated Cmd1p. Moreover, to investigate if the intramolecular interaction in Myo5p affects its Arp2/3 activator activity, purified neck-TH1 protein with associated Cmd1p will be analyzed for its effect on Arp2/3-dependent actin polymerization induced by a construct of the Myo5p C-terminus.

Using time-lapse microscopy, the lifespan and the number of GFP-Myo5p patches at the plasma membrane will be analyzed in a collection of strains expressing *cmd1* point mutations, which differentially affect binding to Myo5p. If our hypothesis is correct, we expect to find a strong correlation between the mutations that disrupt the interaction between Myo5p and Cmd1p, and those that elongate the GFP-Myo5p lifespan and/or increase the number of Myo5p patches at the plasma membrane. Further, different GFP-tagged endocytic proteins will be analyzed in the cmd1 mutants that exhibit an elongated GFP-Myo5p lifespan in order to assess the specificity of the observed phenotype. We also plan to analyze if the detected elongated lifespan of Myo5p patches in the *cmd1-226* mutant is a consequence of premature Myo5p-association to Vrp1p or of delayed dissociation of Myo5p from the plasma membrane. Both effects could also work together. To analyze this point, GFP-Myo5p will be coexpressed with RFP-tagged Vrp1p or Abp1p, and the time-course of patch association of the fluorescent proteins will be observed using dual-color imaging.

For a more detailed analysis of the lipid-binding properties of Myo5p, liposomes with different lipid compositions will be prepared and used for *in vitro* binding experiments with purified ProtA-nT. Again, experiments will also be performed with a Cmd1p-free ProtA-nT construct and with and without the addition of purified Cmd1p. Since the TH1 domain alone could not be expressed in yeast or bacteria, we will try to express the domain *in vitro*. The comparison of liposome-binding by the TH1 domain with liposome-binding by a construct bearing the neck and TH1 domains will demonstrate the effect of the neck domain on lipid binding and show if the TH1 domain alone binds lipids with strong affinity.

Competition experiments between different acidic phospholipids and Cmd1p for binding to a construct of the neck and TH1 domain will be performed, to analyze the possibility that the local production of a specific lipid at endocytic sites causes Cmd1p release from the Myo5p neck. Searching for the signal that causes Cmd1p dissociation, we will also analyze possible phosphorylation sites at the Myo5p neck domain. We will mutate these sites and analyze their functional relevance for Cmd1p binding, Myo5p recruitment to cortical patches and endocytosis.

Finally, purification of high amounts of Myo5p using the bacculovirus system may allow the visualization of the structural change in Myo5p induced by calmodulin dissociation, using cryo-electron microscopy.

9. Materials and methods

9.1. Cell culture

9.1.1. *E. coli* cell culture

E. coli cell culture was performed according to standard protocols (Sambrook and Russel, 2001).

9.1.2. *S. cerevisiae* cell culture

S. cerevisiae cell culture was performed as described (Guthrie and Fink, 1991; Sambrook and Russel, 2001). Unless otherwise mentioned, strains were grown in complete yeast peptone dextrose media (YPD) or, if selection was required, in appropriate synthetic dextrose minimal media (SDC) (Sherman, 1991). Complete media contained 1% yeast extract (Difco), 2% peptone (Difco) and 2% glucose (Fluka). Synthetic minimal media consisted of 2% glucose (Fluka), 0.67% yeast nitrogen base (Difco) and 0.075% of CSM (complete synthetic mix; Qbiogene), which contains all required amino acids, purine- and pyrimidine-bases except those required for auxotrophic marker selection. SDC-Ura media, for instance, contained all described components except uracil. The concentrations of all amino acids, purin- and pyrimidin-bases used in CSM were: 10 mg/l adenine, 50 mg/l L-arginine, 80 mg/l L-aspartate, 20 mg/l L-histidine-HCl, 50 mg/l L-leucin, 50 mg/l L-lysine, 20 mg/l L-methionine, 50 mg/l L-phenylalanine, 100 mg/l L-threonine, 50 mg/l tryptophane, 50 mg/l L-tyrosine, 20 mg/l uracil and 140 mg/l valine. Solid media additionally contained 2% agar (Fluka).

For the induction of proteins under a GAL1-promoter, the galactose containing medium (SGC) was prepared like SDC, just substituting glucose by 1% raffinose and the adequate amount of galactose. For YPD solid medium containing kanamycin, the drug was added at a concentration of 0.03 mg/ml. For contraselection of cells carrying URA3 plasmids, 5-fluoro-orotic acid (FOA) (Fluorochem) was added to the solid medium at a concentration of 1 mg/ml.

Yeast cells were grown at 30°C unless otherwise mentioned.

9.2. Genetic techniques

9.2.1. Generation of yeast strains

9.2.1.1. Generation of double mutants by diploid construction, sporulation and tetrad dissection

Sporulation, tetrad dissection and scoring of genetic markers were performed as described (Sherman et al., 1974). Briefly, in order to obtain diploid yeast cells, haploid cells of opposite mating types, *Mat***a** and *Mat*α, were mixed on YPD plates and incubated for

approximately 12 hours at room temperature (RT). Subsequently, diploid cells were selected on appropriate minimal media (SDC lacking all amino acids, purine- or pyrimidine-bases that could be synthesized by the diploid but not by the haploid yeast cells). For sporulation, diploid cells were grown for 1 day on complete solid media and subsequently transferred to sporulation media (0.022% raffinose, 3g/l potassium acetate). The spores were separated under a tetrad microscope (Singer Instruments) and allowed to germinate and grow on complete media at RT.

The mating type of haploid cells was tested by plating the corresponding yeast either with *Mat***a** or *Mat*α tester strains bearing a *his1* mutation (not present in any other laboratory strain) on minimal media lacking all amino acids, purine- or pyrimidine-bases. Only yeast cells capable of mating with the testers (*Mat*α or *Mat***a** cells, respectively) were able to produce diploids that grew on the minimal media.

9.2.1.2. Plate assay for the detection of *bar1* mutants

Deletion of the *BAR1* gene was tested using a plate assay. This assay is based on the observation the *Mat***a** cells bearing double mutations in the *BAR1/SST1* and the *SST2* genes cannot recover from the cell cycle arrest induced by the α-factor pheromone (Sst2p is a negative regulator of the α-subunit of the Ste2p coupled heterotrimeric G-protein). Only when another *Mat***a** *BAR1* is plated nearby, the extracellular α-factor is degraded and the *Mat***a** *bar1 sst2* strain is able to grow.

To perform the assay, first, a YPD plate is overlaid with a saturated culture of the α-factor hyper-sensitive yeast strain (*Mat***a** *bar1 sst2* cells (SCMIG31)). A straight line of *Mat*α cells (i.e. SCMIG33) is then streaked in the middle of the plate. *Mat*α cells will secrete α-factor and inhibit growth of the SCMIG31 strain. As a consequence, a halo along both sides of the line of *Mat*α cells will be observed upon incubation at 30°C. The *Mat***a** cells to be analysed for the deletion of the *BAR1* gene are streaked perpendicular to the line of *Mat*α cells. If the tested strain is *BAR1*, the protease will degrade the α-factor secreted by the *Mat*α strain and the *Mat***a** *bar1 sst2* cells will be able to grow closer to the line of *Mat*α cells. In contrast, if a strain is *bar1*Δ, the α-factor will not be degraded and the SCMIG31 cells will not be able to grow close to the *Mat*α cells.

9.2.2. Yeast strains

The yeast strains used in this study are listed in table II. Not previously published strains were generated as follows.

SCMIG958

The strain was constructed by crossing the yeast strains SCMIG682 and SCMIG683. *Sjl1*Δ *sjl2*Δ double knockouts were selected on kanamycin-containing plates, choosing spores of tetrads with a 2:2 segregation of the kanamycin resistance.

Table II. Yeast strains

strain	genotype	reference
EGY48	*Mat*α *ura3 leu2 his3 trp1*	(Gyuris et al., 1993)
SCMIG182	*Mat***a** *ade2 ade3:: cmd1-226::TRP1 his3 leu2 lys2 trp1 ura3 cmd1*Δ*::HIS3 bar1*Δ*::LYS2*	(Geli et al., 1998)
SCMIG187	*Mat***a** *ade2 ade3:: cmd1-231::TRP1 his3 leu2 lys2 trp1 ura3 cmd1*Δ*::HIS3 bar1*Δ*::LYS2*	(Geli et al., 1998)
SCMIG19	*Mat***a** *his3 leu2 trp1 ura3 bar1*	(Idrissi et al., 2002)
SCMIG201	*Mat***a** *ade2 ade3:: cmd1-247::TRP1 his3 leu2 lys2 trp1 ura3 cmd1*Δ*::HIS3 bar1*Δ*::LYS2*	(Geli and Riezman, 1998)
SCMIG229 (RH4165)	*Mat***a** *arp2-2::URA3 ts GAL+ ade2 trp1 leu2 his ura3 bar1*	(Idrissi et al., 2002)
SCMIG271	*Mat*α *ura3 lys2 trp1 his3 leu2 ade2 cdc25-2*	(Aronheim and Karin, 2000)
SCMIG273	*Mat***a** *his3 leu2 ura3 trp1 las17*Δ*::LEU2*	(Naqvi et al., 1998)
SCMIG275	*Mat***a** *his3 leu2 lys2 trp1 ura3 bar1 myo5*Δ*::TRP1*	(Idrissi et al., 2002)
SCMIG304	*Mat***a** *his3 leu2 lys2 trp1 ura3 bar1 end5*Δ*::URA3 myo5*Δ*::TRP1* + pURA3*MYO5*	(Geli et al., 2000a)
SCMIG391 (RH2634)	*Mat***a** *his3 leu2 bar1 ura3 sla1*Δ*::URA*	H. Riezman
SCMIG392 (RH3654)	*Mat***a** *his3 trp1 lys2 leu2 bar1*Δ*::LYS2 ura3 pan1-4*	(Tang et al., 1997)
SCMIG458	*Mat***a** *abp1*Δ*::KMX leu2 his3 ura3 met15*	Euroscarf
SCMIG459	*Mat***a** *ent1*Δ*::KMX leu2 his3 ura3 met15*	Euroscarf
SCMIG533	*Mat***a** *his3 leu2 met15 ura3 bbc1*Δ*::KMX*	Euroscarf
SCMIG55 (RH1995)	*Mat***a** *his4 leu2 bar1 end3*Δ*::URA3*	H. Riezman
SCMIG57 (RH2892)	*Mat***a** *end5*Δ*::URA3 ura3 leu2 his4 lys2 bar1*	Howard Riezman
SCMIG59 (RH2905)	*Mat***a** *leu2 his4 ura3 trp1*Δ*::URA3 rvs167*Δ*::TRP1 bar1*	H. Riezman
SCMIG590	*Mat***a** *his3 leu2 trp1 ura3 bar1 myo3*Δ*::HIS3 myo5*Δ*::TRP1 pMYO5*	(Grosshans et al., 2006)
SCMIG61 (RH2897)	*Mat***a** *his4 leu2 lys2 ura3 bar1 end11(erg2)*Δ*::URA3*	(Munn et al., 1999)
SCMIG669	*Mat***a** *his3 trp1 lys2 ura3 leu2 bar1 sla2*Δ*::HIS3*	(Wesp et al., 1997)
SCMIG682	*Mat***a** *sjl1*Δ*::KMX ura3 his3 leu2 met1*	Euroscarf
SCMIG683	*Mat*α *sjl2*Δ*::KMX ura3 his3 leu2 lys2*	Euroscarf

SCMIG729	*Mat***a** *leu2 ura3 rme1 trp1 his3 GAL+ HMLa TOF3 mss4Δ::HIS3MX6 pYCplac111.MSS4*	(Desrivieres et al., 1998)
SCMIG730	*Mat***a** *leu2 ura3 rme1 trp1 his3 GAL+ HMLa TOF3 mss4Δ::HIS3MX6 pYcplac111.mss4-2ts*	(Desrivieres et al., 1998)
SCMIG754 (SL5006)	*Mat***a** *chc1Δ::LEU2* pRS426	(Tan et al., 1993)
SCMIG762	*Mat***a** *his3 leu2 ura3 met1 sac6Δ::KMX*	Euroscarf
SCMIG806	*Mat***a** *ent1Δ::KMX ent2Δ:: KMX ede1Δ::KMX: ura3 his3 leu2 met1 pent1-UIMΔ (LEU2)*	(Shih et al., 2002)
SCMIG947	*Mat***a** *ade2 ade3:: CMD1::TRP1 his3 his3 leu2 lys2 trp1 ura3 cmd1Δ::HIS3 bar1::LYS2*	(Geli et al., 1998)
SCMIG958	*Matα sjl1Δ::KMX sjl2Δ::KMX ura3 his3 leu2 met1*	this study
SCMIG990	*Mat***a** *his3 leu2 ura3 met1 vps11Δ::KMX*	Euroscarf
SCMIG991	*Mat***a** *his3 leu2 ura3 met1 vps16Δ::KMX*	Euroscarf
SCMIG992	*Mat***a** *his3 leu2 ura3 met1 vps18Δ::KMX*	Euroscarf
SCMIG993	*Mat***a** *his3 leu2 ura3 met1 vps33Δ::KMX*	Euroscarf

9.2.3. Methods of the PRS screening

9.2.3.1. Chemical mutagenesis with ethymethane sulfonate

The protocol for the chemical mutagenesis of yeast cells with ethylmethane sulfonate (EMS) is based on the method published by (Guthrie and Fink, 1991).

5 ml of yeast strain SCMIG271 bearing pYX5'SOS-*MYO5* and pYesM#7 were grown to saturation in medium containing 0.1% galactose at 23°C, harvested at 2400 g for 5 min and washed with 5 ml of 0.1 M Na-PO_4 buffer, pH 7. Cells were again harvested and resuspended in 20 ml 0.1 M Na-PO_4 buffer. 0.5 ml of culture was transferred into a glass tube and 35 µl of EMS (Sigma) was added. After careful mixing, the cells were incubated for 1 h at RT. To stop the mutagenesis 0.5 ml of 12% Na-thiosulfate was added and cells were transferred into a 15 ml Falcon tube. Cells were harvested at 3000 g for 3 min and washed twice with 0.1 M Na-PO_4 buffer, pH 7. After resupension in 1 ml of 0.1 M Na-PO_4 buffer, cells were counted under a microscope (Axiolab, Zeiss), using a Neubauer counting-chamber, and diluted to 500 cells/ml. Finally cells were plated on SGC-Leu-Ura plates containing 0.1% galactose.

9.2.3.2. Selection of *mpr* (myosin plasma membrane recruitment) mutants

The mutagenized *cdc25-2* cells were incubated on SGC-Leu-Ura plates for 3 days at 24°C. Colonies were then replica-plated on SGC-Leu medium selecting only for the pYX5'SOS-*MYO5* plasmid and incubated again at 24°C. After 2 days of growth the colonies were plated on SGC-Leu medium containing 1 mg/ml 5'-fluoroorotic acid (FOA). Also the original

plates of the screening were replica-plated, again on SGC-Leu-Ura medium selecting for the 2 plasmids. Both types of replicas (SGC-Leu plates with FOA and SGC-Leu-Ura plates) were incubated at 31°C and the following 2-4 days growth of corresponding colonies was observed. Colonies that showed clearly better growth on the SGC-Leu-Ura medium than on the FOA-medium were selected.

9.2.3.3. Outcrossing of *mpr* mutants

For the purification of the *mpr* mutations from the *cdc25-2* mutation, the temperature sensitive *mpr* mutants were crossed to a wild-type strain (SCMIG19). After tetrad dissection and sporulation, those spores were selected which were bearing the *mpr* mutation alone. For the identification of the *mpr* mutants, spores that were bearing the pYX5'SOS-*MYO5* plasmid were selected on SDC-Leu medium, transferred to new SDC-Leu plates and incubated at 37°C. If 4 spores of the same tetrad were not growing on SDC-Leu at 37°C, 2 spores were ts due to the *cdc25-2* mutation and 2 spores were ts due to the *mpr* mutation. The *mpr* mutants could then be identified by a growth defect on SGC-Leu at 37°C. As all spores were bearing the pYX5'SOS-*MYO5* plasmid, *cdc25-2* cells could be rescued by 5'Sos-Myo5p expression, while *mpr* mutants were still defective in growth.

9.2.3.4. Identification of mutants by complementation with a genetic library

For the identification of the temperature sensitive *mpr* mutants, cells were transformed with the genomic plasmid library, plated on YPD plates and incubated at RT. After 12 hours, the cells were shifted to 37°C. 3 days later, colonies were picked and the plasmid DNA was purified. Isolated plasmids were digested with restriction enzymes to check if they have an insert and if perhaps similar digestion patterns could be observed for plasmids isolated from the same mutant. Plasmids were retransformed into the original mutant and cells were grown as before to control again the effect of the plasmid. Finally, the DNA sequence of the genomic insert of the plasmid was identified by sequencing with primers #140 and #141.

9.2.3.4.1. The yeast genomic library

The yeast genomic library used in this study was constructed by Brian Stevenson from the H. Riezman lab. Genomic DNA was partially digested with Sau3A and partially filled in using the Klenow DNA polymerase fragment in the presence of dGTP and dATP. Fragments were ligated into the *Sal*I site of Ycplac111, which had been partially filled in using the Klenow DNA polymerase fragment in the presence of dTTP and dCTP.

9.3. DNA techniques and plasmid construction

Standard DNA manipulations (gel electrophoresis, enzymatic digestion, ligation, transformation, plasmid preparation and polymerase chain reaction) were performed as described (Sambrook et al., 1989; Sambrook and Russel, 2001)

Enzymes for molecular biology were obtained from New England Biolabs or Roche.

Plasmids were purified with the *Nucleospin* plasmid purification kit (Macherey-Nagel).

DNA was purified from agarose gels using the gel extraction kit from Qiagen.

PCRs were performed using a DNA polymerase with proof-reading activity (Vent polymerase; New England Biolabs) and a TRIO-thermoblock (Biometra).

9.3.1. Introduction of DNA into cells

Electroporation of *E. coli* was performed as described (Sambrook et al., 1989).

Transformation of yeast was accomplished by the lithium acetate method (Ito et al., 1983).

9.3.2. Extraction and purification of plasmid DNA from *S. cerevisiae*

A 5 ml culture of yeast in stationary phase was harvested at 2300 g for 5 min. Cells were resuspended in 0.4 ml of lysis buffer (0.2 M Tris-HCl pH 7.5, 0.5 M NaCl, 1% SDS, 10 mM EDTA) and transferred to a 1.5 ml Eppendorf tube. 150 µl of glass beads and 300 µl of phenol:chloroform:isoamyl alcohol (25:24:1) were added and cells were lysed by vortexing for 2 min. Upon centrifugation at 20,000 g for 5 min, the aqueous phase (upper phase) was transferred into a new 1.5 ml tube and the DNA was further purified by phenol:chloroform extraction. The plasmid DNA was then concentrated by ethanol precipitation and finally resuspended in 50 µl H_2O. To obtain pure plasmid DNA, electro-competent *E.coli* cells were transformed with the plasmid prepared from the yeast cells. Plasmid DNA was purified from single colonies and analyzed by digestion with restriction enzymes and analytical agarose gel-electrophoresis.

9.3.3. Extraction and purification of genomic DNA from *S. cerevisiae*

20 ml of yeast cells were grown to 10^7 cells/ml, harvested at 2300 g for 5 min and resuspended in 1 ml of 1 M sorbitol. Cells were collected in an Eppendorf tube at 5200 g for 2 min and resuspended in 0.5 ml of 1 M sorbitol, 50 mM potassium phosphate buffer pH 7.5, 14 mM β-mercaptoethanol, 40 µg/ml Zymolyase 20T (Seikagaku). After incubation for 30 min at 30°C spheroblasts were collected at 5200 g for 2 min and resupended in 0.5 ml of 50 mM EDTA pH 8.0, 0.2% SDS. The sample was then incubated for 15 min at 65°C. 50 µl of 5 M potassium acetate pH 7.5 was added and the tube was incubated on ice for 1 h. The precipitate was sedimented at 20,000 g for 15 min and the supernatant was transferred into a new Eppendorf tube. 1 ml ethanol was added and the genomic DNA precipitate was

collected at 20,000 g for 15 sec. The supernatant was discarded and the pellet was air-dried and resuspended in 200 µl of TE. The DNA was then incubated at 37°C for 15 min in the presence of RNase A (50 µg/ml). For further purification the sample was extracted 3 times with phenol:chloroform:isoamyl alcohol (25:24:1). Finally, the genomic DNA was precipitated with ethanol and resuspended in 50µl of TE-buffer (10 mM Tris pH 7.5, 1 mM EDTA).

9.3.4. Plasmids

Plasmids used in this study and their relevant features are listed in table III. Primers used in this study are listed in table IV.

Table III. Plasmids

Plasmid*	Yeast marker	Insert	Reference
p181*LAS17*	*LEU2*	*LAS17*	(Naqvi et al., 1998)
p33myc*MYO5*	*LEU2*	*myc-MYO5*	I.M. Fernandez
p33*MYO5*	*URA3*	*MYO5*	(Geli and Riezman, 1996)
p33*myo5*-996STOP	*URA3*	myo5 aa 1-996	(Geli et al., 2000a)
p33*MYO5*-HA_3	*URA3*	*MYO5* + 3HA	(Idrissi et al., 2002)
p33myo5Δ IQ	*URA3*	myo5 (aa 1-1219-(aa 725-735)Δ, (aa 743-753)Δ)	(Geli et al., 1998)
p33*myo5*Δn	*URA3*	*myo5* (aa 1-1219-(aa 705-773)Δ)	this study
p33*myo5*ΔT	*URA3*	*myo5* (aa 1-1219-(aa 774-905)Δ)	this study
pEG202	*HIS3*	LexA	(Gyuris et al., 1993)
pEG202-nT	*HIS3*	myo5 aa 1-996	this study
pEG202-T	*HIS3*	myo5 aa 757-996	M.I. Geli
p*ENT1*-GFP	*URA3*	*ENT1*-GFP	this study
pFA6a-GFP(S65T)TRP1	-	*GFP-TRP1 cassette*	(Longtine et al., 1998)
pGEX-4T-1	-	GST	Pharmacia
pGEX-5X-3	-	GST	Pharmacia
pGFP-*ABP1*	*URA3*	GFP-*ABP1*	this study
pGFP-GSa	*URA3*	GFP-*myo5* (aa 996-1219)	this study
pGFP-H	*URA3*	GFP-*myo5* (aa 1-704)	this study
pGFP-Hn	*URA3*	GFP-*myo5* (aa 1-773)	this study
pGFP-HnT	*URA3*	GFP-*myo5* (aa 1-996)	this study
pGFP-*MYO5*	*URA3*	GFP-*MYO5*	this study
pGFP-*MYO5*.LEU	*LEU2*	GFP-*MYO5*	this study
pGFP*myo5*Δn	*URA3*	GFP-*myo5* (aa 1-1219 -(aa 705-773)Δ)	this study
pGFP*myo5*ΔT	*URA3*	GFP-*myo5* (aa 1-1219 -(aa 774-905)Δ)	this study

pGFP-n	*URA3*	GFP-*myo5* (aa705-773)	this study
pGFP-nT	*URA3*	GFP-*myo5* (aa 705-996)	this study
pGFP-nTC	*URA3*	GFP-*myo5* (aa 705-1219)	this study
pGFP-TC	*URA3*	GFP-*myo5* (aa 774-1219)	this study
pGST-C	-	GST-*myo5* (aa 982-1219)	(Geli et al., 2000a)
pGST-*CMD1*	-	GST-*CMD1*	this study
pJG4-5	*TRP1*	B42	(Gyuris et al., 1993)
pLH309	-	*bar1Δ::URA3* (*BAR1* k.o.)	L. Hicke
p*MYO5*	*LEU2*	*MYO5*	(Geli et al., 2000a)
p*MYO5*-YFP (Ycplac112 background)	*TRP1*	*MYO5*-YFP	F. Idrissi
p*myo5*Δn	*LEU2*	*myo5* (aa 1-1219-(aa 705-773)Δ)	this study
p*myo5*ΔT	*LEU2*	*myo5* (aa 1-1219-(aa 774-905)Δ)	this study
pmyrRin	*URA3*	*myristoylation site-RIN*	A. Aronheim
pNOPGFP2L	*LEU2*	*NOP1* promoter-GFP	E. Hurt
pProtA-GSa	*URA3*	ProtA-*myo5* (aa996-1219)	this study
pProtA-*MYO5*	*URA3*	*MYO5*	(Grosshans et al., 2006)
pProtA-myo5ΔC	*URA3*	myo5 (aa 1-996)	this study
pProtA-myo5ΔIQ	*URA3*	myo5 (aa 1-1219- (aa 725-735)Δ, (aa 743-753)Δ)	this study
pProtA-nT	*URA3*	ProtA-*myo5* (aa705-996)	this study
pProtA-nTC	*URA3*	ProtA-*myo5* (aa705-1219)	F. Idrissi
pProtA-TC	*URA3*	ProtA-*myo5* (aa774-1219)	this study
pRFM-1	*HIS3*	LexA-Bicoid	(Gyuris et al., 1993)
pYES-5'SOS	*URA3*	*5'Sos* (aa 1-1068)	(Aronheim and Karin, 2000)
pYX243	*LEU2*	-	R&D Systems Europe Ltd
pYX5'SOS	*LEU2*	5'Sos (aa 1-1068)	this study
pYX5'SOS.TRP	*TRP1*	5'Sos (aa 1-1068)	this study
pYX5'SOS-*ABP1*	*LEU2*	5'Sos-*ABP1*	this study
pYX5'SOS-C	*LEU2*	5'Sos-*myo5* (aa 996-1219)	this study
pYX5'SOS-*ENT1*	*LEU2*	5'Sos-*ENT1*	this study
pYX5'SOS-H	*LEU2*	5'Sos-*myo5* (aa 1-704)	this study
pYX5'SOS-Hn	*LEU2*	5'Sos-*myo5* (aa 1-773)	this study
pYX5'SOS-HnT	*LEU2*	5'Sos-*myo5* (aa 1-995)	this study
pYX5'SOS-*MYO5*	*LEU2*	*5*'Sos-*MYO5*	this study
pYX5'SOS-*myo5*Δn	*LEU2*	5'Sos-*myo5* (aa 1-1219 -(aa 705-773)Δ)	this study
pYX5'SOS-*myo5*ΔT	*LEU2*	5'Sos-*myo5* (aa 1-1219 -(aa 774-905)Δ)	this study
pYX5'SOS-nT	*LEU2*	5'Sos-*myo5* (aa 705-995)	this study
pYX5'SOS-nTC	*LEU2*	5'Sos-*myo5* (aa 705-1219)	this study
pYX5'SOS-T	*LEU2*	5'Sos-*myo5* (aa 774-995)	this study
pYX5'SOS-TC	*LEU2*	5'Sos-*myo5* (aa 774-1219)	this study

pYX*MYO5*	*LEU2*	*MYO5*	F. Idrissi
YCplac111	*LEU2*	-	(Gietz and Sugino, 1988)
YCplac22	*TRP1*	-	(Gietz and Sugino, 1988)
YCplac33	*URA3*	-	(Gietz and Sugino, 1988)
YDP-L	*LEU2*	-	(Berben et al., 1991)
YDp-W	*TRP1*	-	(Berben et al., 1991)

*All plasmids listed in this table carry a bacterial *ori* and an *Amp*^{R} resistance gene.
Plasmids of the pEG202, pJG4-5, Ycplac112 and pYX243 series are 2µ (multi-copy) plasmids. All other plasmids, which contain a yeast marker, are *CEN* (low-copy) plasmids.

Not previously published plasmids were generated as follows.

pGST-*CMD1*

A DNA fragment encoding *Cmd1p* was amplified by PCR using the primers CMD1.1D.MfeI and CMD1.444U.XhoI and pYXCMD1 as template. The PCR fragment was digested with *Mfe*I and *Xho*I and cloned into *EcoR*I/*Sal*I cut pGEX-4T-1, inserting the *CMD1* sequence in frame downstream of the glutathione-S-transferase.

p33*myo5*Δn

A *MYO5* DNA fragment missing the sequence encoding the myosin neck (aa 705-773) was synthesized by a 2-step PCR. First, 2 overlapping DNA fragments were amplified by PCR using p33*MYO5* as the template and the primer pairs M1502D/ M5.Th1.2112U and M5.2320D/ M52955U. The second PCR reaction used the 2 PCR fragments as template and the primers M1502D and M52955U.
For homologous recombination the product of the 2-step PCR was co-transformed into yeast with *Kpn*I/*Bst*EII digested p33*MYO5*. Cells were selected on SDC-Ura, plasmids were recovered and successful recombination was identified by restriction analyses.

p33*myo5*ΔT

This plasmid was constructed as described for **p33*myo5*Δn**, using the primer pairs M1502D /M5.Th2.2319U and M5.2986D/ C9E1 for the first PCRs and the primers M1502D and C9E1 for the final PCR.

p*myo*5Δn and **p*myo*5ΔT**

These plasmids were constructed by homologous recombination in yeast, substituting *URA3* in p33*myo5*-(N)Δ and p33*myo5*-(T)Δ by *LEU2*. A DNA fragment containing *LEU2* flanked by sequences upstream of the ATG and downstream of the STOP of *URA3* was

amplified by PCR using the primers URAD.D and URAD.U and YDp-L as template. The DNA fragment was co-transformed with p33*myo5*-(N)Δ and p33*myo5*-(T)Δ into yeast and cells were selected on SDC-Leu. Plasmids were recovered from yeast and p33*myo5*-(N)Δ.LEU and p33*myo5*-(T)Δ.LEU were identified by restriction analysis.

pYX5'SOS

The vector pYX243 was digested with *Eco*RI and the 5' overhangs were filled in using the Klenow DNA polymerase fragment. The linearized plasmid was then digested with *Bam*HI and a *Sma*I/*Bam*HI cut 5'Sos DNA fragment, isolated from pYes-5'Sos, was ligated into it.

pYX5'SOS.TRP

This plasmid was obtained by substituting *URA3* in pYX5'SOS by *TRP1* by homologous recombination in yeast. A DNA fragment containing *TRP1* flanked by sequences upstream of the ATG and downstream of the STOP codon of the URA3 gene was amplified by PCR using the primers URAD.D and URAD.U and YDp-W as template. The DNA fragment was then co-transformed with pYX5'SOS into yeast and cells were selected on SDC-Trp. Plasmids were recovered from yeast and pYX5'SOS.TRP1 was identified by restriction analysis.

9.3.4.1. Plasmids for expression of 5'Sos constructs

pYX5'SOS-*ENT1*

The DNA sequence encoding the *ENT1* ORF was amplified by PCR from genomic DNA using the primers Ent1.ApaI.1D and Ent1.XhoI.1565U. The PCR fragment was digested with *Apa*I and *Xho*I and ligated into *Apa*I/*Sal*I cut pYX5'SOS.

pYX5'SOS-*ABP1*

The DNA sequence encoding the *ABP1* ORF was amplified by PCR from genomic DNA using the primers Abp1.1D.ApaI and Abp1.2779U.MluI. The PCR fragment was cut with *Apa*I and *Mlu*I and ligated into *Apa*I /*Mlu*I cut pYX5'SOS.

Plasmids for expression of the 5'Sos Myo5p constructs

The plasmids were obtained by inserting different PCR fragments in frame downstream of 5'SOS into pYX5'SOS.

MYO5 and *myo5* fragments were amplified from the plasmids listed in the table below. pYX5'SOS and PCR fragments were digested with *Apa*I and *Mlu*I and the PCR fragments were subsequently ligated into pYX5'SOS.

plasmid	Myo5p-fragment	primer	template
pYX5'SOS-*MYO5*	aa 1-1219	Myo5.1.ApaI.D, M5.3660U.SOS	p33*MYO5*
pYX5'SOS-nTC	aa 705-1219	M5.2113D.SOS, M5.3660U.SOS	p33*MYO5*
pYX5'SOS-TC	aa 774-1219	M5.2320D.SOS, M5.3660U.SOS	p33*MYO5*
pYX5'SOS-C	aa 996-1219	M5.2986D.SOS, M5.3660U.SOS	p33*MYO5*
pYX5'SOS-HnT	aa 1-995	Myo5.1.ApaI.D, M5.2985U.SOS	p33*MYO5*
pYX5'SOS-Hn	aa 1-773	Myo5.1.ApaI.D, M5.2319U.SOS	p33*MYO5*
pYX5'SOS-H	aa 1-704	Myo5.1.ApaI.D, M5.2112U.SOS	p33*MYO5*
pYX5'SOS-nT	aa 705-995	M5.2113D.SOS, M5.2985U.SOS	p33*MYO5*
pYX5'SOS-T	aa 774-995	M5.2320D.SOS, M5.2985U.SOS	p33*MYO5*
pYX5'SOS-*myo5*Δn	aa 1-1219 -(aa 705-773)Δ	Myo5.1.ApaI.D, M5.3660U.SOS	p33*myo5*Δn
pYX5'SOS-*myo5*ΔT	aa 1-1219 -(aa 774-905)Δ	Myo5.1.ApaI.D, M5.3660U.SOS	p33*myo5*Δn

9.3.4.2. Plasmids for expression of GFP constructs

pGFP-*ABP1*

The sequence encoding the *ABP1* gene was amplified by PCR from genomic DNA using the primers ABP1.-522D.BamHI and ABP1.2239U.SphI. The PCR product was cut with *Bam*HI and *Sph*I and ligated into the *Bam*HI/*Sph*I cut Ycplac33 to generate p33*ABP1*.

The START codon of *ABP1* was then exchanged by 2 restriction sites of *Pme*I. A DNA-fragment bearing the restriction sites was synthesized by a 2-step PCR. First 2 DNA fragments were amplified by PCR using the primer pairs Abp1.-522D.BamHI / 2PmeI.Abp1.-1U and Abp1.479U / 2PmeI.Abp1.3D and p33*ABP1* as template. The second PCR reaction used the 2 PCR products as template and the primers Abp1.-522D.BamHI and 2PmeI.Abp1.3D. The second PCR product was digested with *BamH*I and *Eag*I and ligated into the *BamH*I/*Eag*I cut *p33*ABP1.

Finally, the DNA fragment coding for GFP was inserted upstream of *ABP1*. The GFP-fragment was amplified by PCR with the primers GFP.SmaI.D and GFP.SmaI.U and pNOPGFP2L as template, cut with *Sma*I and ligated into the previously inserted *Pme*I site of p33*ABP1*.

p*ENT1*-GFP:

A DNA sequence encoding the Ent1p ORF was amplified by PCR from genomic DNA using the primers Ent1.HdIII.-600D and Ent1.XhoI.1565U, cut with *Hind*III and *Xho*I and ligated into the *Hind*III/*Sal*I cut Ycplac33 (p33*ENT1*). The GFP sequence, together with *TRP1*, was then cloned downstream of the last codon of *ENT1* by homologous recombination. A PCR fragment was amplified using the primers Ent1.F2 and Ent1.R1 and pFA6a-GFP(S65T)-TRP1 as template. The PCR product was transformed into yeast cells, together with p33*ENT1*. Cells were selected on SDC-Trp, plasmids were recovered and successful recombination was identified by restriction analysis.

Plasmids for expression of GFP-Myo5p constructs

For construction of **pGFP-*MYO5*** and **pGFP-HnT** a PCR-product of the sequence encoding for GFP was amplified from pNOP-GFP2L with the primers GFP.SmaI.D and GFP.SmaI.U, cut with *Sma*I and ligated into the *Msc*I site upstream of the *MYO5* sequence in p33*MYO5* and p33myo5-996STOP, respectively. **pGFP*myo5*ΔT** and **pGFP*myo5*Δn** were obtained by ligating the same PCR fragment into the *Msc*I site of p33*myo5-(T)Δ* or p33*myo5-(N)Δ.*

pGFP-nTC, pGFP-TC, pGFP-C and **GFP-nT** were obtained by homologous recombination in yeast. For each plasmid, a PCR-fragment was amplified with the primers listed below and p33*MYO5* as template. The PCR products were then co-transformed into yeast with *Kpn*I/*Bst*EII digested pGFP-MYO5 or *Kpn*I/*Bst*EII digested pGFP-HnT (see table). Cells were selected on SDC-Ura, plasmids were recovered and successful recombination was identified by restriction analyses.

plasmid	primers	*Kpn*I/*Bst*EII cut plasmid for recombination
pGFP-nTC	5RU1, M5-27.neck.D	pGFP-*MYO5*
pGFP-TC	5RU1, M5-27.TH1.D	pGFP-*MYO5*
pGFP-C	C9E1, M5-27.TH2.D	pGFP-*MYO5*
pGFP-nT	M52955U, M5-27.neck.D	pGFP-HnT

For construction of **pGFP-H**, **pGFP-Hn** and **pGFP-n** PCR fragments were amplified with the primers and templates listed in the table below, cut with *Eco*RI and *Bam*HI and ligated into the *Eco*RI/*Bam*HI cut Ycplac33.

plasmid	primers	template
pGFP-H	M5.-640D, M5.2112U.STOP.BamHI	pGFP-MYO5
pGFP-Hn	M5.-640D, M5.2320U.STOP.BamHI	pGFP-MYO5
pGFP-n	M5.-640D, M5.2320U.STOP.BamHI	pGFP-nTC

pGFP-*MYO5*.LEU was constructed by substituting *URA3* in pGFP-*MYO5* by *LEU2* by homologous recombination in yeast. A DNA fragment encoding *LEU2* flanked by sequences upstream of the ATG and downstream of the STOP codon of *URA3* was amplified by PCR using the primers URAD.D and URAD.U and YDp-L as template. The DNA fragment was co-transformed with pGFP-*MYO5* into yeast and cells were selected on SDC-Leu. Plasmids were recovered from yeast and pGFP-*MYO5*.LEU was identified by restriction analysis.

9.3.4.3. Plasmids for expression of ProtA-Myo5p constructs

In these plasmids 2 IgG-binding motifs of the Protein A from *Staphylococcus aureus* followed by a TEV (tobacco etch virus) protease restriction site was cloned upstream of the *myo5* sequence.

pProtA-myo5Δn, **pProtA-myo5ΔT**, **pProt-myo5ΔC** and **pProtA-myo5ΔIQ** were constructed by ligating a *Sna*BI/*Hpa*I fragment, which was cut out from pProtA-*MYO5*, into the plasmids p33*myo5*-(N)Δ, p33*myo5*-(T)Δ, p33*myo5*-996STOP and p33myo5-(IQ)Δ, respectively

pProtA-TC, and **pProtA-C** were constructed by homologous recombination. A PCR-fragment was amplified with the primers listed in the table below and p33*MYO5* as template and then co-transformed into yeast with *Kpn*I/*Bst*EII digested p33ProtA-*MYO5*. Cells were selected on SDC-Ura, plasmids were recovered and successful recombination was identified by restriction analyses.

plasmid	primers
pProtA-TC	C9E1, ProtA.M5.2320D
pProtA-C	C9E1, ProtA.M5.2986D

pProtA-nT was also constructed by homologous recombination in yeast. A PCR was performed with the primers M52955 and M1502D and pProtA-nTC as template. The amplified fragment was co-transformed with pGFP-HnT for recombination. Cells were selected on SDC-Ura, plasmids were recovered and successful recombination was identified by restriction analyses.

9.3.5. Primers

Table IV. Primers

Name	Sequence*	Restriction site	Direction#
2PmeI.Abp1.-1U	GTTTAAACGGTTGGTTGTTTAAACT GTGATTGATAGGTGTGTGCG		3’
2PmeI.Abp1.3D	GTTTAAACAACCAACCGTTTAAACG CTTTGGAACCTATTGATTATACTACT C		5’
5RU1	GGTGGTGGGGCAGGCTTTTTAGA		3’
ABP1.2239U.SphI	AACCAAGCATGCTGGGAGACTCTTC ATGCATTTC	*Sph*I	3’
Abp1.479U	CGGGAGGAGTGGAAG		3’
ABP1.-522D.BamHI	ACCAAGGATCCCAGAATACTCTTAG AGCTCATCGC	*Bam*HI	5’
C9E1	GCCCTAGCAGCAAGCG		3’
CMD1.1D.MfeI	AACCAACCCAATTGATGTCCTCCAA TCTTACCGAAGAAC	*Mfe*I	5’
CMD1.444U.XhoI	AACCAACTCGAGCTATTTAGATAAC AAAGCAGC	*Xho*I	3’
Ent1.F2	AATGGCTCAAATAACCGGGGATATA CTCTAATTGATTTACGGATCCCCGG GTTAATTAA		5’
Ent1.HdIII.-600D	AACCAAAAGCTTGGAAGTGAAGAA TCTAGCCAAAG	*Hind*III	5’
Ent1.R1	CATCTGATTAGAAATGCGGACTGGA ATGACAGAATCACTGAATTCGAGCT CGTTTAAAC		3’
Ent1.XhoI.1565U	AACCAACTCGAGCGTCCTGAACTAC GTTAGTTTAC	*Xho*I	3’
GFP.SmaI.D	AACCACCCGGGATGTCAGCATGCAG TAAAGGAGAAGAAC	*Sma*I	5’
GFP.SmaI.U	AACCACCCGGGAGTTTGTATAGTTC ATCCATGCCATGTG	*Sma*I	3’
M1502D	GTTATTAAGCATTATGCCGG		5’
M5.2112U.SOS	CAACCACGCGTAGGTGTTTTGATGA AAACACTTGTG	*Mlu*I	3’
M5.2112U.STOP.BamHI	ACCAAGGATCCTTAAGGTGTTTTGA TGAAAACACTTGTG	*Bam*HI	3’
M5.2113D.SOS	CTTCCGGGCCCGAAACATTATTTGC TTTGGAGCATATGAG	*Apa*I	5’
M5.2319U.SOS	CAACCACGCGTTCTTTCTTTTCTTCC ACCCAAAACC	*Mlu*I	3’
M5.2320D	AGGTCTATGTCCTTATTAGGTTACA GAGC		5’
M5.2320D.SOS	CAACCGGGCCCAGGTCTATGTCCTT ATTAGGTTACAG	*Apa*I	5’
M5.2320U.STOP.BamHI	ACCAAGGATCCTTATCTTTCTTTTCT TCCACCCAAAACC	*Bam*HI	3’

M5.2985U.SOS	CAACCACGCGTTGCAGCAATCGAAACTGGCC	*Mlu*I	3’
M5.2986D	GCCCAGCATGTTCCCACC		5’
M5.2986D.SOS	ACCAAGGGCCCGCCCAGCATGTTCCCACC	*Apa*I	5’
M5.3660U.SOS	CAACCACGCGTTTACCAATCATCTTCCTCTTCATCTTC	*Mlu*I	3’
M5.-640D	CAAGAGGAATTGGACGCTAAG		5’
M5.Th1.2112U	GCTCTGTAACCTAATAAGGACATAGACCTAGGTGTTTTGATGAAAACACTTG		3’
M5.Th2.2319U	GGTGGGAACATGCTGGGCTCTTTCTTTTCTTCCACCCAAAAC		3’
M5-27.neck.D	CAATACGAATTTAACCGCTTTATAGAAATGGAAACATTATTTGCTTTGGAGCATATGAG		5’
M5-27.TH1.D	CAATACGAATTTAACCGCTTTATAGAAATGAGGTCTATGTCCTTATTAGGTTACAG		5’
M5-27.TH2.D	CAATACGAATTTAACCGCTTTATAGAAATGGCCCAGCATGTTCCCACC		5’
M52955U	GTTGCTTGCGAGGAACTAGC		3’
Myo5.1.ApaI.D	GCCGGGGGCCCATGGCTATCTTAAAAAGAGGAGC	*Apa*I	5’
PEP5.1D.EcoRV	AACCAAGATATCCATGTCCCTGAGCTCCTGG	*Eco*RV	5’
PEP5.3087U.XhoI	AACCAACTCGAGTTAAATAGTGATGTCAGAATAACTGATGG	*Xho*I	3’
ProtA.M5.2320D	CTGCAGGAATTCGATATCCCAACGACCGAAAACCTGTATTTTCAGGGCAGGTCTATGTCCTTATTAGGTTACAG		5’
ProtA.M5.2986D	CGTCAGGAATTCGATATCCCAACGACCGAAAACCTGTATTTTCAGGGCGCCCAGCATGTTCCCACC		5’
ProtA-M5.2113D	CTGCAGGAATTCGATATCCCAACGACCGAAAACCTGTATTTTCAGGGCGAAACATTATTTGCTTTGGAGCATATGAG		5’
URA3D.D	CACAGAACAAAAACCTGCAGGAAACGAAGATAAATC GAATTCCCGGGGATCCGGTGATG		5’
URA3D.U	GTGAGTTTAGTATACATGCATTTACTTATAATACAGTGCAGGTCGACGGATCCGGTGATTG		3’
#140	AACAGCTATGACCATG		5’
#141	TGAAAACGACGGCCAGT		3’

*The sequences of the primers are written from the 5’ to the 3’ end.
#Primers amplifying the coding strand are named 5’ primers, primers amplifying the complementary strand are 3’ primers.

9.4. Purification of yeast plasma membrane and cytosol

The isolation of highly enriched plasma membrane fractions and the preparation of cytosol were performed in parallel (see figure 31). The purification of plasma membrane on a discontinuous sucrose gradient is based on the protocol from R. Serrano (Serrano, 1988).

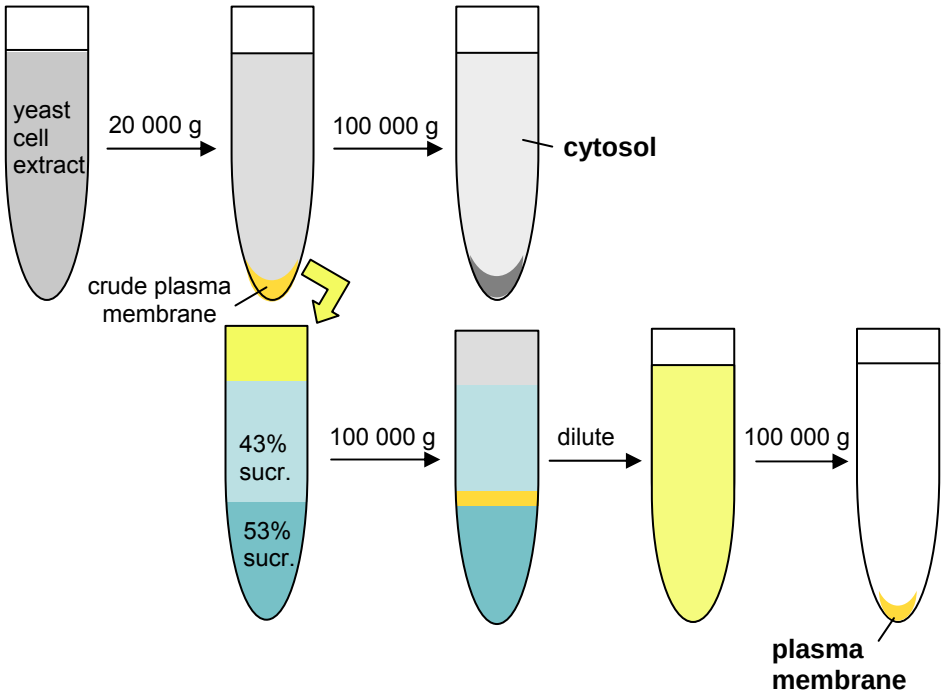

Figure 31. Scheme of the protocol for the purification of plasma membrane and cytosolic fractions (see text for details).

2 l of yeast cells were grown to an OD_{600} of 1.0, washed once with water and once with lysis buffer (25 mM Tris, pH 8.5, 5 mM EDTA), harvested into 2 50 ml centrifugation tubes at 2400 g for 5 min and frozen at -20°C.

Cells were thawed, one-tenth pellet volume of lysis buffer was added and the cells were glass bead-lysed in the presence of protein inhibitors (0.5 mM PMSF, 1µg/ml aprotinin, 1µg/ml pepstatin, 1µg/ml leupeptin, 1µg/ml antipain). The cell extract was recovered, transferred into a single 50 ml Falcon tube and diluted with lysis buffer, 0.5 mM PMSF up to a volume of 12.5 ml. Unbroken cells and cell debris were eliminated by centrifugation at 700 g for 10 min at 4°C. The supernatant was recovered (supernatant A) and the pellet was resuspended in 12.5 ml of breakage buffer (10 mM Tris, pH 7.5, 0.2 mM EDTA, 0.2 mM DTT), 0.5 mM PMSF. After centrifugation at 700 g for 10 min at 4°C, the supernatant (supernatant B) was mixed with the same volume of supernatant A. The combined supernatants (= total) were then centrifuged in a swing out rotor (JS-13.1, Beckman) at 20,000 g for 20 min at 4°C. The supernatant was collected (= precytosol) and the pellet was resupended in 10 ml of

breakage buffer, 0.5 mM PMSF. To eliminate non-solubilized material the membrane suspension was again centrifuged at 700 g for 10 min at 4°C. The supernatant was then applied to a discontinuous sucrose gradient made of 9 ml of 53% (w/w) and 18 ml of 43% sucrose in breakage buffer in an Ultra-Clear ultracentrifuge tube (#344058, Beckman).
Centrifugation was carried out in a SW-28 Beckman rotor at 100,000 g for 3h at 4°C. The 43% / 53% interphase of the sucrose gradient was recovered, diluted with 6 volumes of water and the plasma membrane was recovered by centrifugation at 80,000 g for 20 min at 4°C. The plasma membrane pellet was dissolved in 1.3 ml of breakage buffer plus lysis buffer (1:1), 0.5mM PMSF. To obtain the cytosol, the precytosol was cleared from membranes by centrifugation in a SW-28 Beckman rotor at 100,000 g for 3h at 4°C. The supernatant was recovered.

9.5. Protein techniques

9.5.1. SDS-PAGE, immunoblots and antibodies

SDS-PAGE was performed as described (Laemmli, 1970) using a Minigel system (BioRad Laboratories, München). High and low range SDS-PAGE molecular weight standards (BioRad Laboratories, München) were used for determination of apparent molecular weights. Coomassie Brilliant blue staining (colloidal Brilliant Blue G, Sigma) was used for detection of total protein on acrylamide gels.
Protein concentrations were determined with a BioRad Protein assay (BioRad Laboratories).
Immunoblots were performed as described (Geli et al., 1998).
For detection of peroxidase-conjugated antibodies an enhanced chemoluminescence (ECL) detection kit (Amersham Biosciences) was used.
Proteins on nitrocellulose membranes were stained with Ponceau Red
The primary and secondary antibodies used for detection of proteins are listed in the tables V and VI.

Table V. Primary Antibodies

Primary antibody	Type	Source/ Reference	Dilution
PAP (Peroxidase-anti-peroxidase)	rabbit anti-horseradish peroxidase conjugated to horseradish peroxidase	DAKO A/S	1:1000
anti-Gas1	rabbit-serum raised against recombinant Gas1p	(Muniz et al., 2000)	1:50,000
anti-Hxk1	rabbit-serum raised against recombinant Hxk1p	(van Tuinen and Riezman, 1987)	1.2000
anti-Cmd1	rabbit-serum raised against recombinant purified Cmd1p	(Geli et al., 1998)	1:1000
anti-HA	rat monoclonal antibody (3F10) against a hemagglutinin epitope	Roche	1:1000
anti-HA-perox	rat monoclonal antibody (3F10) against a hemagglutinin epitope, peroxidase conjugated	Roche	1:500
anti-myc-perox	mouse monoclonal antibody (9E10) against a peptide of human c-myc protein	Roche	1:2000
anti-GST	goat-serum against schistosomal glutathion-S-transferase	Amersham Biocsciences,	1:2000
anti-LexA	mouse monoclonal antibody, peroxidase conjugated	Santa Cruz	1:2000
anti-Myo5p	Rabbit-serum raised agains a C-terminal peptide of Myo5p (IPTPPQNRDVPK)	(Geli et al., 1998)	1:1000

Table VI. Secondary antibodies

Secondary antibody	Type	Source/ Reference	Dilution
goat anti-mouse	horseradish peroxidase goat anti-mouse IgG	Sigma	1:4000
goat anti-rabbit	horseradish peroxidase goat anti-rabbit IgG	Sigma	1:5000
goat anti-rat	horseradish peroxidase goat anti-rat IgG	Sigma	1:5000
rabbit anti-goat	horseradish peroxidase goat anti-rat IgG	Sigma	1:2000

9.5.2. Purification of recombinant GST fusion proteins

GST fusion proteins were purified from BL21 *E.coli* strains (Novagen). Glutathion Sepharose beads were obtained from Amersham Biosciences.

9.5.2.1. Purification of GST

For purification of GST BL21 cells carrying pGEX-5X-3 were grown in LB media containing 50 mg/l ampicillin at 37°C. At OD_{600} 0.6, isopropyl-β-D-thiogalactopyranoside (IPTG) was added to a concentration of 1 mM and the culture was incubated for 4 h at 37°C. Cells were harvested and frozen at -20°C.

Cells were thawed in PBS, 0.5% Tween, 0.5 mM PMSF and lysed by sonication (10 x 20 sec.). Cell debris was eliminated by centrifugation at 12,000 g for 20 min.

For the preparation of GST-coated beads 30 µl of 50% glutathione Sepharose beads were added to the protein extract obtained from 200 ml of BL21 pGEX-5X-3 culture. After incubation for 1 h shaking at 4°C, the beads were recovered on an econocolumn (BioRad), washed several times with PBS, 0.5% Tween and then PBS, and finally equilibrated in the buffer used for the binding experiment.

For purification of soluble GST the protein was eluted from the glutathione beads by incubating with 20 mM glutathione, 50 mM Tris pH8, 5 mM $CaCl_2$ at 24°C for 5 min. Several eluted fractions were collected and analyzed by SDS-PAGE and Coomassie Blue staining.

9.5.2.2. Purification of GST-C

For purification of GST-GSa coated beads an *E.coli* culture carrying pGST-GSa was grown in minimal media (MM; (Sambrook et al., 1989)) containing 50 mg/l ampicillin. At OD_{600} 0.4 cells were shifted to 24°C and induced at OD_{600} 0.7-0.8 with 0.1 mM IPTG for 2 h. Cells were harvested and frozen at -20°C.

The *E.coli* cell extract was prepared as described for GST (8.5.2.1), but additionally to the PMSF, protease inhibitors (Complete Protease Inhibitor tablets, Roche) were added to the buffer for sonication (1 tablet/ 50 ml buffer).

30 µl of 50% glutathione Sepharose beads were added to the protein extract obtained from 2 l of BL21 pGST-C culture, and were incubated for 1 h shaking at 4°C. Beads were recovered, washed as explained previously (see 8.5.2.1.), and finally equilibrated in the buffer used for the binding experiment.

9.5.2.3. Purification of GST-Cmd1p and Cmd1p

For the purification of GST-Cmd1p, an *E.coli* culture carrying the plasmid pGST*CMD1* was grown in LB-medium. Induction of protein, purification of protein coated glutathione beads and elution of GST-Cmd1p was done like described for the GST protein (see 8.5.2.1.).

Cmd1p was cleaved from GST by adding 30 µl of 50% thrombin-agarose (Thrombin clean cleavage kit; Sigma) to 50 µl eluted GST-Cmd1 protein and incubating over night shaking at 4°C.

In order to purify Cmd1p from GST and uncut GST-Cmd1p, the supernatant was recovered from the thrombin-agarose, diluted 1:25 with 10 mM Tris pH 8, 150 mM $NaCl_2$, 0.1% Tween and incubated with 50 µl of 50% glutathione Sepharose over night, shaking at 4°C. The supernatant was recovered and analyzed by SDS-PAGE and Coomassie Blue staining.

9.5.3. Purification of Protein A-tagged proteins from yeast

N-terminal Protein A-tagged proteins were purified from yeast strain SCMIG275 transformed with the corresponding plasmid (pProtA-nT or pProtA-C). 1 l of cells were grown to OD_{600} 1.0, harvested and frozen at -20°C. After thawing, one-tenth pellet volume of IP buffer (50 mM Tris, pH 7.5, 150 mM $NaCl_2$, 5 mM EDTA) was added to the cell pellet and the cells were glass bead lysed in the presence of protein inhibitors (0.5 mM PMSF, 1 µg/ml aprotinin, 1 µg/ml pepstatin, 1 µg/ml leupeptin, 1 µg/ml antipain). 1 ml of IP buffer containing 0.5 M $NaCl_2$, 1% Triton and protein inhibitors was added, mixed and incubated for 10 min on ice. Unbroken cells and cell debris were eliminated by centrifugation at 2500 g for 5 min. The cell extract was centrifuged at 20,000 g for 10 min at 4°C. The supernatant was recovered and incubated with 40 µl of 50% IgG-Sepharose (Amersham Biocsciences) for 2 h rotating at 4°C.

For the purification of Cmd1p free ProtA-nT, 5mM $CaCl_2$ was added to the cell extract before addition of the sepharose.

Beads were collected on Mobicol-columns (MoBiTec) and washed 4 times with IP buffer, 0.5 M $NaCl_2$, 1% Triton and 3 times with IP buffer, 0.5 M $NaCl_2$, 0.1% Tween. The protein was then eluted from the beads by adding 0.5 M acetic acid pH 3.4 (adjusted with ammonium acetate), 0.5 M $NaCl_2$, 0.1% Tween. The eluted protein was rapidly centrifuged from the column into half the volume of 1 M Tris pH 9 for neutralization. The protein content of the eluted fractions was determined by SDS-PAGE and Coomassie staining.

9.5.4. *In vitro* protein binding assay

For the binding assays, Gutathion Sepharose beads covered with GST-C or GST, ProtA-nT or Cmd1p free ProtA-nT, and Cmd1p were purified as described before. 1 µg of GST-C or GST bound to Glutathion Sepharose beads were incubated with 0.03 µg of ProtA-nT in 1 ml

TBS-TB (10 mM Tris pH 8.0, 150 mM $NaCl_2$, 0.1% Tween-20, 1.5% BSA) for 3 h at 4°C on a turning wheel.

For the experiment with purified Cmd1p, 1 µg of Cmd1p was preincubated with ProtA-nT (purified in the presence of 5 mM $CaCl_2$) in TBS-TB buffer before addition of the beads, 1 mM EGTA was added to the binding assay.

For the binding experiment in the presence of Ca^{2+} ProtA-nT was preincubated for 2 h in TBS-TB buffer containing 5 mM $CaCl_2$ before addition of the beads.

Beads were collected on Mobicol-columns (MoBiTec), washed 2 times with TBS-TB and 3 times with TBS-T (10 mM Tris pH 8.0, 150 mM $NaCl_2$, 0.1% Tween-20) and finally boiled in 30 µl SDS-sample buffer. Bound proteins were analyzed by SDS-PAGE and Western blot.

9.5.5. Protein overlay assay

For the overlay assay, IgG-Sepharose covered with ProtA-nT was purified as explained before (3.5.2.4). The beads were collected on Mobicol-columns (MoBiTec) and washed 7 times with 50 mM Tris pH 7.5, 0.5 M $NaCl_2$, 5 mM EDTA, 1% Triton. The nT-fragment was then cut off from the Protein A-tag with TEV protease. The protein-coated beads were incubated in 30 µl of 50 mM Tris, pH 8, 0.5 mM EDTA and 10 Units (1 µl) of AcTEV (Invitrogen) over night shaking at 4°C. The supernatant was discarded and the protein was eluted from the beads by incubating in 30 µl of 50 mM Tris, pH 8, 1 M $NaCl_2$, 0.5 mM EDTA for 30 min shaking at 4°C.

After analysis of the eluted fractions by SDS-PAGE and Coomassie Blue staining, the nT-protein (0.15 µg) was separated on SDS-PAGE and transferred to nitrocellulose in 30 mM Tris, 240 mM glycine. Proteins were then partially renaturated by washing 3 times for 30 min at RT with 10 mM Tris, pH 8, 150 mM $NaCl_2$, 0.05% Tween, and the membrane was blocked over night at 4°C in blocking buffer (10 mM Tris, pH 8, 150 mM $NaCl_2$, 0.05% Tween 3% BSA). The membrane was then probed with purified GST or GST-C protein in blocking buffer for 3 h at 4°C. After 3 washing steps with blocking buffer for 20 min at 4°C, anti-GST antibody diluted 1:2000 in blocking buffer was added and the membrane was incubated for 1.5 h at RT. Again, the membrane was washed 3 times for 20 min with blocking buffer and then incubated for 1 h with the anti-goat antibody diluted 1:2000 in blocking buffer. After washing 2 times with blocking buffer and 2 times with 10 mM Tris, pH 8, 150 mM $NaCl_2$, 0.05% Tween the membrane-bound peroxidase-conjugated antibody was detected with an enhanced chemoluminescence detection kit.

9.5.6. Binding of purified proteins to lipid strips

The PIP lipid strips (p-6001,Echelon) were first blocked with 3% fatty acid free BSA (Sigma) in TBS-T buffer (10 mM Tris pH 8.0, 150 mM NaCl, 0.1% Tween-20) at RT for 1 h. The

strips were then incubated with the Protein A-tagged protein at a concentration of 0.005 µg/ml in TBS-T with 3% BSA (=TBS-TB) over night at 4°C. The strip was washed 3 times with TBS-TB for 10 min at RT and the peroxidase-conjugated antibody for detection of the protein A (PAP, DAKO) was added 1:1000 in TBS-TB. After incubation for 1h at RT the strip was washed 3 times for 10 min with TBS-TB and 3 times for 10 min with TBS-T. Finally, bound protein was detected using an enhanced chemoluminescence detection kit.

9.5.7. IgG pull-down experiments

9.5.7.1. IgG pull-downs from yeast extract

0.4 l of yeast cells were grown to OD_{600} 0.8, washed once with water and once with lysis buffer (25 mM Tris, pH 8.5, 5 mM EDTA), harvested at 2400 g for 5 min and frozen at -20°C. Cells were thawed, 100 µl of lysis buffer was added and the cells were glass bead-lysed in the presence of protein inhibitors (0.5 mM PMSF, 1µg/ml aprotinin, 1µg/ml pepstatin, 1µg/ml leupeptin, 1µg/ml antipain). The cell extract was recovered and diluted with 1 ml of lysis buffer containing protein inhibitors. Unbroken cells and cell debris were eliminated by centrifugation at 700 g for 10 min at 4°C. The supernatant was recovered and diluted with the same volume of breakage buffer (10 mM Tris, pH 7.5, 0.2 mM EDTA, 0.2 mM DTT) containing protein inhibitors. After another centrifugation at 700 g for 10 min at 4°C the yeast extract was adjusted to a concentration of 10 mg/ml with breakage buffer plus lysis buffer (1:1) (BLB). 1% Triton and 150 mM $NaCl_2$ was added, the extract was incubated for 30 min shaking at 4°C and cleared again by centrifugation at 700 g for 10 min at 4°C. 1 ml of extract was incubated with 25 µl of 50% IgG-Sepharose (Amersham Biosciences) in siliconized tubes for 2 h at 4°C on a turning wheel. The beads were washed three times with BLB containing 1% Triton and 150 mM $NaCl_2$ and 2 times with BLB and finally boiled in 25 µl SDS-sample buffer. Precipitated proteins were analyzed by SDS-PAGE and immunoblot.
Note: Since we observed that ProtA-Myo5p from the plasma membrane was binding less efficient to the IgG-beads than ProtA-Myo5p from cytosol, probably with this method mainly cytosolic Myo5p was precipitated.

9.5.7.2. IgG pull-down from plasma membrane and cytosolic fractions

0.5 ml purified plasma membrane and cytosolic fraction (see section 8.4.) was diluted with 0.5 ml BLB buffer (see 8.5.7.1.). 1% Triton, 150 mM $NaCl_2$, and protein inhibitors (0.5 mM PMSF, 1µg/ml aprotinin, 1µg/ml pepstatin, 1µg/ml leupeptin, 1µg/ml antipain) were added, and samples were incubated with 40 µl of 50% IgG-Sepharose (Amersham Biosciences) for 2 h at 4°C on a turning wheel. Beads were washed 5 times with BLB, 1% Triton, 150 mM $NaCl_2$, and finally boiled in 25 µl SDS-sample buffer. Immunoprecipitated proteins were analyzed by SDS-PAGE and Western blot.

9.5.8. Immunoprecipitations from plasma membrane and cytosolic fractions

Myc-tagged Myo5p was precipitated from plasma membrane and cytosol under the same conditions as described for the IgG-pull down (see 8.5.7.2.). Samples were incubated with 50 µl of 50% a-myc-agarose (Roche) and the beads were washed and analyzed as described before.

9.6. The α-factor internalization assay

The α-factor pheromone is a small peptide secreted by yeast cells of the mating type α (*Matα*). The peptide binds to a G-coupled receptor (Ste2p) that is exclusively expressed in cells of the opposite mating type (*Mat***a** cells). Binding of the pheromone triggers a signal transduction cascade that results in the transcriptional activation of genes involved in the mating response.

After binding of the α-factor to its receptor the complex is rapidly internalized by endocytosis and is then transported to the vacuole for degradation. Such a mechanism significantly contributes to desensitization of the pheromone (Bardwell et al., 1994). Based on the observation that α-factor which is bound to its receptor on the cell surface, but not internalised α-factor, can be dissociated from the cells by a short incubation in an acidic buffer, a quantitative assay to monitor the internalization kinetics of ^{35}S-radiolabelled α–factor was developed by Dulic *et al* (Dulic et al., 1991).

The [^{35}S] α-factor uptake assays were performed as described for the continuous-presence protocol (Dulic et al., 1991).

Cells were grown to 0.5 - 1 x 10^7 cells/ml, harvested and resuspended to 5 x 10^8 cells/ml in YPD of 37°C. Cells were pre-incubated for 15 min at 37°C and 100,000 dpm/ml of purified ^{35}S-α-factor was added. 2 x 100 µl of culture were taken at the indicated time points and the uptake was stopped by 1/100 dilution into ice-cold pH 1 (50 mM sodium citrate) or pH 6 (50 mM potassium phosphate) buffers, respectively. Cells were incubated for 20 min on ice to allow the dissociation of the □-factor from its receptor at pH 1. Subsequently, cells were recovered by filtration onto GF/C filters (Whatman) using a 10 PLC filter holder (Amersham Biocsciences) and cell-associated counts were measured in a □-counter (Beckman LS 6000 TA).

Internalized counts were calculated by dividing pH 1-resistant (internal) by pH 6-resistant (total cell-bound) counts per time point. Uptake assays were performed at least three times and the mean and standard deviations were calculated per time point.

9.7. Fluorescence microscopy

9.7.1. Fluorescence microscopy of living cells expressing GFP-Myo5p constructs

Cells encoding GFP-constructs were grown to mid-log phase in SCD medium, selecting for the transformed plasmid. Cells were harvested, diluted in a small volume of medium and directly visualized on poly-lysine coated slides using an *Axiophot* fluorescence microscope (Zeiss) equipped with a GFP-filter (excitation 470/40, LP520). Images were taken with a Olympus DP70 camera.

9.7.2. Time-lapse fluorescence microscopy of cortical patches in living cells

Cells expressing GFP-Myo5p were grown to mid-log phase in SDC medium. Time-lapse videos were collected from cells immobilized in 0.8% low-melt agarose prepared in complete synthetic medium. Microscopy was performed using an Olympus fluorescence BX61 microscope equipped with Nomarski differential interference contrast (DIC) optics, a 100 x objective (NA 1.35) , a Roper Cool-SNAP HQ camera, Sutter Lambda 10 x 2 automated excitation and emission filter wheels and a 175 W Xenon remote source lamp with liquid light guide. Images were taken every 2 seconds and were acquired/processed using the SlideBook image analysis software from Intelligent Imaging Innovations.

9.7.3. Plasma membrane staining with FM4-64 and confocal fluorescence microscopy

For staining of the plasma membrane with the lyophilic dye FM4-64, the yeast cells were grown to 10^7 cells/ml, harvested and resuspended in 25 µl of YPD. The cells were incubated for 15 min on ice, FM4-64 (Molecular Probes) was added to a concentration of 8 µM and the cells were kept on ice for another 15 min. Cells were harvested at 4°C and resuspended in 50 µl of ice-cold 2% alginate in 50 mM glycine, pH 6.2, containing 8 µM FM4-64. 2 µl of sample were placed on an ice-cold slide, covered with a coverslip and 2 µl of 50 mM $CaCl_2$ was added to the sample from every side of the coverslip to solidify the alginate. Cells were immediately visualized using a Leica TCS SP confocal laser scanning microscope. The microscope fitted to/with spectrophotometers for emission band wavelength selection was used with 2 lasers, i.e., an argon ion laser emitting at 488 nm and an HeNe laser emitting at 543 nm to excite YFP and FM4-64, respectively. During scanning, we used a triple-dichroic beam splitter (TD 488/543/633). For visualization of YFP, the emission window was set at 500–535 nm. For visualization of FM4-64, the emission window was set at 563–607 nm. Serial optical slices were taken each 0.5 µm. Confocal image stacks were combined as x–y projection images.

10. Literature

Adams, A.E., D. Botstein, and D.G. Drubin. 1991. Requirement of yeast fimbrin for actin organization and morphogenesis in vivo. *Nature*. 354:404-8.

Adams, R.J., and T.D. Pollard. 1986. Propulsion of organelles isolated from Acanthamoeba along actin filaments by myosin-I. *Nature*. 322:754-6.

Adams, R.J., and T.D. Pollard. 1989. Binding of myosin I to membrane lipids. *Nature*. 340:565-8.

Albanesi, J.P., H. Fujisaki, J.A. Hammer, 3rd, E.D. Korn, R. Jones, and M.P. Sheetz. 1985. Monomeric Acanthamoeba myosins I support movement in vitro. *J Biol Chem*. 260:8649-52.

Anderson, B.L., I. Boldogh, M. Evangelista, C. Boone, L.A. Greene, and L.A. Pon. 1998. The Src homology domain 3 (SH3) of a yeast type I myosin, Myo5p, binds to verprolin and is required for targeting to sites of actin polarization. *J Cell Biol*. 141:1357-70.

Antonny, B. 2006. Membrane deformation by protein coats. *Curr Opin Cell Biol*. 18:386-94.

Aronheim, A., and M. Karin. 2000. Analysis and identification of protein-protein interactions using protein recruitment systems. *Methods Enzymol*. 328:47-59.

Audhya, A., R. Loewith, A.B. Parsons, L. Gao, M. Tabuchi, H. Zhou, C. Boone, M.N. Hall, and S.D. Emr. 2004. Genome-wide lethality screen identifies new PI4,5P2 effectors that regulate the actin cytoskeleton. *Embo J*. 23:3747-57.

Ayscough, K.R. 2000. Endocytosis and the development of cell polarity in yeast require a dynamic F-actin cytoskeleton. *Curr Biol*. 10:1587-90.

Ayscough, K.R. 2005. Coupling actin dynamics to the endocytic process in Saccharomyces cerevisiae. *Protoplasma*. 226:81-8.

Ayscough, K.R., J. Stryker, N. Pokala, M. Sanders, P. Crews, and D.G. Drubin. 1997. High rates of actin filament turnover in budding yeast and roles for actin in establishment and maintenance of cell polarity revealed using the actin inhibitor latrunculin-A. *J Cell Biol*. 137:399-416.

Bahler, M., and A. Rhoads. 2002. Calmodulin signaling via the IQ motif. *FEBS Lett*. 513:107-13.

Baines, I.C., H. Brzeska, and E.D. Korn. 1992. Differential localization of Acanthamoeba myosin I isoforms. *J Cell Biol*. 119:1193-203.

Baines, I.C., A. Corigliano-Murphy, and E.D. Korn. 1995. Quantification and localization of phosphorylated myosin I isoforms in Acanthamoeba castellanii. *J Cell Biol*. 130:591-603.

Bardwell, L., J.G. Cook, C.J. Inouye, and J. Thorner. 1994. Signal propagation and regulation in the mating pheromone response pathway of the yeast Saccharomyces cerevisiae. *Dev Biol*. 166:363-79.

Barritt, G.J. 1999. Receptor-activated Ca2+ inflow in animal cells: a variety of pathways tailored to meet different intracellular Ca2+ signalling requirements. *Biochem J*. 337 (Pt 2):153-69.

Barylko, B., D.D. Binns, and J.P. Albanesi. 2000. Regulation of the enzymatic and motor activities of myosin I. *Biochim Biophys Acta*. 1496:23-35.

Berben, G., J. Dumont, V. Gilliquet, P.A. Bolle, and F. Hilger. 1991. The YDp plasmids: a uniform set of vectors bearing versatile gene disruption cassettes for Saccharomyces cerevisiae. *Yeast*. 7:475-7.

Berg, J.S., B.C. Powell, and R.E. Cheney. 2001. A millennial myosin census. *Mol Biol Cell*. 12:780-94.

Bose, A., A. Guilherme, S.I. Robida, S.M. Nicoloro, Q.L. Zhou, Z.Y. Jiang, D.P. Pomerleau, and M.P. Czech. 2002. Glucose transporter recycling in response to insulin is facilitated by myosin Myo1c. *Nature*. 420:821-4.

Broder, Y.C., S. Katz, and A. Aronheim. 1998. The ras recruitment system, a novel approach to the study of protein-protein interactions. *Curr Biol*. 8:1121-4.

Brown, S.S. 1997. Myosins in yeast. *Curr Opin Cell Biol*. 9:44-8.

Bugnicourt, A., M. Froissard, K. Sereti, H.D. Ulrich, R. Haguenauer-Tsapis, and J.M. Galan. 2004. Antagonistic roles of ESCRT and Vps class C/HOPS complexes in the recycling of yeast membrane proteins. *Mol Biol Cell*. 15:4203-14.

Coluccio, L.M. 1997. Myosin I. *Am J Physiol*. 273:C347-59.

Cordonnier, M.N., D. Dauzonne, D. Louvard, and E. Coudrier. 2001. Actin filaments and myosin I alpha cooperate with microtubules for the movement of lysosomes. *Mol Biol Cell*. 12:4013-29.

Cyr, J.L., R.A. Dumont, and P.G. Gillespie. 2002. Myosin-1c interacts with hair-cell receptors through its calmodulin-binding IQ domains. *J Neurosci*. 22:2487-95.

Dawson, J.C., J.A. Legg, and L.M. Machesky. 2006. Bar domain proteins: a role in tubulation, scission and actin assembly in clathrin-mediated endocytosis. *Trends Cell Biol*. 16:493-8.

De La Cruz, E.M., and E.M. Ostap. 2004. Relating biochemistry and function in the myosin superfamily. *Curr Opin Cell Biol*. 16:61-7.

Desrivieres, S., F.T. Cooke, P.J. Parker, and M.N. Hall. 1998. MSS4, a phosphatidylinositol-4-phosphate 5-kinase required for organization of the actin cytoskeleton in Saccharomyces cerevisiae. *J Biol Chem*. 273:15787-93.

Di Fiore, P.P., and P. De Camilli. 2001. Endocytosis and signaling. an inseparable partnership. *Cell*. 106:1-4.

Di Paolo, G., and P. De Camilli. 2006. Phosphoinositides in cell regulation and membrane dynamics. *Nature*. 443:651-7.

Doberstein, S.K., I.C. Baines, G. Wiegand, E.D. Korn, and T.D. Pollard. 1993. Inhibition of contractile vacuole function in vivo by antibodies against myosin-I. *Nature*. 365:841-3.

Doberstein, S.K., and T.D. Pollard. 1992. Localization and specificity of the phospholipid and actin binding sites on the tail of Acanthamoeba myosin IC. *J Cell Biol*. 117:1241-9.

Dulic, V., M. Egerton, I. Elguindi, S. Raths, B. Singer, and H. Riezman. 1991. Yeast endocytosis assays. *Methods Enzymol*. 194:697-710.

Duncan, M.C., M.J. Cope, B.L. Goode, B. Wendland, and D.G. Drubin. 2001. Yeast Eps15-like endocytic protein, Pan1p, activates the Arp2/3 complex. *Nat Cell Biol*. 3:687-90.

Durrbach, A., G. Raposo, D. Tenza, D. Louvard, and E. Coudrier. 2000. Truncated brush border myosin I affects membrane traffic in polarized epithelial cells. *Traffic*. 1:411-24.

El Mezgueldi, M., N. Tang, S.S. Rosenfeld, and E.M. Ostap. 2002. The kinetic mechanism of Myo1e (human myosin-IC). *J Biol Chem*. 277:21514-21.

Engqvist-Goldstein, A.E., and D.G. Drubin. 2003. Actin assembly and endocytosis: from yeast to mammals. *Annu Rev Cell Dev Biol*. 19:287-332.

Evangelista, M., B.M. Klebl, A.H. Tong, B.A. Webb, T. Leeuw, E. Leberer, M. Whiteway, D.Y. Thomas, and C. Boone. 2000. A role for myosin-I in actin assembly through interactions with Vrp1p, Bee1p, and the Arp2/3 complex. *J Cell Biol*. 148:353-62.

Fath, K.R., G.M. Trimbur, and D.R. Burgess. 1994. Molecular motors are differentially distributed on Golgi membranes from polarized epithelial cells. *J Cell Biol*. 126:661-75.

Fazi, B., M.J. Cope, A. Douangamath, S. Ferracuti, K. Schirwitz, A. Zucconi, D.G. Drubin, M. Wilmanns, G. Cesareni, and L. Castagnoli. 2002. Unusual binding properties of the SH3 domain of the yeast actin-binding protein Abp1: structural and functional analysis. *J Biol Chem*. 277:5290-8.

Friant, S., R. Lombardi, T. Schmelzle, M.N. Hall, and H. Riezman. 2001. Sphingoid base signaling via Pkh kinases is required for endocytosis in yeast. *Embo J*. 20:6783-92.

Fujisaki, H., J.P. Albanesi, and E.D. Korn. 1985. Experimental evidence for the contractile activities of Acanthamoeba myosins IA and IB. *J Biol Chem*. 260:11183-9.

Geli, M.I., R. Lombardi, B. Schmelzl, and H. Riezman. 2000a. An intact SH3 domain is required for myosin I-induced actin polymerization. *Embo J*. 19:4281-91.

Geli, M.I., R. Lombardi, B. Schmelzl, and H. Riezman. 2000b. An intact SH3 domain is required for myosin I-induced actin polymerization. *Embo J*. 19:4281-91.

Geli, M.I., and H. Riezman. 1996. Role of type I myosins in receptor-mediated endocytosis in yeast. *Science*. 272:533-5.

Geli, M.I., and H. Riezman. 1998. Endocytic internalization in yeast and animal cells: similar and different. *J Cell Sci*. 111 (Pt 8):1031-7.

Geli, M.I., A. Wesp, and H. Riezman. 1998. Distinct functions of calmodulin are required for the uptake step of receptor-mediated endocytosis in yeast: the type I myosin Myo5p is one of the calmodulin targets. *Embo J*. 17:635-47.

Gietz, R.D., and A. Sugino. 1988. New yeast-Escherichia coli shuttle vectors constructed with in vitro mutagenized yeast genes lacking six-base pair restriction sites. *Gene*. 74:527-34.

Gillespie, P.G., and J.L. Cyr. 2002. Calmodulin binding to recombinant myosin-1c and myosin-1c IQ peptides. *BMC Biochem*. 3:31.

Gillespie, P.G., and J.L. Cyr. 2004. Myosin-1c, the hair cell's adaptation motor. *Annu Rev Physiol*. 66:521-45.

Goldman, Y.E. 1998. Wag the tail: structural dynamics of actomyosin. *Cell*. 93:1-4.

Goley, E.D., and M.D. Welch. 2006. The ARP2/3 complex: an actin nucleator comes of age. *Nat Rev Mol Cell Biol*. 7:713-26.

Goode, B.L., A.A. Rodal, G. Barnes, and D.G. Drubin. 2001. Activation of the Arp2/3 complex by the actin filament binding protein Abp1p. *J Cell Biol*. 153:627-34.

Goodson, H.V., B.L. Anderson, H.M. Warrick, L.A. Pon, and J.A. Spudich. 1996. Synthetic lethality screen identifies a novel yeast myosin I gene (MYO5): myosin I proteins are required for polarization of the actin cytoskeleton. *J Cell Biol*. 133:1277-91.

Grosshans, B.L., H. Grotsch, D. Mukhopadhyay, I.M. Fernandez, J. Pfannstiel, F.Z. Idrissi, J. Lechner, H. Riezman, and M.I. Geli. 2006. TEDS site phosphorylation of the yeast myosins I is required for ligand-induced but not for constitutive endocytosis of the G protein-coupled receptor Ste2p. *J Biol Chem*. 281:11104-14.

Guthrie, C., and G.R. Fink. 1991. *Methods in Enzymology*.

Gyuris, J., E. Golemis, H. Chertkov, and R. Brent. 1993. Cdi1, a human G1 and S phase protein phosphatase that associates with Cdk2. *Cell*. 75:791-803.

Hasson, T., and M.S. Mooseker. 1996. Vertebrate unconventional myosins. *J Biol Chem*. 271:16431-4.

Haucke, V. 2005. Phosphoinositide regulation of clathrin-mediated endocytosis. *Biochem Soc Trans*. 33:1285-9.

Hayden, S.M., J.S. Wolenski, and M.S. Mooseker. 1990. Binding of brush border myosin I to phospholipid vesicles. *J Cell Biol*. 111:443-51.

Hirono, M., C.S. Denis, G.P. Richardson, and P.G. Gillespie. 2004. Hair cells require phosphatidylinositol 4,5-bisphosphate for mechanical transduction and adaptation. *Neuron*. 44:309-20.

Hokanson, D.E., J.M. Laakso, T. Lin, D. Sept, and E.M. Ostap. 2006. Myo1c binds phosphoinositides through a putative pleckstrin homology domain. *Mol Biol Cell*. 17:4856-65.

Hokanson, D.E., and E.M. Ostap. 2006. Myo1c binds tightly and specifically to phosphatidylinositol 4,5-bisphosphate and inositol 1,4,5-trisphosphate. *Proc Natl Acad Sci U S A*. 103:3118-23.

Howard, J.P., J.L. Hutton, J.M. Olson, and G.S. Payne. 2002. Sla1p serves as the targeting signal recognition factor for NPFX(1,2)D-mediated endocytosis. *J Cell Biol*. 157:315-26.

Huber, L.A., I. Fialka, K. Paiha, W. Hunziker, D.B. Sacks, M. Bahler, M. Way, R. Gagescu, and J. Gruenberg. 2000. Both calmodulin and the unconventional myosin Myr4

regulate membrane trafficking along the recycling pathway of MDCK cells. *Traffic*. 1:494-503.

Hwang, K.J., F. Mahmoodian, J.A. Ferretti, E.D. Korn, and J.M. Gruschus. 2007. Intramolecular interaction in the tail of Acanthamoeba myosin IC between the SH3 domain and a putative pleckstrin homology domain. *Proc Natl Acad Sci U S A*. 104:784-9.

Idrissi, F.Z., B.L. Wolf, and M.I. Geli. 2002. Cofilin, but not profilin, is required for myosin-I-induced actin polymerization and the endocytic uptake in yeast. *Mol Biol Cell*. 13:4074-87.

Ishikawa, T., N. Cheng, X. Liu, E.D. Korn, and A.C. Steven. 2004. Subdomain organization of the Acanthamoeba myosin IC tail from cryo-electron microscopy. *Proc Natl Acad Sci U S A*. 101:12189-94.

Ito, H., Y. Fukuda, K. Murata, and A. Kimura. 1983. Transformation of intact yeast cells treated with alkali cations. *J Bacteriol*. 153:163-8.

Jenkins, G.M., and M.A. Frohman. 2005. Phospholipase D: a lipid centric review. *Cell Mol Life Sci*. 62:2305-16.

Jonsdottir, G.A., and R. Li. 2004. Dynamics of yeast Myosin I: evidence for a possible role in scission of endocytic vesicles. *Curr Biol*. 14:1604-9.

Jontes, J.D., R.A. Milligan, T.D. Pollard, and E.M. Ostap. 1997. Kinetic characterization of brush border myosin-I ATPase. *Proc Natl Acad Sci U S A*. 94:14332-7.

Jontes, J.D., E.M. Ostap, T.D. Pollard, and R.A. Milligan. 1998. Three-dimensional structure of Acanthamoeba castellanii myosin-IB (MIB) determined by cryoelectron microscopy of decorated actin filaments. *J Cell Biol*. 141:155-62.

Jung, G., and J.A. Hammer, 3rd. 1990. Generation and characterization of Dictyostelium cells deficient in a myosin I heavy chain isoform. *J Cell Biol*. 110:1955-64.

Jung, G., K. Remmert, X. Wu, J.M. Volosky, and J.A. Hammer, 3rd. 2001. The Dictyostelium CARMIL protein links capping protein and the Arp2/3 complex to type I myosins through their SH3 domains. *J Cell Biol*. 153:1479-97.

Kaksonen, M., Y. Sun, and D.G. Drubin. 2003. A pathway for association of receptors, adaptors, and actin during endocytic internalization. *Cell*. 115:475-87.

Kaksonen, M., C.P. Toret, and D.G. Drubin. 2005. A modular design for the clathrin- and actin-mediated endocytosis machinery. *Cell*. 123:305-20.

Kaksonen, M., C.P. Toret, and D.G. Drubin. 2006. Harnessing actin dynamics for clathrin-mediated endocytosis. *Nat Rev Mol Cell Biol*. 7:404-14.

Kim, K., A. Yamashita, M.A. Wear, Y. Maeda, and J.A. Cooper. 2004. Capping protein binding to actin in yeast: biochemical mechanism and physiological relevance. *J Cell Biol*. 164:567-80.

Kim, S.V., W.Z. Mehal, X. Dong, V. Heinrich, M. Pypaert, I. Mellman, M. Dembo, M.S. Mooseker, D. Wu, and R.A. Flavell. 2006. Modulation of cell adhesion and motility in the immune system by Myo1f. *Science*. 314:136-9.

Kooijman, E.E., V. Chupin, B. de Kruijff, and K.N. Burger. 2003. Modulation of membrane curvature by phosphatidic acid and lysophosphatidic acid. *Traffic*. 4:162-74.

Krauss, M., M. Kinuta, M.R. Wenk, P. De Camilli, K. Takei, and V. Haucke. 2003. ARF6 stimulates clathrin/AP-2 recruitment to synaptic membranes by activating phosphatidylinositol phosphate kinase type Igamma. *J Cell Biol*. 162:113-24.

Krauss, M., V. Kukhtina, A. Pechstein, and V. Haucke. 2006. Stimulation of phosphatidylinositol kinase type I-mediated phosphatidylinositol (4,5)-bisphosphate synthesis by AP-2mu-cargo complexes. *Proc Natl Acad Sci U S A*. 103:11934-9.

Krendel, M., and M.S. Mooseker. 2005. Myosins: tails (and heads) of functional diversity. *Physiology (Bethesda)*. 20:239-51.

Kubler, E., and H. Riezman. 1993. Actin and fimbrin are required for the internalization step of endocytosis in yeast. *Embo J*. 12:2855-62.

Kubler, E., F. Schimmoller, and H. Riezman. 1994. Calcium-independent calmodulin requirement for endocytosis in yeast. *Embo J*. 13:5539-46.

Kuriyan, J., and D. Cowburn. 1997. Modular peptide recognition domains in eukaryotic signaling. *Annu Rev Biophys Biomol Struct*. 26:259-88.

Laemmli, U.K. 1970. Cleavage of structural proteins during the assembly of the head of bacteriophage T4. *Nature*. 227:680-5.

Lechler, T., G.A. Jonsdottir, S.K. Klee, D. Pellman, and R. Li. 2001. A two-tiered mechanism by which Cdc42 controls the localization and activation of an Arp2/3-activating motor complex in yeast. *J Cell Biol*. 155:261-70.

Lechler, T., A. Shevchenko, and R. Li. 2000. Direct involvement of yeast type I myosins in Cdc42-dependent actin polymerization. *J Cell Biol*. 148:363-73.

Lee, M.C., L. Orci, S. Hamamoto, E. Futai, M. Ravazzola, and R. Schekman. 2005. Sar1p N-terminal helix initiates membrane curvature and completes the fission of a COPII vesicle. *Cell*. 122:605-17.

Lee, W.L., M. Bezanilla, and T.D. Pollard. 2000. Fission yeast myosin-I, Myo1p, stimulates actin assembly by Arp2/3 complex and shares functions with WASp. *J Cell Biol*. 151:789-800.

Lee, W.L., E.M. Ostap, H.G. Zot, and T.D. Pollard. 1999. Organization and ligand binding properties of the tail of Acanthamoeba myosin-IA. Identification of an actin-binding site in the basic (tail homology-1) domain. *J Biol Chem*. 274:35159-71.

Lombardi, R., and H. Riezman. 2001. Rvs161p and Rvs167p, the two yeast amphiphysin homologs, function together in vivo. *J Biol Chem*. 276:6016-22.

Longtine, M.S., A. McKenzie, 3rd, D.J. Demarini, N.G. Shah, A. Wach, A. Brachat, P. Philippsen, and J.R. Pringle. 1998. Additional modules for versatile and economical PCR-based gene deletion and modification in Saccharomyces cerevisiae. *Yeast*. 14:953-61.

Lynch, T.J., J.P. Albanesi, E.D. Korn, E.A. Robinson, B. Bowers, and H. Fujisaki. 1986. ATPase activities and actin-binding properties of subfragments of Acanthamoeba myosin IA. *J Biol Chem*. 261:17156-62.

Machesky, L.M. 2000. The tails of two myosins. *J Cell Biol*. 148:219-21.

Machesky, L.M., and R.H. Insall. 1999. Signaling to actin dynamics. *J Cell Biol*. 146:267-72.

Madania, A., P. Dumoulin, S. Grava, H. Kitamoto, C. Scharer-Brodbeck, A. Soulard, V. Moreau, and B. Winsor. 1999. The Saccharomyces cerevisiae homologue of human Wiskott-Aldrich syndrome protein Las17p interacts with the Arp2/3 complex. *Mol Biol Cell*. 10:3521-38.

Mallik, R., and S.P. Gross. 2004. Molecular motors: strategies to get along. *Curr Biol*. 14:R971-82.

McGoldrick, C.A., C. Gruver, and G.S. May. 1995. myoA of Aspergillus nidulans encodes an essential myosin I required for secretion and polarized growth. *J Cell Biol*. 128:577-87.

Mellman, I. 1996. Endocytosis and molecular sorting. *Annu Rev Cell Dev Biol*. 12:575-625.

Mermall, V., P.L. Post, and M.S. Mooseker. 1998. Unconventional myosins in cell movement, membrane traffic, and signal transduction. *Science*. 279:527-33.

Miyata, H., B. Bowers, and E.D. Korn. 1989. Plasma membrane association of Acanthamoeba myosin I. *J Cell Biol*. 109:1519-28.

Mochida, J., T. Yamamoto, K. Fujimura-Kamada, and K. Tanaka. 2002. The novel adaptor protein, Mti1p, and Vrp1p, a homolog of Wiskott-Aldrich syndrome protein-interacting protein (WIP), may antagonistically regulate type I myosins in Saccharomyces cerevisiae. *Genetics*. 160:923-34.

Mooseker, M.S., and R.E. Cheney. 1995. Unconventional myosins. *Annu Rev Cell Dev Biol*. 11:633-75.

Mullins, R.D. 2000. How WASP-family proteins and the Arp2/3 complex convert intracellular signals into cytoskeletal structures. *Curr Opin Cell Biol*. 12:91-6.

Muniz, M., C. Nuoffer, H.P. Hauri, and H. Riezman. 2000. The Emp24 complex recruits a specific cargo molecule into endoplasmic reticulum-derived vesicles. *J Cell Biol*. 148:925-30.

Munn, A.L., A. Heese-Peck, B.J. Stevenson, H. Pichler, and H. Riezman. 1999. Specific sterols required for the internalization step of endocytosis in yeast. *Mol Biol Cell*. 10:3943-57.

Naqvi, S.N., R. Zahn, D.A. Mitchell, B.J. Stevenson, and A.L. Munn. 1998. The WASp homologue Las17p functions with the WIP homologue End5p/verprolin and is essential for endocytosis in yeast. *Curr Biol*. 8:959-62.

Neuhaus, E.M., and T. Soldati. 2000. A myosin I is involved in membrane recycling from early endosomes. *J Cell Biol*. 150:1013-26.

Newpher, T.M., R.P. Smith, V. Lemmon, and S.K. Lemmon. 2005. In vivo dynamics of clathrin and its adaptor-dependent recruitment to the actin-based endocytic machinery in yeast. *Dev Cell*. 9:87-98.

Novak, K.D., M.D. Peterson, M.C. Reedy, and M.A. Titus. 1995. Dictyostelium myosin I double mutants exhibit conditional defects in pinocytosis. *J Cell Biol*. 131:1205-21.

Novak, K.D., and M.A. Titus. 1998. The myosin I SH3 domain and TEDS rule phosphorylation site are required for in vivo function. *Mol Biol Cell*. 9:75-88.

Oberholzer, U., T.L. Iouk, D.Y. Thomas, and M. Whiteway. 2004. Functional characterization of myosin I tail regions in Candida albicans. *Eukaryot Cell*. 3:1272-86.

Odorizzi, G., M. Babst, and S.D. Emr. 1998. Fab1p PtdIns(3)P 5-kinase function essential for protein sorting in the multivesicular body. *Cell*. 95:847-58.

Okeley, N.M., and M.H. Gelb. 2004. A designed probe for acidic phospholipids reveals the unique enriched anionic character of the cytosolic face of the mammalian plasma membrane. *J Biol Chem*. 279:21833-40.

Ostap, E.M., P. Maupin, S.K. Doberstein, I.C. Baines, E.D. Korn, and T.D. Pollard. 2003. Dynamic localization of myosin-I to endocytic structures in Acanthamoeba. *Cell Motil Cytoskeleton*. 54:29-40.

Ostap, E.M., and T.D. Pollard. 1996. Biochemical kinetic characterization of the Acanthamoeba myosin-I ATPase. *J Cell Biol*. 132:1053-60.

Peter, B.J., H.M. Kent, I.G. Mills, Y. Vallis, P.J. Butler, P.R. Evans, and H.T. McMahon. 2004. BAR domains as sensors of membrane curvature: the amphiphysin BAR structure. *Science*. 303:495-9.

Peterson, M.R., and S.D. Emr. 2001. The class C Vps complex functions at multiple stages of the vacuolar transport pathway. *Traffic*. 2:476-86.

Phillips, K.R., S. Tong, R. Goodyear, G.P. Richardson, and J.L. Cyr. 2006. Stereociliary myosin-1c receptors are sensitive to calcium chelation and absent from cadherin 23 mutant mice. *J Neurosci*. 26:10777-88.

Pichler, H., and H. Riezman. 2004. Where sterols are required for endocytosis. *Biochim Biophys Acta*. 1666:51-61.

Pollard, T.D. 1982. Assays for myosin. *Methods Enzymol*. 85 Pt B:123-30.

Pollard, T.D., and E.D. Korn. 1973. Acanthamoeba myosin. I. Isolation from Acanthamoeba castellanii of an enzyme similar to muscle myosin. *J Biol Chem*. 248:4682-90.

Pollard, T.D., and E.M. Ostap. 1996. The chemical mechanism of myosin-I: implications for actin-based motility and the evolution of the myosin family of motor proteins. *Cell Struct Funct*. 21:351-6.

Powner, D.J., and M.J. Wakelam. 2002. The regulation of phospholipase D by inositol phospholipids and small GTPases. *FEBS Lett*. 531:62-4.

Raposo, G., M.N. Cordonnier, D. Tenza, B. Menichi, A. Durrbach, D. Louvard, and E. Coudrier. 1999. Association of myosin I alpha with endosomes and lysosomes in mammalian cells. *Mol Biol Cell*. 10:1477-94.

Rieder, S.E., and S.D. Emr. 1997. A novel RING finger protein complex essential for a late step in protein transport to the yeast vacuole. *Mol Biol Cell*. 8:2307-27.

Rodal, A.A., L. Kozubowski, B.L. Goode, D.G. Drubin, and J.H. Hartwig. 2005. Actin and septin ultrastructures at the budding yeast cell cortex. *Mol Biol Cell*. 16:372-84.

Rodal, A.A., A.L. Manning, B.L. Goode, and D.G. Drubin. 2003. Negative regulation of yeast WASp by two SH3 domain-containing proteins. *Curr Biol*. 13:1000-8.

Rohatgi, R., H.Y. Ho, and M.W. Kirschner. 2000. Mechanism of N-WASP activation by CDC42 and phosphatidylinositol 4, 5-bisphosphate. *J Cell Biol*. 150:1299-310.

Rosenfeld, S.S., and B. Rener. 1994. The GPQ-rich segment of Dictyostelium myosin IB contains an actin binding site. *Biochemistry*. 33:2322-8.

Sambrook, J., E.F. Fritsch, and T. Maniatis. 1989. Molecular Cloning: A laboratory Manual, 2nd ed. *Cold Spring Harbor, New York: Cold Spring Harbor Laboratory Press*.

Sambrook, J., and D.W. Russel. 2001. Molecular Cloning: A laboratory Manual, 3rd ed. . *Cold Spring Harbor, New York: Cold Spring Harbor Laboratory Press*.

Sato, T.K., P. Rehling, M.R. Peterson, and S.D. Emr. 2000. Class C Vps protein complex regulates vacuolar SNARE pairing and is required for vesicle docking/fusion. *Mol Cell*. 6:661-71.

Sellers, J.R. 2000. Myosins: a diverse superfamily. *Biochim Biophys Acta*. 1496:3-22.

Serrano, R. 1988. H+-ATPase from plasma membranes of Saccharomyces cerevisiae and Avena sativa roots: purification and reconstitution. *Methods Enzymol*. 157:533-44.

Seth, A., C. Otomo, and M.K. Rosen. 2006. Autoinhibition regulates cellular localization and actin assembly activity of the diaphanous-related formins FRLalpha and mDia1. *J Cell Biol*. 174:701-13.

Sherman, F. 1991. Getting started with yeast. *Methods Enzymol*. 194:3-21.

Sherman, S., G. Fink, and C. Lawrence. 1974. Methods in yeast genetics. *Cold Spring Harbor, New York: Cold Spring Harbor Laboratory Press*.

Shih, S.C., D.J. Katzmann, J.D. Schnell, M. Sutanto, S.D. Emr, and L. Hicke. 2002. Epsins and Vps27p/Hrs contain ubiquitin-binding domains that function in receptor endocytosis. *Nat Cell Biol*. 4:389-93.

Singer-Kruger, B., Y. Nemoto, L. Daniell, S. Ferro-Novick, and P. De Camilli. 1998. Synaptojanin family members are implicated in endocytic membrane traffic in yeast. *J Cell Sci*. 111 (Pt 22):3347-56.

Sirotkin, V., C.C. Beltzner, J.B. Marchand, and T.D. Pollard. 2005. Interactions of WASp, myosin-I, and verprolin with Arp2/3 complex during actin patch assembly in fission yeast. *J Cell Biol*. 170:637-48.

Sokac, A.M., C. Schietroma, C.B. Gundersen, and W.M. Bement. 2006. Myosin-1c couples assembling actin to membranes to drive compensatory endocytosis. *Dev Cell*. 11:629-40.

Soldati, T. 2003. Unconventional myosins, actin dynamics and endocytosis: a menage a trois? *Traffic*. 4:358-66.

Soulard, A., T. Lechler, V. Spiridonov, A. Shevchenko, A. Shevchenko, R. Li, and B. Winsor. 2002. Saccharomyces cerevisiae Bzz1p is implicated with type I myosins in actin patch polarization and is able to recruit actin-polymerizing machinery in vitro. *Mol Cell Biol*. 22:7889-906.

Stefan, C.J., S.M. Padilla, A. Audhya, and S.D. Emr. 2005. The phosphoinositide phosphatase Sjl2 is recruited to cortical actin patches in the control of vesicle formation and fission during endocytosis. *Mol Cell Biol*. 25:2910-23.

Stoffler, H.E., and M. Bahler. 1998. The ATPase activity of Myr3, a rat myosin I, is allosterically inhibited by its own tail domain and by Ca2+ binding to its light chain calmodulin. *J Biol Chem*. 273:14605-11.

Sun, Y., M. Kaksonen, D.T. Madden, R. Schekman, and D.G. Drubin. 2005. Interaction of Sla2p's ANTH domain with PtdIns(4,5)P2 is important for actin-dependent endocytic internalization. *Mol Biol Cell*. 16:717-30.

Sun, Y., A.C. Martin, and D.G. Drubin. 2006. Endocytic internalization in budding yeast requires coordinated actin nucleation and myosin motor activity. *Dev Cell*. 11:33-46.

Swanljung-Collins, H., and J.H. Collins. 1992. Phosphorylation of brush border myosin I by protein kinase C is regulated by Ca(2+)-stimulated binding of myosin I to phosphatidylserine concerted with calmodulin dissociation. *J Biol Chem*. 267:3445-54.

Tan, P.K., N.G. Davis, G.F. Sprague, and G.S. Payne. 1993. Clathrin facilitates the internalization of seven transmembrane segment receptors for mating pheromones in yeast. *J Cell Biol*. 123:1707-16.

Tang, H.Y., A. Munn, and M. Cai. 1997. EH domain proteins Pan1p and End3p are components of a complex that plays a dual role in organization of the cortical actin cytoskeleton and endocytosis in Saccharomyces cerevisiae. *Mol Cell Biol*. 17:4294-304.

Tang, N., T. Lin, and E.M. Ostap. 2002. Dynamics of myo1c (myosin-ibeta) lipid binding and dissociation. *J Biol Chem*. 277:42763-8.

Temesvari, L.A., J.M. Bush, M.D. Peterson, K.D. Novak, M.A. Titus, and J.A. Cardelli. 1996. Examination of the endosomal and lysosomal pathways in Dictyostelium discoideum myosin I mutants. *J Cell Sci*. 109 (Pt 3):663-73.

Titus, M.A., D. Wessels, J.A. Spudich, and D. Soll. 1993. The unconventional myosin encoded by the myoA gene plays a role in Dictyostelium motility. *Mol Biol Cell*. 4:233-46.

Tong, A.H., B. Drees, G. Nardelli, G.D. Bader, B. Brannetti, L. Castagnoli, M. Evangelista, S. Ferracuti, B. Nelson, S. Paoluzi, M. Quondam, A. Zucconi, C.W. Hogue, S. Fields, C. Boone, and G. Cesareni. 2002. A combined experimental and computational strategy to define protein interaction networks for peptide recognition modules. *Science*. 295:321-4.

Tong, A.H., G. Lesage, G.D. Bader, H. Ding, H. Xu, X. Xin, J. Young, G.F. Berriz, R.L. Brost, M. Chang, Y. Chen, X. Cheng, G. Chua, H. Friesen, D.S. Goldberg, J. Haynes, C. Humphries, G. He, S. Hussein, L. Ke, N. Krogan, Z. Li, J.N. Levinson, H. Lu, P. Menard, C. Munyana, A.B. Parsons, O. Ryan, R. Tonikian, T. Roberts, A.M. Sdicu, J. Shapiro, B. Sheikh, B. Suter, S.L. Wong, L.V. Zhang, H. Zhu, C.G. Burd, S. Munro, C. Sander, J. Rine, J. Greenblatt, M. Peter, A. Bretscher, G. Bell, F.P. Roth, G.W. Brown, B. Andrews, H. Bussey, and C. Boone. 2004. Global mapping of the yeast genetic interaction network. *Science*. 303:808-13.

Toshima, J., J.Y. Toshima, M.C. Duncan, J.T. Cope, Y. Sun, A.C. Martin, S. Anderson, J.R. Yates, 3rd, K. Mizuno, and D.G. Drubin. 2006a. Negative Regulation of Yeast Eps15-like Arp2/3 Complex Activator, Pan1p, by the Hip1R-related Protein, Sla2p, during Endocytosis. *Mol Biol Cell*.

Toshima, J.Y., J. Toshima, M. Kaksonen, A.C. Martin, D.S. King, and D.G. Drubin. 2006b. Spatial dynamics of receptor-mediated endocytic trafficking in budding yeast revealed by using fluorescent alpha-factor derivatives. *Proc Natl Acad Sci U S A*. 103:5793-8.

Tyska, M.J., A.T. Mackey, J.D. Huang, N.G. Copeland, N.A. Jenkins, and M.S. Mooseker. 2005. Myosin-1a is critical for normal brush border structure and composition. *Mol Biol Cell*. 16:2443-57.

Vaduva, G., N.C. Martin, and A.K. Hopper. 1997. Actin-binding verprolin is a polarity development protein required for the morphogenesis and function of the yeast actin cytoskeleton. *J Cell Biol*. 139:1821-33.

Valdez-Taubas, J., and H.R. Pelham. 2003. Slow diffusion of proteins in the yeast plasma membrane allows polarity to be maintained by endocytic cycling. *Curr Biol*. 13:1636-40.

van Tuinen, E., and H. Riezman. 1987. Immunolocalization of glyceraldehyde-3-phosphate dehydrogenase, hexokinase, and carboxypeptidase Y in yeast cells at the ultrastructural level. *J Histochem Cytochem*. 35:327-33.

Veigel, C., L.M. Coluccio, J.D. Jontes, J.C. Sparrow, R.A. Milligan, and J.E. Molloy. 1999. The motor protein myosin-I produces its working stroke in two steps. *Nature*. 398:530-3.

Wang, G., and R.J. Deschenes. 2006. Plasma membrane localization of Ras requires class C Vps proteins and functional mitochondria in Saccharomyces cerevisiae. *Mol Cell Biol*. 26:3243-55.

Warren, D.T., P.D. Andrews, C.W. Gourlay, and K.R. Ayscough. 2002. Sla1p couples the yeast endocytic machinery to proteins regulating actin dynamics. *J Cell Sci*. 115:1703-15.

Welch, M.D., and R.D. Mullins. 2002. Cellular control of actin nucleation. *Annu Rev Cell Dev Biol*. 18:247-88.

Wendland, B., K.E. Steece, and S.D. Emr. 1999. Yeast epsins contain an essential N-terminal ENTH domain, bind clathrin and are required for endocytosis. *Embo J*. 18:4383-93.

Wesp, A., L. Hicke, J. Palecek, R. Lombardi, T. Aust, A.L. Munn, and H. Riezman. 1997. End4p/Sla2p interacts with actin-associated proteins for endocytosis in Saccharomyces cerevisiae. *Mol Biol Cell*. 8:2291-306.

Wessels, D., J. Murray, G. Jung, J.A. Hammer, 3rd, and D.R. Soll. 1991. Myosin IB null mutants of Dictyostelium exhibit abnormalities in motility. *Cell Motil Cytoskeleton*. 20:301-15.

Wessels, D., M. Titus, and D.R. Soll. 1996. A Dictyostelium myosin I plays a crucial role in regulating the frequency of pseudopods formed on the substratum. *Cell Motil Cytoskeleton*. 33:64-79.

Whittaker, M., and R.A. Milligan. 1997. Conformational changes due to calcium-induced calmodulin dissociation in brush border myosin I-decorated F-actin revealed by cryoelectron microscopy and image analysis. *J Mol Biol*. 269:548-57.

Williams, R., and L.M. Coluccio. 1995. Phosphorylation of myosin-I from rat liver by protein kinase C reduces calmodulin binding. *Biochem Biophys Res Commun*. 216:90-102.

Winter, D., T. Lechler, and R. Li. 1999. Activation of the yeast Arp2/3 complex by Bee1p, a WASP-family protein. *Curr Biol*. 9:501-4.

Wolenski, J.S. 1995. Regulation of calmodulin-binding myosins. *Trends Cell Biol*. 5:310-6.

Wolenski, J.S., S.M. Hayden, P. Forscher, and M.S. Mooseker. 1993. Calcium-calmodulin and regulation of brush border myosin-I MgATPase and mechanochemistry. *J Cell Biol*. 122:613-21.

Yamashita, R.A., N. Osherov, and G.S. May. 2000. Localization of wild type and mutant class I myosin proteins in Aspergillus nidulans using GFP-fusion proteins. *Cell Motil Cytoskeleton*. 45:163-72.

Young, M.E., J.A. Cooper, and P.C. Bridgman. 2004. Yeast actin patches are networks of branched actin filaments. *J Cell Biol*. 166:629-35.

11. Publications

Grosshans BL, Grotsch H, Mukhopadhyay D, Fernandez IM, Pannsfield J, Idrissi FZ, Lechner J, Riezman H, Geli MI.
Teds site phosphorylation of the yeast myosins-I is required for ligand-induced but not for constitutive endocytosis of the G protein-coupled receptor Ste2p.
J Biol Chem. 2006 Feb 21;281(16):11104-14

Singh GP, Creely CM, Volpe G, Grotsch H, Petrov D.
Real-time detection of hyperosmotic stress response in optically trapped single yeast cells using Ramanmicrospectroscopy.
Anal Chem. 2005 Apr 15;77(8):2564-8